THE JOURNAL
OF
CHEMICAL PHYSICS

VOLUME 8 FEBRUARY, 1940 NUMBER 2

The Infra-Red Absorption Spectrum of Methylphenylacetylene

M. J. MURRAY, *Chemical Laboratory, Armour Institute of Technology, Chicago, Illinois*

AND

FORREST F. CLEVELAND, *Physical Laboratory, Armour Institute of Technology, Chicago, Illinois*

(Received November 8, 1939)

The infra-red spectrum of methylphenylacetylene between 500 and 2300 cm^{-1} has been measured with the aid of a prism spectrometer. The results are compared with the Raman spectrum of this compound, previously measured by the authors. The results are inconclusive as regards the assignment of the fundamental whose overtone, according to Badger's hypothesis, is responsible for the resonance splitting of the frequency near 2230 cm^{-1}.

INTRODUCTION

BADGER[1] has suggested that the appearance of two strong frequencies in the 2200-cm^{-1} region in the Raman spectra of nearly all of the disubstituted acetylenes is attributable to a Fermi resonance interaction between the fundamental frequency expected in this region and an overtone of a lower frequency near 750 or 1100 cm^{-1}. Since the latter frequency is inactive in the Raman spectrum, he suggested that an infra-red study would best decide which of the two frequencies more nearly satisfied the condition for resonance.

At the time the present investigation was begun, the authors had just completed a study of the Raman spectra of a series of derivatives of phenylacetylene and had found that the second overtone of a frequency near 750 cm^{-1} was considerably greater than the mean of the doublet near 2230 cm^{-1}. It was therefore of interest to measure the infra-red spectrum of one of the compounds in order to find if the expected frequency in the infra-red would better satisfy the frequency condition for resonance. Methylphenylacetylene was chosen for the study because in this compound the two lines in the 2200-cm^{-1} region were well separated and approximately equal in intensity.

[1] R. M. Badger, J. Chem. Phys. **5**, 178 (1937).

EXPERIMENTAL PROCEDURE

The methylphenylacetylene was synthesized by the action of dimethylsulfate on sodium phenylacetylide in ether solution and was purified by distillation in an efficient heated column using a high reflux ratio. The boiling point of the liquid was 72°–73°C at a pressure of 15 mm of mercury. The sample was the same as that used in obtaining the Raman spectrum.

The infra-red spectrum was obtained with the recording prism spectrometer described by Randall and Strong[2] with the addition of the periodic radiometer designed by Firestone[3] to eliminate extraneous effects. The slit width varied from 0.5 mm at 500 cm^{-1} to 0.10 mm at 2000 cm^{-1}; near 1100 cm^{-1} it was 0.2 mm.

[2] H. M. Randall and John Strong, Rev. Sci. Inst. **2**, 585 (1931).

[3] F. A. Firestone, Rev. Sci. Inst. **3**, 163 (1932).

Data were first secured with the empty cell alone in order to make possible corrections for the absorption of carbon dioxide and water vapor in the atmosphere. The thickness of the liquid in the sodium chloride absorption cell was 0.1 mm.

TABLE I. *Infra-red and Raman spectra of* $C_6H_5C{\equiv}CCH_3$.

INFRA-RED		RAMAN		
FREQUENCY (cm^{-1})	APPROXIMATE INTENSITY	DISPLACEMENT (cm^{-1})	ESTIMATED INTENSITY	DEPOLARIZATION FACTOR
		149	2	—
		298	3	0.8
		388	4	0.7
		401	2	—
		510	1	—
526	8	528	3	0.9
546	4			
594	6			
611	2			
624	4	626	3	—
631	4			
649	6			
702	10	701	3	—
754	10	758	2	—
825	6			
839	4			
909	10			
963	6	953	1	—
981	2	971	6	0.3
999	4	1001	7	0.3
1024	8	1030	2	—
1064	8	1053	½	—
1095	4			
1153	6	1160	4	<0.5
1196	6	1181	4	
1256	4	1245	1	—
		1262	8	0.3
1300	2	1286	2	—
1326	2	1328	1	—
1359	6	1382	4*b*	0.9
1418	8	1436	3	0.7
1468	8	1450	3	
		1489	4	0.7
		1500	4	
1572	6	1601	9	0.7
1667	6			
1821	4			
1890	4			
1957	4			
2137	6			
		2214	9	0.6
		2254*	10	0.6

* A frequency 2231(4) was observed on three different spectrograms and 2254 appeared resolved into the doublet 2246(10), 2262(6) when the camera lens was diaphragmed to 1.0 cm.

The source of radiation was a Nernst glower heated by current from a 220-v, a.c. power line.

RESULTS

Comparison of the results with the Raman data obtained by the authors is made in Table I.

DISCUSSION OF RESULTS

The frequency in the 1100 cm^{-1} region which most nearly satisfies the frequency condition for resonance is the weak one at 1095 cm^{-1}. The first overtone of this frequency, 2190 cm^{-1}, is seen to have a value even less than that of the smaller frequency of the doublet, 2214, 2254. The second overtone of the 756 cm^{-1} frequency, 2268 cm^{-1}, on the other hand, is greater than the larger frequency of the doublet. The results are thus inconclusive.

Soon after these measurements were completed, a paper by Crawford[4] appeared which reported the results of an infra-red and Raman study of dimethylacetylene. A weak frequency was observed at 1126 cm^{-1}. The first overtone of this frequency, 2252 cm^{-1}, falls between the doublet frequencies, 2233, 2310, but is somewhat less than the mean, 2272 cm^{-1}. The mean of the doublet, 693, 774 cm^{-1}, is near the value 725 cm^{-1} which Crawford assigns as one of the fundamental frequencies of dimethylacetylene. The second overtone of this frequency, 2175 cm^{-1}, is much lower than the mean, 2272 cm^{-1}.

ACKNOWLEDGMENT

The experimental work reported in this paper was done in the Physics Department at the University of Michigan. The authors wish to express their appreciation to Professor H. M. Randall for putting the facilities of his laboratory at their disposal. They also wish to express their thanks to Mr. Robert A. Oetjen for his assistance in obtaining the experimental record.

[4] Bryce L. Crawford, Jr., J. Chem. Phys. **7**, 555 (1939).

The Rotational Structure of the Hydrazoic Acid Bands in the Photographic Infra-Red

EUGENE H. EYSTER*
Department of Physics, University of Michigan, Ann Arbor, Michigan
(Received November 28, 1939)

The third and fourth harmonics of the N—H stretching frequency in hydrazoic acid, at 9547.31 and 12,412.19 cm^{-1}, respectively, have been studied photographically under high dispersion. The rotational structure has been well resolved and completely analyzed, to yield the rotational constants in the ground and excited states. The effective moments of inertia in the ground state have been combined with other information to determine the structure of the molecule; the best values of the molecular parameters are:

$N_1-H = 1.012A$ $N_2-N_3 = 1.128A$
$N_1-N_2 = 1.241A$ $\Delta HN_1N_2 = 110° 52'$.

ELECTRON and x-ray diffraction experiments have fully confirmed the predictions of the modern structural theory concerning the structure of the azide group in ionic crystals and in covalent compounds.[1] The infra-red spectra of covalent azides have not, however, been satisfactorily correlated with acceptable structures. It has been asserted that the rotational structure of the hydrazoic acid bands in the photographic infra-red demands the existence of two kinds of HN_3 molecules, one of which is structurally inacceptable, and that the envelopes of methyl azide bands in the same region indicate that this molecule has a linear C—N—N—N group, contrary to the electron diffraction results.[2] It has consequently been thought useful to reinvestigate these spectra in order to determine whether or not these reported inconsistencies are real. The present paper presents the complete analysis of the rotational structure of the two strongest bands of hydrazoic acid in the photographic region, and demonstrates the fact that the resulting rotational constants determine a structure which is in complete harmony with theoretical predictions and with previous structure determinations in other covalent azides.

EXPERIMENTAL

The infra-red spectrum of hydrazoic acid was photographed by the author in the spectroscopic laboratory of the Gates and Crellin Laboratories of Chemistry of the California Institute of Technology. The acid was prepared from recrystallized sodium azide (Eimer and Amend) by the method of Dennis and Isham.[3] The gas was swept from the generator in a current of dry nitrogen, through a 50-cm calcium chloride drying tube, and into a trap cooled in liquid air. This trap, attached to the generator by a Pyrex standard taper, was then transferred to a similar fitting on the six-meter Pyrex absorption tube, which was at once evacuated and sealed off while the explosive acid was still at liquid-air temperatures. The gas pressure was subsequently regulated by adjusting the temperature of the liquid acid in this trap. The whole of the absorption tube was shielded from stray radiation with black cloth, and a filter which cut out all wave-lengths shorter than 7000A was interposed between the source and the tube to protect its contents from possible photochemical decomposition in the direct beam.

With the trap at room temperature, exploration photographs were taken with a Bausch and Lomb glass Littrow spectrograph set to record the region between 7500 and 12,000A on Eastman I-Z plates. Four bands were observed, and the two stronger ones were then rephotographed in the first order of a twenty-one-foot concave grating spectrograph. For the band at 10,477A, the trap was held at 0°C, and for the weaker 8058A band it was held at 25°C. Wave-length measurements on the prism spectrograms were

* National Research Fellow in Chemistry.

[1] The considerations leading to a prediction of the structures of the azide group in covalent and ionic compounds are summarized on page 185, L. Pauling, *The Nature of the Chemical Bond* (Cornell University Press, 1939).

[2] A discussion of these results, with references to the original papers, is given in an interesting review article by Verleger, Physik. Zeits. **38**, 83 (1937).

[3] L. M. Dennis and H. Isham, J. Am. Chem. Soc. **29**, 216 (1907).

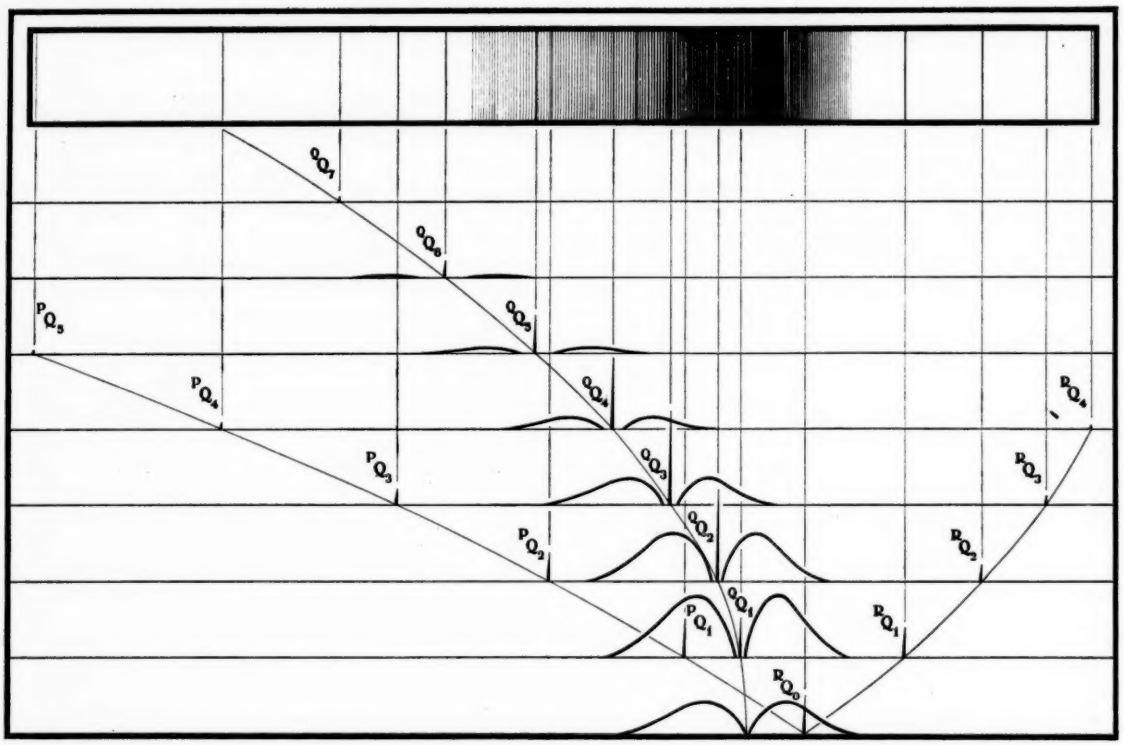

FIG. 1. The hydrazoic acid band at 9547 cm^{-1}, and its analysis into constituent sub-bands and branches. Calculated intensities of the K-structure lines are indicated by their heights, and the intensities of the J-structure lines are given as envelopes.

made with respect to infra-red emission lines of copper, sodium, potassium, barium, and calcium, and on the grating spectrograms with respect to iron arc standards in the second and third orders. Eastman 144-R and I-Z plates, hypersensitized in ammonia, were used, and higher order spectra from the grating were removed by the filter already mentioned.

ROTATIONAL STRUCTURE

Since one may confidently expect the structures of hydrazoic acid and its methyl derivative to be analogous, the results of the electron diffraction study of methyl azide[4] should provide a basis for the calculation of approximate moments of inertia for the acid itself. Such approximate moments enable one to estimate as probable values for Badger's rotational parameters S and ρ[5] the following:

$$S=-0.999; \quad \rho=+61.4.$$

These values constitute a numerical statement of the fact that the rotational levels of hydrazoic acid should approximate those of a symmetric rotator of an extreme spindle shape. Hence it should be possible to treat the hydrazoic acid bands as symmetric rotator bands, except that lines receiving a large portion of their intensity from levels of high J and low K may show a splitting or fuzziness as the result of asymmetry.

The bands at 10,477A and 8058A undoubtedly correspond to the third and fourth harmonics of the N−H stretching frequency, and both the third and fourth harmonic states of this vibration belong to the irreducible representation A' of the group C_s of the planar hydrazoic acid. Molecular symmetry then does not require that these bands present rotational structures of pure types, and if we imagine the direction of electric moment change to be the N−H bond direction, parallel-perpendicular hybrid bands will in fact be anticipated.[6]

[4] L. Pauling and L. O. Brockway, J. Am. Chem. Soc. **59**, 13 (1937).

[5] R. M. Badger and L. R. Zumwalt, J. Chem. Phys. **6**, 713 (1938).

[6] This molecule is so nearly symmetric that the type B and C bands may well be called perpendicular, and the

General features of observed bands

These general expectations are well fulfilled by the observed bands. The third harmonic band is a hybrid of predominantly parallel structure, whose most striking feature is provided by the fact that the various parallel sub-bands, which usually coalesce to form a single parallel band, are here clearly separated as a result of the strong dependence of the small moment of inertia upon vibrational state; unusually marked convergence is correspondingly present in the perpendicular component. Fig. 1 shows a representation of the complete band, with its analysis into constituent branches. The coarse structure lines are separately represented and named, while only the envelopes of the closely spaced ${}^{Q}R_K$ and ${}^{Q}P_K$ branches are shown; though these latter are not specifically named, their naming is uniquely implied by the associated ${}^{Q}Q_K$ branches. The nomenclature of lines will be evident from the following: the large letter describes the behavior of J in the transition, the left-hand superscript describes the behavior of K, the right-hand subscript gives the value of K'', and the value of J'' follows the large letter in parentheses.

The fourth harmonic is a pure parallel band, and hence much simpler in appearance than the band of Fig. 1. As might be anticipated, the ${}^{Q}Q$ branch sweeps back even more rapidly than in the third harmonic. Since the appearance of this band can be readily visualized from a consideration of the parallel component of the third harmonic band, it has not been separately illustrated. The frequencies and identifications of

TABLE I. *The third* N—H *harmonic band of hydrazoic acid at 9547.31 cm*$^{-1}$.

J	${}^{Q}P_5(J)$	${}^{Q}P_4(J)$	${}^{Q}P_3(J)$	${}^{Q}R_2(J)$	${}^{Q}P_2(J)$	${}^{Q}R_1(J)$	${}^{Q}P_1(J)$	K	${}^{P}Q_K$	${}^{Q}Q_K$	${}^{R}Q_K$
6							9539.95	0	——	——	9564.82
7							39.09	1	9527.07	9544.60	597.44
8	9474.37						38.35	2	485.10	537.50	622.02
9	73.69	9497.53		9545.30			——	3	438.00	522.92	642.93
10	72.89	96.92		46.02			36.71	4	384.25	504.74	657.30
11	71.88	95.96	9514.03	46.73			35.92	5	326.40	480.76	666.32
12	71.14	95.14	13.24	47.51	9527.74		35.02	6		452.62	
13	70.32	94.22	12.50		26.89		34.15	7		420.20	
14	69.40	93.32	——		26.08		33.41	8		384.14	
15	68.60	92.46	——		25.23		32.50				
16	67.74	91.60	10.04		24.45		31.68				
17	66.99	90.73	09.20		23.64	9558.21	30.84				
18	66.04	89.91	08.27		——	58.96	30.02				
19	65.19	89.02	07.41		22.03	59.69	29.16				
20	64.34	88.11	06.56		21.15	60.40	28.35				
21	63.55	87.36	05.72		20.31	61.10	27.30				
22	62.64	86.39	——		19.39	61.78	26.46				
23		85.62	03.97		18.47	62.48	25.58				
24		84.76	03.14		17.57	63.17	24.74				
25		83.77	02.29		16.64	63.88	23.86				
26		82.99	01.36		15.68	64.61					
27		82.11	00.40		14.79	65.25					
28		——				65.97					
29		80.08				66.65					
30		79.33				67.32					
31		78.44				68.06					
32		77.47				68.76					
33		76.59				69.44					
34						70.12					
35						70.91					
36						71.60					
37						72.29					
38						72.95					
39						73.60					
40						74.25					
41						74.92					
42						75.54					
43						76.21					
44						76.80					

type A bands parallel. For a discussion of pure and hybrid bands and their dependence on molecular symmetry see E. H. Eyster, J. Chem. Phys. **6**, 577 (1938).

TABLE II. *The fourth* N−H *harmonic band of hydrazoic acid at 12,412.19 cm*$^{-1}$.

J	$^{Q}P_4(J)$	$^{Q}R_3(J)$	$^{Q}P_3(J)$	$^{Q}R_2(J)$	$^{Q}P_2(J)$	$^{Q}R_1(J)$	$^{Q}P_1(J)$	K	$^{Q}Q_K$
6							12,405.40	1	12,410.60
7				12,406.03			04.72	2	399.91
8				06.71			03.99	3	382.21
9	12,350.64			07.54			03.12	4	357.69
10	49.69			08.39			02.18	5	326.59
11	48.92			09.14		12,419.73	01.34	6	289.66
12	48.02			09.87	12,390.03	20.33	00.67		
13	47.10			10.52	89.26	21.05			
14	46.26			11.34	88.45	21.77			
15	45.47	12,394.41		12.04	87.57	22.31			
16	44.62	95.14	12,369.13	12.80	86.69	23.06			
17	43.73	95.77	68.18	13.40	85.87	23.97			
18	42.86	96.50	67.19	14.19	84.91	24.71			
19	42.06	97.19	66.34	14.90	84.04	25.30			
20	41.15	97.93	65.52	15.54	83.17	25.97	393.58		
21	40.42	98.68	64.70	16.25	——	26.61	92.76		
22	39.38		63.83	16.93	81.45	27.31	91.82		
23	38.47		62.87	17.61	80.52		90.80		
24	37.56		61.94	18.29	79.72				
25	36.66		61.03	19.03	78.87				
26	35.77		60.10		77.96				
27	34.88		59.21						
28	34.01		58.34						
29	33.07		56.64						
30	31.99		55.64						
31	31.05		54.69						
32	30.21		53.83						
33	29.35		52.83						
34	28.37								
35	27.32								

the 250 lines that were measurable in these bands are given in Tables I and II. Missing lines and branches in these tables are ones which are completely obscured by stronger components of the bands; many of the reported lines are blends, and subject to unavoidable errors of measurement for that reason. This is especially true of lines in the third harmonic band, where there are several regions in which the overlapping is so multifold as to produce utter confusion in the fine structure.

Rotational constants

In the absence of strong perturbations by adjacent vibrational states, the rotational energy of a symmetric rotator may be conveniently written as follows:

$$F(J,K,v)=\sum_{i,j}{}'X_{ij}{}^{v}\{J(J+1)\}^{i}\{K^2\}^{j}. \quad (1)$$

The primed summation indicates the omission of the constant term $X_{00}{}^{v}$, and v is to be considered as the totality of quantum numbers required to specify the vibrational state; in our case it will simply be v_1, the quantum number associated with the N−H stretching frequency. A formula of this type should be expected to describe the majority of the rotational levels of a molecule so nearly symmetric as hydrazoic acid; the leading coefficients will then be related to the effective moments of inertia as follows:

$$X_{01}{}^{v}=A_v-\tfrac{1}{2}(B_v+C_v);\quad X_{10}{}^{v}=\tfrac{1}{2}(B_v+C_v), \quad (2)$$

where

$$A_v=h/8\pi^2I_A{}^{v}c;\quad B_v=h/8\pi^2I_B{}^{v}c;$$
$$C_v=h/8\pi^2I_C{}^{v}c;\quad A_v\gg B_v>C_v. \quad (3)$$

It was found best to evaluate $X_{01}{}^{0}$ and $X_{02}{}^{0}$ in the third harmonic band, with the aid of the following relations:

$$\Delta F''(K)/(2K+1)=X_{01}{}^{0}+2X_{02}{}^{0}M+\cdots;\quad M=(K+\tfrac{1}{2})^2+\tfrac{1}{4}$$
$$\Delta_2F''(K)/4K=X_{01}{}^{0}+2X_{02}{}^{0}M+\cdots;\quad M=K^2+1. \quad (4)$$

The term differences of (4) are given by:

$$\Delta F''(K)={}^{Q}Q_K-{}^{P}Q_{K+1}={}^{R}Q_K-{}^{Q}Q_{K+1},$$
$$\Delta_2F''(K)={}^{R}Q_{K-1}-{}^{P}Q_{K+1}. \quad (5)$$

Eqs. (4) were tested with the experimental combinations, and found to represent the data within experimental error. The constants of the equations were then determined by the method of least squares to be:

$$X_{01}^{0}=19.946\ \text{cm}^{-1};\quad X_{02}^{0}=-0.05616\ \text{cm}^{-1}.$$

The dependence of X_{01}^{v} and X_{02}^{v} upon v was established by the determination of X_{01}^{3}, X_{01}^{4}, X_{02}^{3}, and X_{02}^{4} with the aid of the relation:

$$({}^{Q}Q_1-{}^{Q}Q_K)/(K^2-1)=X_{01}''-X_{01}'+(X_{02}''-X_{02}')M+\cdots;\quad M=K^2+1. \tag{6}$$

This relation was first tested with the observed combinations in both the third and fourth harmonic bands, and found to be well fulfilled; deviations from linearity in M were within the error of observation. The constants were then determined by the method of least squares, and it was found possible to represent the dependence of the terms X_{01}^{v} and X_{02}^{v} upon the vibrational quantum number v_1 of the N−H stretching frequency as:

$$X_{01}^{v_1}=X_{01}^{0}-\alpha_{01}^{1}v_1;\quad \alpha_{01}^{1}=0.905\ \text{cm}^{-1},$$
$$X_{02}^{v_1}=X_{02}^{0}-\alpha_{02}^{1}v_1;\quad \alpha_{02}^{1}=-0.000904\ \text{cm}^{-1}. \tag{7}$$

It must be realized, of course, that the "lines" used in the above formulas are actually whole branches, and that the appropriate averages over their J structures should appear in Eqs. (4), (5), and (6) to render them precise. This effect will be small, however, since these "lines" are surprisingly sharp. It must also be admitted that the constants X_{01}^{v} and X_{02}^{v} which we have determined in this way may contain small contributions from cross product terms like X_{11}^{v} and X_{12}^{v}, but we shall find in the following section that these cross product terms appear to be exceedingly small.

Determination of the constants X_{10}^{0} and X_{20}^{0} was made by the usual method, with the aid of the expressions:

$$\Delta_2F_K''(J)/2(2J+1)=X_{10}^{0}+K^2X_{11}^{0}+2(X_{20}^{0}+K^2X_{21}^{0})M+\cdots;\quad M=\{(J+\tfrac{1}{2})^2+\tfrac{3}{4}\}. \tag{8}$$

The combinations of (8) are the familiar ones:

$$\Delta_2F_K''(J)={}^{Q}R_K(J-1)-{}^{Q}P_K(J+1). \tag{9}$$

When these combinations were evaluated from the three available values of K in the fourth harmonic, their dependence upon K was found to be too small to detect. Hence it has been concluded that the cross terms in the energy expression are too small to be considered in this treatment. The constants X_{10}^{0} and X_{20}^{0} were then determined by fitting an equation of the form of (8), without the K dependence, to the observed combinations by the method of least squares. The resulting constants, evaluated from the data from the fourth harmonic where overlapping was least serious, were:

$$X_{10}^{0}=0.3996\ \text{cm}^{-1};\quad X_{20}^{0}=-8.1\times10^{-6}\ \text{cm}^{-1}.$$

The variation of X_{10}^{v} with vibrational state was best determined by the following relations:

$$X_{10}^{v_1}=X_{10}^{0}-\alpha_{10}^{1}v_1-\cdots;$$
$$\tfrac{1}{2}\{{}^{Q}R_K(J-1)+{}^{Q}P_K(J)\}=f(K)-\alpha_{10}^{1}v_1M-\cdots;\quad M=J^2. \tag{10}$$

These combinations were made in the two harmonics, and no systematic deviations from linearity in M could be detected. The average value of the constant α_{10}^{1} was 0.000610 cm^{-1}. The change in the small quantity X_{20}^{v} with vibrational state was beyond the limit of experimental determination.

The rotational constants may now be collected:

$$X_{01}^{v}=19.946-0.905v_1-\cdots.$$
$$X_{02}^{v}=-0.05616+0.000904v_1+\cdots.$$
$$X_{10}^{v}=0.3996-0.000610v_1-\cdots.$$
$$X_{20}^{v}=-0.0000081+\cdots.$$

Line intensities

The relative intensities of the lines comprising the parallel component, and the relative intensities of the lines comprising the perpendicular component of the third harmonic band may now be calculated to the symmetric rotator approximation with the aid of the matrix elements of the electric moment given by Dennison for symmetric rotator wave functions.[7] In order to determine the intensity ratio of the two separate com-

[7] D. M. Dennison, Rev. Mod. Phys. **3**, 313 (1931).

ponents, however, one must appeal to the experimental intensities, which are very difficult to measure in this region. Fortunately this task was made easy by the fact that two sharp lines of moderate intensity, ${}^{Q}Q_6$ and ${}^{P}Q_3$, which are close together in the third harmonic and in a region quite free from other lines of appreciable intensity, are found to have equal intensities, both by visual examination of prints of the spectrograms and also by inspection of microphotometer traces of the plates. This useful fact establishes the ratio of the parallel and perpendicular components in the third harmonic. Fig. 1 shows these symmetric rotator intensities for the individual coarse structure lines, and the envelopes of the fine structure intensities. It is interesting to note that the calculated intensities of the ${}^{P}P$, ${}^{R}P$, ${}^{P}R$, and ${}^{R}R$ branches are too small to be represented on the scale of Fig. 1; no lines of these branches were found. Because of the inherent difficulties of intensity measurements in this region it is quite impossible to make any quantitative comparison of theoretical and observed intensities; suffice it to say that a summation of the intensities of Fig. 1 produces a band envelope whose similarity to a microphotometer trace of the third harmonic band is amazingly close, except for two exceptional lines which will be mentioned shortly. A similar comparison in the fourth harmonic yields comparable results.

This treatment also enables one to calculate the ratios of the vibrational matrix elements of the parallel and perpendicular components of the electric moment. One finds:

$$(M_\perp)_{03}/(M_\parallel)_{03}=0.212; \quad (M_\perp)_{04}/(M_\parallel)_{04}\doteq 0.$$

It is of interest to notice that there is no evident relationship between these observed ratios and those which one would calculate on the assumption that the change of electric moment takes place along the N−H bond, for such an assumption would predict a ratio of 6.7, nearly independent of v_1.[8]

Up to this point, no departures from the symmetric rotator intensities have been remarked; such departures do, however, exist, and are found precisely where they should be expected. The ${}^{Q}P_0$ and ${}^{Q}R_0$ branches, whose higher lines should feel the effects of asymmetry most markedly, are completely submerged by stronger branches. The first line of the ${}^{Q}Q$ branch, ${}^{Q}Q_1$, is already very sharp and in the correct position. The lines ${}^{R}Q_0$ and ${}^{P}Q_1$, however, both of which obtain their greatest intensity from transitions involving levels with $K=0$ for J values around 16, are noticeably weak and diffuse, the former merely giving anomalous intensity to two fine structure lines, and the latter being almost indistinguishable. The estimated positions of these lines, however, do not seem to deviate greatly from the symmetric rotator predictions, though they were felt unsuitable to use in determining the rotational constants. The next lines in these branches have become very sharp, and no further deviations from the behavior of a symmetric rotator were found in the third harmonic band. None were observed at all in the fourth harmonic where the perpendicular component is absent.

Vibrational Constants

The vibrational energy expression for hydrazoic acid will have the form:

$$G(v)=Y_1(v_1+\tfrac{1}{2})+\cdots+Y_{11}(v_1+\tfrac{1}{2})^2 +\cdots+\text{cross terms.} \quad (11)$$

Determination of the centers of the third and fourth harmonics of the N−H frequency of quantum number v_1 will make possible the evaluation of the vibrational constants Y_1 and Y_{11}. The band centers are given by:

$$G_0{}^{v}=G(v)-G(0)={}^{Q}Q_K+K^2(X_{01}{}^{0}-X_{01}{}^{v}) +K^4(X_{02}{}^{0}-X_{02}{}^{v})+\cdots. \quad (12)$$

With the aid of the above expression and the values of the rotational constants already determined, values of $G_0{}^{v}$ were calculated from each of the ${}^{Q}Q$ lines in the third and fourth harmonic bands, giving as best values:

$$G_0{}^{3}=9547.31 \text{ cm}^{-1}; \quad G_0{}^{4}=12{,}41\,2.19 \text{ cm}^{-1}.$$

From these the vibrational constants are found

[8] This assumption has been used by Badger and Bauer, J. Chem. Phys. 5, 854 (1937). It is probable that the appearance of the third harmonic of the N−H stretching frequency in ethylene imine is a result of the failure of this assumption, rather than an indication of an abnormally small angle between the N−H bond and the plane of the ring, as was first supposed; see the reference of footnote 6.

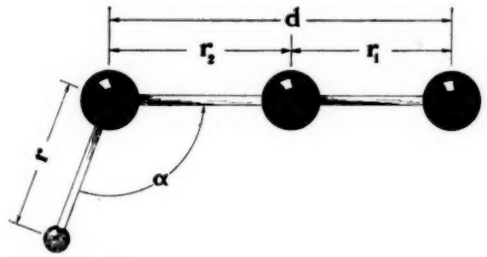

FIG. 2. The assumed model of the hydrazoic acid molecule; the size parameters have the relative values given by this investigation.

to be:

$$Y_1 = 3497.32 \text{ cm}^{-1}; \quad Y_{11} = -78.72 \text{ cm}^{-1}.$$

This information permits the center of the fundamental band to be calculated as 3339.88 cm^{-1}. Davies gives 3336.2 cm^{-1} as the apparent center of the parallel structure of the fundamental,[9] and incomplete results in this laboratory give 3335.6 cm^{-1}. Since the apparent minimum of the parallel component will be found at a frequency somewhat lower than that of the actual band center, this agreement seems adequate, and constitutes the justification for the vibrational assignments made for the photographic bands.

STRUCTURE OF THE MOLECULE

In order to interpret the rotational constants X_{01}^0 and X_{10}^0 in terms of effective moments of inertia of the ground state of the molecule, it is necessary not only to assume the planar structure, but also to assume explicitly that $I_A^0 + I_B^0 = I_C^0$; the latter assumption will of course be only approximately true since the I^0's are effective moments of inertia, but for the present purpose this is one of the least important errors. With this assumption and Eqs. (2) and (3), we may obtain:

$$A_0 = 20.346 \text{ cm}^{-1}; \quad B_0 = 0.4035 \text{ cm}^{-1};$$
$$C_0 = 0.3957 \text{ cm}^{-1}.$$

The effective moments of inertia, expressed in the convenient chemical units, i.e., mass on the chemical atomic weight scale and distance in A, are:

$$I_A^{0\prime} = 0.8286; \quad I_B^{0\prime} = 41.78; \quad I_C^{0\prime} = 42.61.$$

[9] M. M. Davies, Trans. Faraday Soc. **35**, 1184 (1939).

The assumed shape of the hydrazoic acid molecule is shown in Fig. 2. Having assumed the planarity of the molecule and the linearity of the azide group—assumptions in which one has great confidence—the molecule still has four structural parameters, which are conveniently chosen as: r, the N−H distance; α, the H−N−N bond angle; d, the length of the azide group; and $k = r_2/d$, which places the central nitrogen atom. The moments of inertia can define only two of these parameters, so that we must assume values for the other two. The following have been chosen as the most suitable assumptions:

(1) The parameter r has been chosen as 1.012A, on the basis of the 1.016A N−H distance in the ground state of ammonia. It is felt a decrease of 0.004A should be made to care for the absence of the H−H repulsions in HN_3 and for the fact that the nitrogen atom involved in N−H bonding in HN_3 is partially double-bonded in the azide group.

(2) The parameter k has been chosen as 0.524. If one assumes the structures

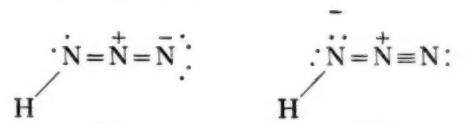

(a) (b)

to be the only ones contributing appreciably to the ground state of hydrazoic acid, then one can make an approximate calculation of the dependence of both d and k upon x, the "hybridization ratio," which is a quantity ranging from zero to one which measures the fractional contribution of state (a) to the ground state.[10] Fig. 3 shows the result of this calculation. Unfortunately we do not know the value of x which will prevail in the actual molecule, but one sees from Fig. 3 that the azide group can achieve greatest compactness, and hence presumably the greatest binding energy by choosing an x of about 0.63; the corresponding k is 0.524.

One may now determine the values of α and d from the moments of inertia and the assumed values for k and r. One finds:

$$\alpha = 110° 52'; \quad d = 2.369\text{A}.$$

[10] This method is described and applied to a somewhat different case on page 180, L. Pauling, *The Nature of the Chemical Bond* (Cornell University Press, 1939).

Though one might expect the value of d to be less accurately given by the curves of Fig. 3 than is k, it is interesting to note that the minimum value of d given by the simple theory is 2.371A. Such close agreement is of course accidental, but fortunately neither α nor d are very sensitive to reasonable changes of k. Table III shows a comparison of the parameters of the azide group as determined by this method, as calculated by the simple theory, and as determined in other compounds containing the azide group. The differences between the values obtained by these four methods are gratifyingly small, being within the limits of error of the diffraction and crystal structure determinations. It is consequently felt that the values

$$N_1-H=1.012A \qquad N_2-N_3=1.128A$$
$$N_1-N_2=1.241A \qquad \measuredangle H-N_1-N_2=110°\ 52'$$

constitute a reasonably precise description of the mean positions of the atoms in the ground state of hydrazoic acid. The structure of the azide group is in complete agreement with the structural theory, and hence tells us nothing new in principle. The angle α is of greater interest, since it might seem somewhat smaller than one would expect on the basis of structures (a) and (b) and a hybridization ratio $(a)/(b)=0.63$. It is felt, however, that this is a real effect, and is another example of the tendency of the unshared electron pairs on the nitrogen atom to prefer the $2s$ orbital, and hence to give to the bonding orbitals somewhat more than the usual $2p$ character, a procedure which leads to smaller angles.

TABLE III. *Parameters of the covalent azide group.*

PARAMETER	ELECTRON DIFFRACTION CH_3N_3	X-RAY CRYSTAL STRUCTURE $C_2N_3(N_3)_3$	PRESENT STUDY HN_3	SIMPLE THEORY $-N_3$
k	0.530	0.532	—	0.524
d	2.34	2.37	2.369	2.371
α	120°	—	110° 52′	—

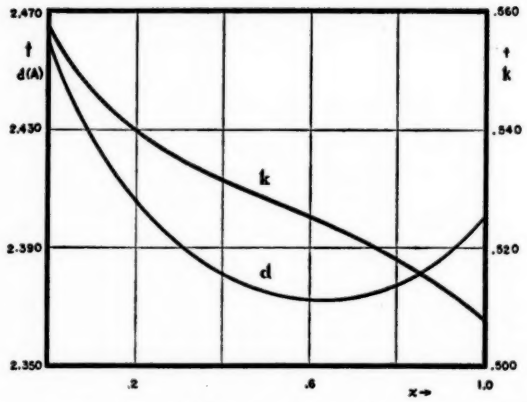

FIG. 3. Dependence of the parameters d and $k=r_2/d$ upon the hybridization ratio x.

Finally, this structure makes it easy to understand the large value of the constant $\alpha_{01}{}^1$, which is responsible for the unusual nature of the photographic bands. In fact this constant can be roughly predicted, for with this molecular structure, one sees that $\alpha_{01}{}^1$ should be given approximately by the value of α_e for a diatomic molecule with $B_e=20.8$, $\omega_e=3497$, and $\omega_e x_e=78.7$. The Morse approximation, which usually gives too small values for α_e, then gives $\alpha_e=0.705$, which is certainly of the right order of magnitude.

In conclusion, the author is pleased to acknowledge his special indebtedness to the National Research Council, and to express his gratitude to Professor Richard M. Badger of the California Institute of Technology, in whose laboratory the experimental part of this investigation was completed, for his helpful advice and for his continued interest in this problem.

Normal Vibrations of Chains of Similar and Similarly Situated Dynamical Systems and the Infra-Red Spectrum of Undecane

S. E. WHITCOMB, H. H. NIELSEN AND L. H. THOMAS
Mendenhall Laboratory of Physics, Ohio State University, Columbus, Ohio

(Received September 23, 1939)

Theory indicates that the normal modes of vibration of chain molecules fall into two classes; *end vibrations* in which the amplitude falls off exponentially from the ends towards the middle, and *chain vibrations* in which it varies harmonically as in a standing wave. The transition from one class to the other takes place via chain vibrations with a small number of nodes of amplitude along the chain. For a long chain we expect only those chain vibrations to show up in the infra-red spectrum for which the phase of the electric moment is constant along the chain.

These considerations have been applied to predict the vibration spectra of the straight chain paraffins, assumed to consist of a zigzag chain of carbon atoms each carrying two hydrogen atoms in a plane perpendicular to the chain and alternately above and below it.

The infra-red spectrum of undecane has been measured from 1 to 15μ on a prism spectrometer, the positions of 31 bands being determined. Accepted values of the interatomic distances and angles were assumed and force constants were adjusted to fit four of the fundamental frequencies to observed bands. Bands were observed near all the other fundamental frequencies predicted certainly to occur (as chain vibrations) and near one out of three that should possibly occur (as end vibrations near chain vibrations with few nodes). All but three of the observed bands could be accounted for as fundamentals, harmonics, or simple combination frequencies.

I. INTRODUCTION

THE spectrum of undecane and those of similar compounds have been measured by several investigators. The first investigation was carried out by Coblentz.[1, 2] Later Lambert and Lecomte[3, 4] measured the spectrum in the region between 6μ and 16μ and Liddell and Kaspar[5] the region from 0.5 to 1.8μ. More recently Barca-Galateanu[6, 7] has measured the spectrum of dodecane, the next member of the series, from 2 to 15μ, and the results are very similar to those for undecane. The work of Lambert and Lecomte on the other members of this series also shows this similarity.

Various attempts have been made to explain the observed spectra. The first was by Ellis[8] and was purely empirical. He interpreted part of the bands as being harmonic members of a series whose fundamental at 3.3μ was due to a C−H vibration. Other bands were attributed to a C−C vibration with an unobserved fundamental at 28μ. Other observers have applied these series with fair success to various members of the methane series. However, without making use of improbable combination frequencies, they could not account for all of the observed bands, nor could they explain the intensities. Later workers have attempted to explain the observed spectra on the basis of a model of the molecule. Lennart Simons[9] assumed a model composed only of carbon atoms arranged in a straight line and obtained expressions for the normal frequencies of vibration. Kassel[10] has obtained the normal frequencies of pentane taking account of the carbon atoms and assuming an angle of 110° between the C−C bonds. Kirkwood[11] more recently has worked out the normal frequencies for a model of any length taking into account the angle between the C−C bonds. All of these workers have, however, neglected altogether the effect of the hydrogen atoms, which must certainly be important. Accordingly it was thought worthwhile to investigate the whole problem taking into account all of these factors and thus to set up a fairly complete theory of the vibration spectra of these long chain compounds.

[1] Coblentz, Astrophys. J. **20**, 207 (1903).
[2] Coblentz, Phys. Rev. **16**, 385 (1903).
[3] Lecomte, Comptes rendus **183**, 27 (1926).
[4] Lambert and Lecomte, Ann. de physique **18**, 329 (1932).
[5] Liddell and Kaspar, Nat. Bur. Stand. J. Research **11**, 599 (1933).
[6] Barca-Galateanu, Bull. Soc. Roum. de Phys. **37–67**, 19 (1936).
[7] Barca-Galateanu, Bull. Soc. Roum. de Phys. **38–70**, 104 (1938).
[8] Ellis, Phys. Rev. **27**, 298 (1926).
[9] Lennart Simons, Soc. Scient. Fenn. Com. Phys. Math. **8–16**, 1 (1935).
[10] Kassel, J. Chem. Phys. **3**, 326 (1935).
[11] Kirkwood, J. Chem. Phys. **7**, 506 (1939).

II. The Theory of the Vibrations of Chains of Similar Dynamical Systems[12]

Consider a chain of m links each described by r coordinates, y_{uh}, $u=1, 2, \cdots r$, $h=1, 2, \cdots m$, completed at the ends before $h=1$ and after $h=m$ by systems described by q coordinates, x_t, $t=1, 2, \cdots q$, and s coordinates, z_w, $w=1, 2, \cdots s$, chosen so that the kinetic energy has the form

$$\tfrac{1}{2}[\sum \dot{x}^2+\sum\sum \dot{y}^2+\sum \dot{z}^2]. \qquad (1)$$

The total number of degrees of freedom is thus $q+mr+s$.

Suppose that the potential energy contains no product terms involving x_t and y_{uh} if $h>l$; y_{uh} and y_{vk} if $|h-k|>l$; or y_{uh} and z_w if $h<m+1-l$; where l is a small integer usually 1 or 2. Suppose further that the coefficients of the terms in $y_{uh}y_{vh+k}$ (which differ from zero only for $|k|\geqslant l$) are independent of h.

This form does not represent a finite chain molecule exactly because of progressive small changes in the internal and relative equilibrium distances of the links as the ends are approached. On the other hand, the coordinates may be defined differently for these links so as partly to compensate this. (Indeed for C_nH_{2n+2} with $r=9$ we may perhaps take $m=n$, $q=s=3$; x_1, x_2, and x_3, being combinations of coordinates of the end CH_3 group, chosen with y_{11}, y_{12}, $\cdots y_{19}$, so that these are coupled to y_{21} etc. by nearly the same potential energy terms as these with y_{31} etc.; but it is safer to take whole CH_3 groups as end groups.)

If the system is vibrating in a normal mode with frequency ω we may write

$$x_t=a_te^{i\omega t}, \quad y_{uh}=b_{uh}e^{i\omega t}, \quad z_w=c_we^{i\omega t}. \qquad (2)$$

We then regard the b_{uh} as linear combinations of terms of the form

$$b_ue^{ih\lambda}. \qquad (3)$$

The equations of motion for y_{uh}, $h=l+1, l+2, \cdots m-l$, give a set of r homogeneous linear equations in b_u, linear in ω^2, and of degree l in $\cos\lambda$, the term in ω^2 not containing λ. The equation

$$D=0, \qquad (4)$$

formed by equating to zero the determinant of the coefficients of b_u in these, is an equation of degree r in ω^2, the coefficient of ω^{2s} being in general of degree $l(r-s)$ in $\cos\lambda$. This equation connects the simultaneously possible values of ω and λ for the oscillations of an infinite chain with phase difference λ from link to link.

For a given value of ω there are in general lr values of $\cos\lambda$ and sets of ratios of b_u. If we take for b_{uh} linear combinations of the $2lr$ terms $b_ue^{\pm ih\lambda}$, and substitute these, together with a_t and c_w, in the end conditions, the equations of motion, that is, for x_t; y_{uh}, $h=1, 2, \cdots l, m+1-l, m+2-l, \cdots m$; and z_w: we obtain a set of $q+2lr+s$ homogeneous linear equations in $2lr+q+s$ variables. The determinant formed by the coefficients of these equations when equated to zero must give the condition that ω is a normal frequency. This determinant contains only symmetrical functions of the $2lr$ values of $e^{i\lambda}$ for given ω and can therefore be expressed without actually solving the Eq. (4) for $\cos\lambda$. So expressed it must be equivalent to that obtained by eliminating all of a_t, b_{uh}, and c_w, from the (original) equations of motion.

If the r values of ω^2 satisfying $D=0$ are given as functions of λ from $\lambda=0$ to $\lambda=2\pi$, it may happen that some of them vary little over this range and lie in bands separated from those covered by other roots. If any normal frequency lies in such a band, the corresponding normal mode must be a linear combination of at least one pair of sets of terms $b_ue^{\pm ih\lambda}$ with λ real and at most $lr-1$ pairs of sets with λ complex, which must die off exponentially from the ends towards the center. The mode, for a sufficiently long chain, is then given by a sum over the sets with λ real

$$b_{uh}=\sum b_{u\lambda}\cos(h\lambda-\epsilon), \qquad (5)$$

modified near the ends to satisfy the end conditions. The modifications near the ends are usually small for vibrations that can be regarded as near the internal vibrations of the separate groups and of the order of 1 for those that can be regarded as relative motions of the groups, but may exceptionally be much larger. Such modes we shall term *chain vibrations*. (Fig. 1, A.)

[12] Routh, *Advanced Rigid Dynamics* (Macmillan, 1930), p. 287, where some references are given. The first consideration of problems of this kind seems to be due to Lagrange; chains of gyrostats were considered by Kelvin; the general theory is not difficult to set up and presents analogies with the theory of electronic states of linear crystals.

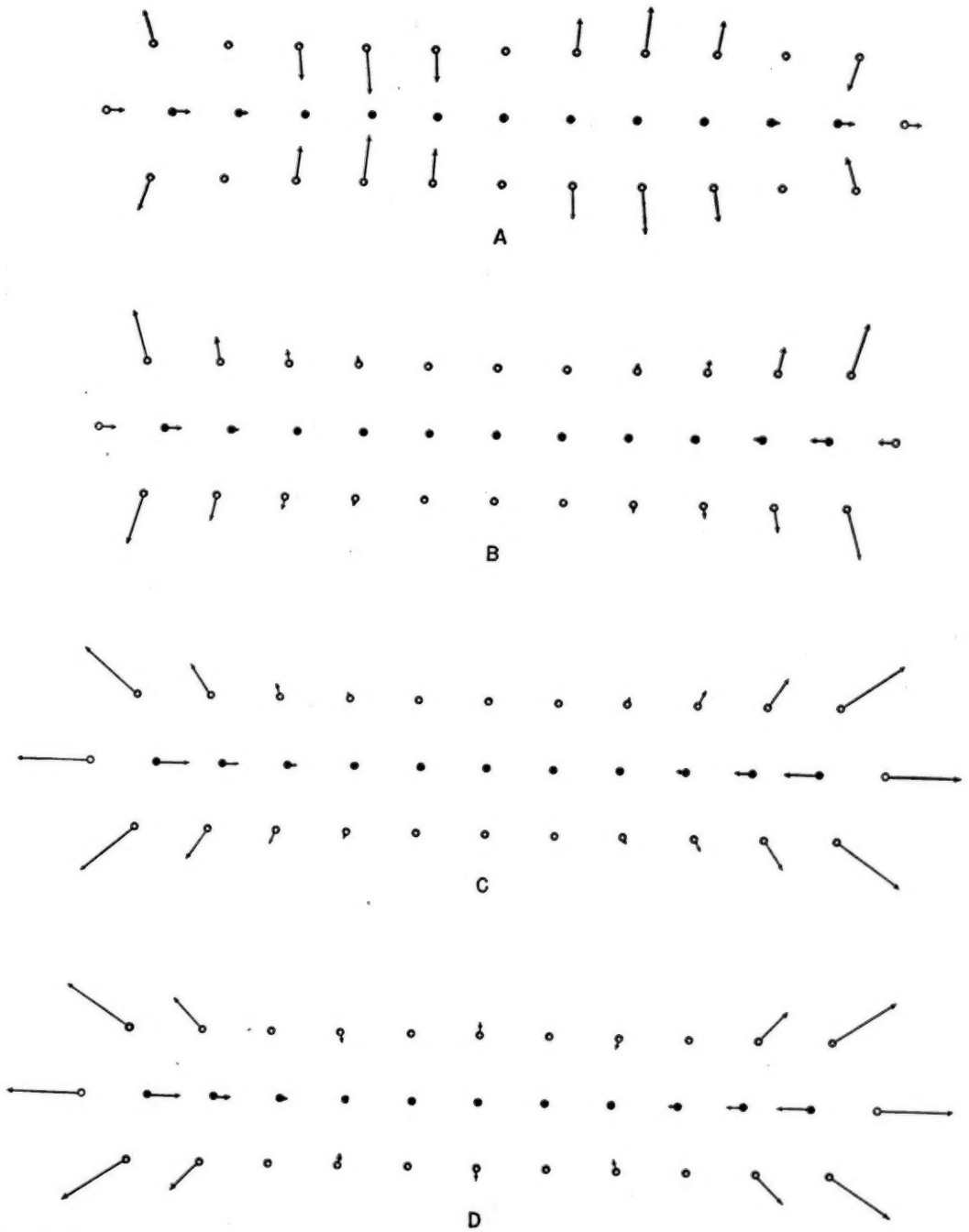

FIG. 1. These diagrams represent a chain molecule (e.g., undecane with black spots for C nuclei, open circles for H nuclei, looked at perpendicular to its length and parallel to the plane containing the C nuclei). The arrows represent (exaggerated) maximum displacements of the nuclei in certain normal modes of oscillation. (A) Represents a typical chain vibration ($\lambda = \pi/4$); (B) the last member of a set of m such modes, of which the frequency happens to lie outside the band of chain frequencies. (C) Represents a typical end vibration; (D) a similar mode of which the frequency happens to lie inside a band of chain frequencies. For (A) and (B) the displacements with amplitude varying trigonometrically or exponentially along the chain are most important, for (C) and (D) these are small compared with the displacements of mixed type near the end groups.

If a normal frequency does not lie in any of these bands, the corresponding mode must be compounded entirely of sets of terms with λ complex falling off exponentially from the ends towards the middle. Such modes will be termed *end vibrations*. (Fig. 1, C.)

In the simpler situations all the modes including translations and rotations of the whole chains are accounted for as follows: one end vibration with frequency near that of each internal vibration of an end group by itself, and one for each vibration of an end group relative to the chain, $q+s$ modes in all; and m modes for each of the r values of ω^2 satisfying (4). Of the latter all, except, for some end conditions, a few, are chain vibrations, a few may be end vibrations with only complex values of λ, the frequencies corresponding to which lie outside but near the bands of chain frequencies. (Fig. 1, B.) These modes have in the simplest cases just $0, 1, \cdots m-1$, nodes of amplitude along the chain; and when each involves but one real value of λ, these differ from one another, except near $\lambda=0$ and $\lambda=\pi$, by approximately π/m.

This simple situation may be complicated by the overlapping of bands by bands, (for links with symmetry, overlapping of bands for modes of different symmetry may be immaterial); or by what would otherwise be frequencies of end vibrations lying within bands, giving rise to chain vibrations with large end modifications. (Fig. 1, D.)

The procedure suggested for a long finite chain, then, is first to solve the equation $D=0$ for r values of ω^2 as functions of λ, essentially the problem of an infinite chain; secondly to solve the equations for a semi-infinite chain from each end with no amplitudes increasing exponentially away from the end, $lr+q$ or $lr+s$ homogeneous linear equations in as many amplitude coefficients, these provide first approximations to the end vibrations (which may in case of resonance or symmetry involve both ends), and, used as end conditions, fix more exactly the chain vibrations.

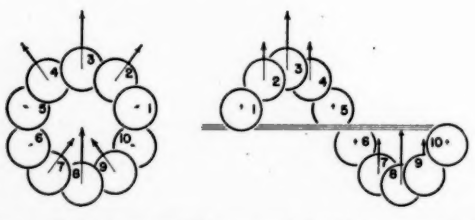

FIG. 2. This diagram illustrates how for a general chain molecule the electric moments perpendicular to the axis are in phase when $\lambda=\pm\theta$ (in this case $\pi/5$).

III. The Optical Activity of Chain Vibrations

The displacement from one member to the next in a chain of similar and similarly situated groups can always be regarded as made up of a translation along and a rotation of not more than two right angles about an axis with unique direction and unique position (unless the rotation vanishes). If this screw has sufficient pitch, chains of indefinite length should be possible. For a long chain molecule with many complete rotations from one end to the other, the axis of this screw may justly be called the axis of the molecule.

A chain vibration will give rise to bands observable in the infra-red only if the electric moments in any direction produced in the successive links are nearly in phase. For electric moment parallel to the axis this means $\lambda\approx 0$; for electric moment perpendicular to the axis $\lambda\approx\pm\theta$, where θ is the angle of rotation from one link to the next. (Fig. 2.) In the special case of no rotation from one group to the next we must have $\lambda\approx 0$ for the electric moment parallel to any direction in space.

If chain vibrations are given roughly by

$$b_{uh}=\sum_{\lambda} b_{u\lambda}\cos(h\lambda-\epsilon), \tag{6}$$

the electric moments for vibration parallel to the axis are proportional roughly to

$$\sum_{h=1}^{m}\sum_{\lambda} b_{u\lambda}\cos(h\lambda-\epsilon)=\sum_{\lambda} b_{u\lambda}\frac{\sin\frac{1}{2}m\lambda}{\sin\frac{1}{2}\lambda}\times\cos\{\tfrac{1}{2}(m+1)\lambda-\epsilon\}, \tag{7}$$

for vibration perpendicular to the axis at angle η to the initial direction from which rotations are measured, to

$$\sum_{h=1}^{m}\sum_{\lambda} b_{u\lambda}\cos(h\lambda-\epsilon)\cos(h\theta-\eta)=\sum_{\lambda} b_{u\lambda}\tfrac{1}{2}\left[\frac{\sin\frac{1}{2}m(\lambda+\theta)}{\sin\frac{1}{2}(\lambda+\theta)}\cos\{\tfrac{1}{2}(m+1)(\lambda+\theta)-(\eta+\epsilon)\}+\frac{\sin\frac{1}{2}m(\lambda-\theta)}{\sin\frac{1}{2}(\lambda-\theta)}\times\cos\{\tfrac{1}{2}(m+1)(\lambda-\theta)-(\epsilon-\eta)\}\right], \tag{8}$$

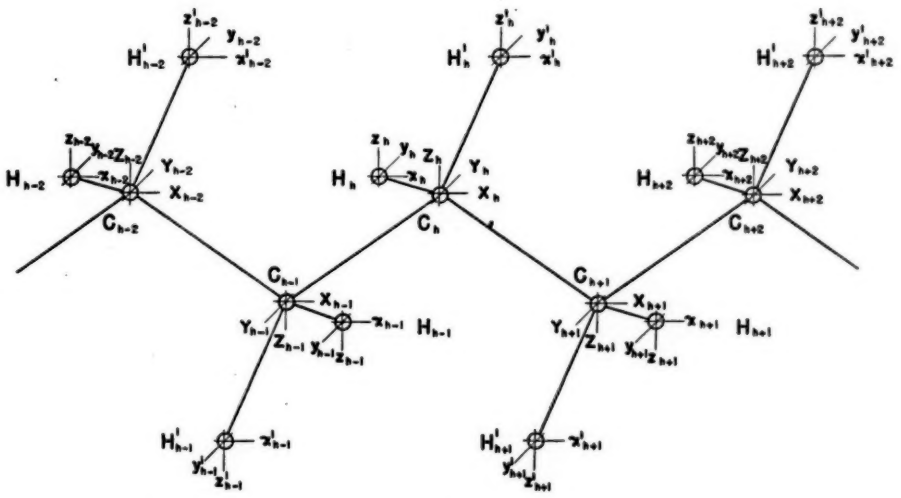

FIG. 3. The structure assumed for the straight chain paraffins.

where as λ varies, the energy of vibration remains nearly the same, of order of magnitude

$$\tfrac{1}{2}m\sum_{\lambda}\sum_{u}b_{u\lambda}{}^{2}\omega^{2}, \tag{9}$$

so long as there is at least one value of λ that is real and not too small.

As the values of λ depart from nearly the above values (0 or $\pm\theta$), the intensity of emission or absorption must fall off rapidly according to the first factors of the above expressions (7) and (8) like that in the diffraction pattern due to a slit. If the molecule is symmetrical end to end, the intensity is exactly zero for modes with an odd number of nodes of electric moment (this applies to C_nH_{2n+2} whether n is even or odd). If but one real λ is involved, changing in steps of π/m, the last factors have one value, $\cos\gamma$ say, for modes with an odd number of nodes of amplitude, and then $\sin\gamma$ for those with an even number of nodes.

If a mode corresponding to a root of $D=0$ is an end vibration, however, the energy of vibration for given $b_{u\lambda}$ may be much smaller than (9), while, for suitable end conditions, any component of electric moment may be appreciable, irrespective of θ.

To a first approximation the infra-red spectrum of such a molecule can therefore be predicted using only the solutions of $D=0$ for $\lambda=0$ for electric moment parallel to the axis and for $\lambda=\pm\theta$ for electric moment perpendicular to the axis, to obtain the frequencies due to chain vibrations. In addition, for suitable end conditions, end vibrations may occur giving frequencies near the limits of the bands of solutions of $D=0$, most usually for $\lambda=0$ or π. Only the $q+s$ modes properly belonging to the end groups are then left out of account.

IV. The Vibrations of Long Straight Chain Paraffins C_nH_{2n+2}

The model assumed for the structure of these members of the methane series consists of n carbon atoms lying along two parallel lines in a plane so that there is an angle of 2β between the C−C bonds of length b. The hydrogen atoms are assumed to be grouped in pairs in perpendicular planes through the carbon atoms, the angle between the C−H bonds of length a at each carbon atom being 2α. The end groups of the chain carry an additional hydrogen atom which is important only in the consideration of end conditions. The arrangement of five CH_2 groups near the middle of the chain is shown in Fig. 3.

We take coordinates X_h, Y_h, Z_h, for the displacements of the carbon atoms along one of the parallel lines, perpendicular to the plane containing the carbon atoms, and perpendicular to these away from the other parallel line, and x_h, y_h, z_h, and x_h', y_h', z_h', correspondingly for the hydrogen atoms of the hth. CH_2 groups. These coordinates are oriented as shown in Fig. 3 in

such a way that a rotation of the whole group through 180° about the parallel line and a translation along a C−C bond lead to the corresponding coordinates of an adjacent group. Thus the rotation angle θ of Section III is just π.

Taking the mass of a carbon atom as M and that of a hydrogen atom as m, the kinetic energy of the hth. CH_2 group is given by

$$\tfrac{1}{2}M(\dot{X}_h^2+\dot{Y}_h^2+\dot{Z}_h^2)+\tfrac{1}{2}m(\dot{x}_h^2+\dot{y}_h^2+\dot{z}_h^2 +\dot{x}_h'^2+\dot{y}_h'^2+\dot{z}_h'^2). \quad (10)$$

The potential energy is assumed to be that due to central forces; a linear combination of squares of the elongations of the distances between atoms. $q_1, q_2, \cdots q_{31}$, denote elongations of distances with equilibrium values as indicated in parentheses:

$q_1(H_h-C_h=a)$, $q_3(H_h-H_h'=2a\sin\alpha)$,
$q_4(C_h-C_{h+1}=b)$, $q_6(C_h-C_{h+2}=2b\sin\beta)$,
$q_8(H_h-C_{h+1}=d)$, $q_{16}(H_h-H_{h+2}=2b\sin\beta)$,
$q_{20}(H_h-C_{h+2}=c)$, $q_{28}(H_h-H_{h+2}'=f)$,

together with the analogous interactions of the other atoms. Here

$$c^2=a^2+4b^2\sin^2\beta,$$
$$d^2=a^2\sin^2\alpha+b^2\sin^2\beta+(a\cos\alpha+b\cos\beta)^2, \quad (11)$$
$$f^2=4a^2\sin^2\alpha+4b^2\sin^2\beta.$$

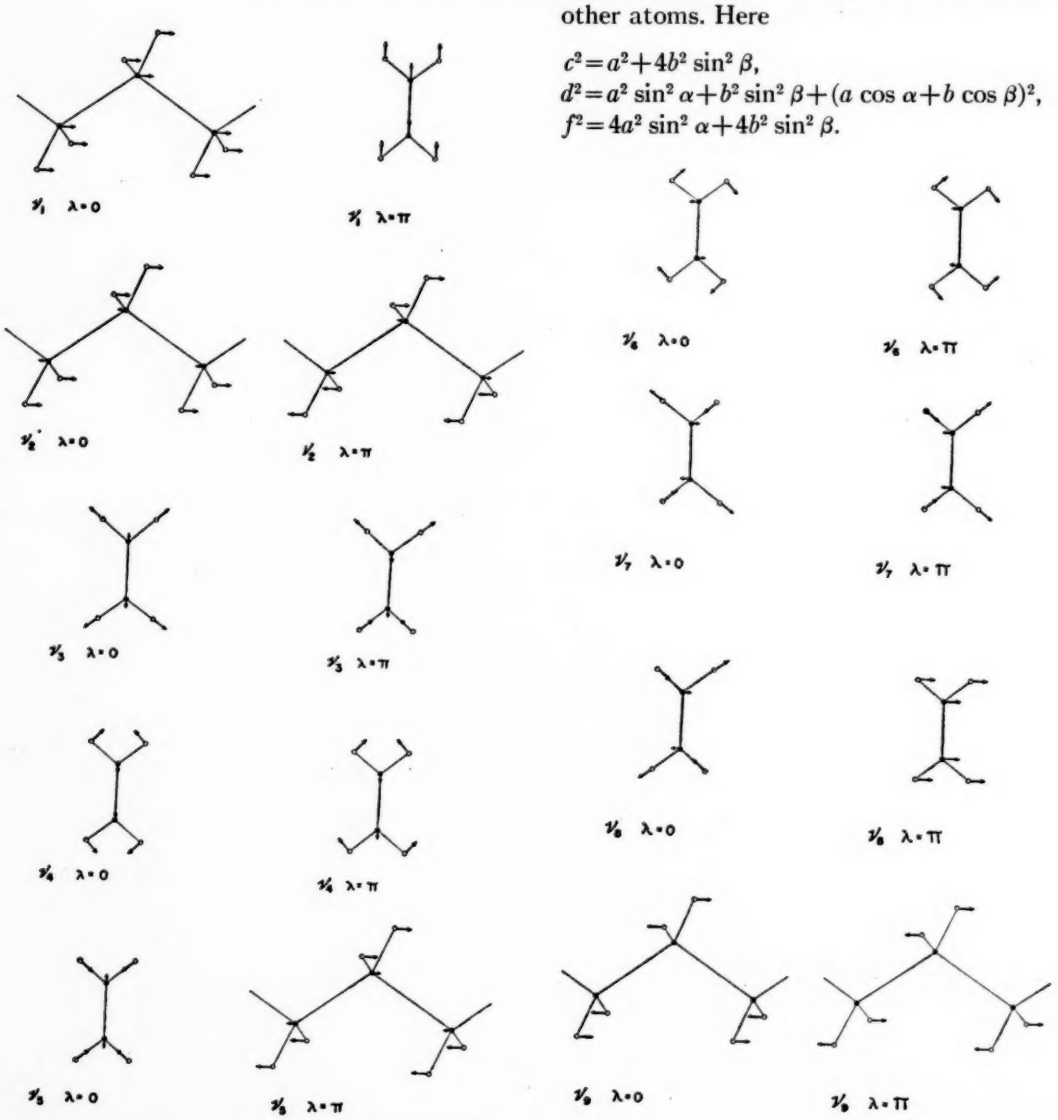

FIG. 4. These diagrams show the nature of the displacements of the atomic nuclei in the chain vibrations of undecane (and of other straight chain paraffins) with $\lambda=0$ or π. For motion perpendicular to the axis, e.g. ν_1, $\lambda=\pi$, a portion of the molecule is viewed along the axis; for motion parallel to the axis, e.g., ν_1, $\lambda=0$, the molecule is viewed nearly perpendicular to the plane containing the carbons, and three consecutive CH_2 groups are shown in projection.

The terms in the potential energy involving the coordinates of the hth. CH_2 group are taken to be

$$\tfrac{1}{2}[K_1(q_1^2+q_2^2)+K_3q_3^2+K_4(q_4^2+q_5^2)+K_6(q_6^2+q_7^2)+K_8\sum_{i=8}^{15}q_i^2+K_9\sum_{i=16}^{19}q_i^2+K_{10}\sum_{i=20}^{27}q_i^2+K_{11}\sum_{i=28}^{31}q_i^2]. \quad (12)$$

When the elongations are replaced by their values in terms of the coordinates, the equations of motion of the hth. CH_2 group, where h may take any value from 3 to $n-2$, can be written down.

We regard the motion in a normal mode with frequency ω as a combination of terms in which successive groups oscillate with phase-difference λ and so substitute in these equations of motion

$$X_h=Xe^{\iota(\omega t+\lambda h)}, \quad \cdots, \quad z_h'=z'e^{\iota(\omega t+\lambda h)}. \quad (13)$$

We thus obtain a set of nine homogeneous linear equations in $X, \cdots, z'$, involving ω, λ, and the angles, dimensions, and force constants. These will have nontrivial solutions if the determinant formed by the coefficients vanishes. This gives the Eq. (4) of the above general case. This ninth-order determinant may be simplified since X, $x+x'$, Z, $z+z'$, and $y-y'$, form a set of coordinates unchanged, Y, $y+y'$, $z-z'$, and $x-x'$, a set changed in sign, by reflection in the plane containing the carbon atoms. Accordingly a new determinant is formed taking rows and columns the proper sums and differences of those of the former to correspond to these new coordinates in the above order, giving

$$\begin{vmatrix}
-R+A_{11}, & A_{12}, & -\iota A_{13}, & -\iota A_{14}, & \iota A_{15}, & 0, & 0, & 0, & 0 \\
A_{21}, & -2r+A_{22}, & -\iota A_{23}, & 0, & \iota A_{25}, & 0, & 0, & 0, & 0 \\
\iota A_{31}, & \iota A_{32}, & -R+A_{33}, & A_{34}, & A_{35}, & 0, & 0, & 0, & 0 \\
\iota A_{41}, & 0, & A_{43}, & -2r+A_{44}, & A_{45}, & 0, & 0, & 0, & 0 \\
-\iota A_{51}, & -\iota A_{52}, & A_{53}, & A_{54}, & -2r+A_{55}, & 0, & 0, & 0, & 0 \\
0, & 0, & 0, & 0, & 0, & -R+A_{66}, & A_{67}, & A_{68}, & -\iota A_{69} \\
0, & 0, & 0, & 0, & 0, & A_{76}, & -2r+A_{77}, & A_{78}, & \iota A_{79} \\
0, & 0, & 0, & 0, & 0, & A_{86}, & A_{87}, & -2r+A_{88}, & 0 \\
0, & 0, & 0, & 0, & 0, & \iota A_{96} & -\iota A_{97}, & 0, & -2r+A_{99}
\end{vmatrix}=0, \quad (14)$$

where $R=\frac{1}{2}M\omega^2$, $r=\frac{1}{2}m\omega^2$, $A_{ij}=A_{ji}$, and with the abbreviations $k=(b/d)\sin\beta$, $l=(a/d)\sin\alpha$, $n=(a/d)\cos\alpha+(b/d)\cos\beta$, $p=(2b/c)\sin\beta$, $q=(a/c)\sin\alpha$, $s=(a/c)\cos\alpha$, $t=(2b/f)\sin\beta$, and $u=(2a/f)\sin\alpha$, we have

$$\begin{aligned}
A_{11}&=K_4\sin^2\beta(1-\cos\lambda)+2K_8k^2+2K_{10}p^2+K_6(1-\cos 2\lambda),\\
A_{22}&=2K_9(1-\cos 2\lambda)+2K_{11}t^2(1-\cos 2\lambda)+2K_8k^2+2K_{10}p^2,\\
A_{33}&=K_1\cos^2\alpha+K_4\cos^2\beta(1+\cos\lambda)+2K_8n^2+2K_{10}s^2,\\
A_{88}&=A_{44}=K_1\cos^2\alpha+2K_8n^2+2K_{10}s^2,\\
A_{55}&=K_1\sin^2\alpha+2K_3+2K_{11}u^2(1+\cos 2\lambda)+2K_8l^2+2K_{10}q^2,\\
A_{66}&=K_1\sin^2\alpha+2K_8l^2+2K_{10}q^2,\\
A_{77}&=K_1\sin^2\alpha+2K_8l^2+2K_{10}q^2+2K_{11}u^2(1-\cos 2\lambda),\\
A_{99}&=2K_9(1-\cos 2\lambda)+2K_{11}t^2(1+\cos 2\lambda)+2K_8k^2+2K_{10}p^2,\\
A_{12}&=-2K_8k^2\cos\lambda-2K_{10}p^2\cos 2\lambda,\\
A_{13}&=K_4\sin\beta\cos\beta\sin\lambda,\\
A_{14}&=2K_8kn\sin\lambda+2K_{10}ps\sin 2\lambda,\\
A_{15}&=2K_8kl\sin\lambda+2K_{10}pq\sin 2\lambda,\\
A_{23}&=2K_8kn\sin\lambda-2K_{10}ps\sin 2\lambda,\\
A_{25}&=2K_{11}tu\sin 2\lambda,\\
A_{34}&=-K_1\cos^2\alpha+2K_8n^2\cos\lambda-2K_{10}s^2\cos 2\lambda,\\
A_{68}&=A_{35}=K_1\sin\alpha\cos\alpha-2K_8ln\cos\lambda+2K_{10}qs\cos 2\lambda,\\
A_{78}&=A_{45}=-K_1\sin\alpha\cos\alpha-2K_8ln-2K_{10}qs,\\
A_{67}&=-K_1\sin^2\lambda+2K_8l^2\cos\lambda-2K_{10}q^2\cos 2\lambda,\\
A_{69}&=2K_8kl\sin\lambda-2K_{10}pq\sin 2\lambda,\\
A_{79}&=2K_{11}tu\sin\lambda.
\end{aligned} \quad (15)$$

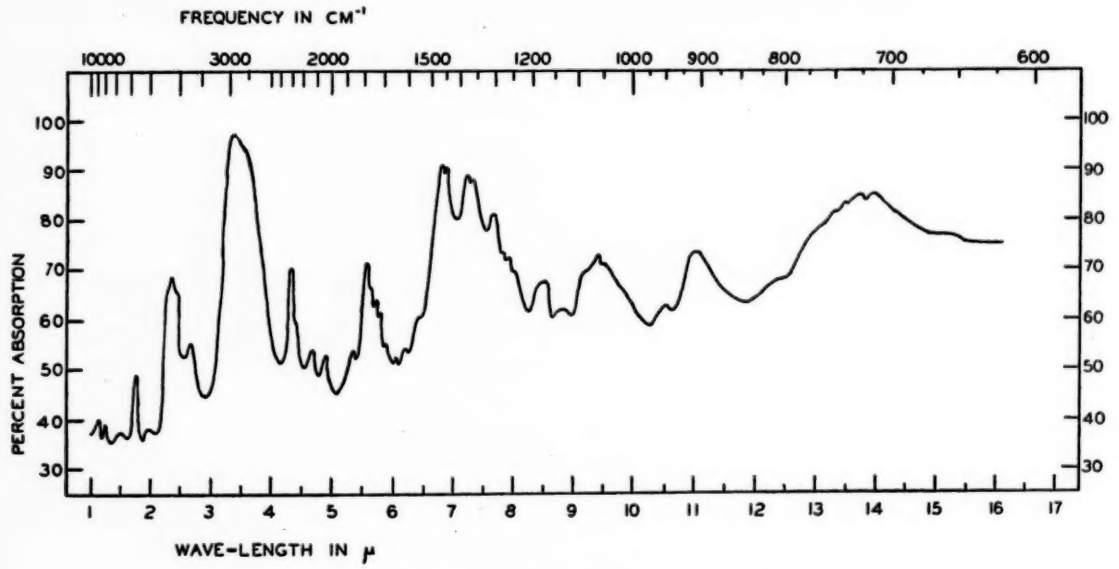

FIG. 5. The infra-red absorption spectrum of $C_{11}H_{24}$.

Thus the ninth-order determinant splits up for all values of λ into one fifth-order determinant and one fourth-order determinant. For the values $\lambda=0$ and $\lambda=\pi$, which are of special interest for the infra-red spectrum, the determinants split up further into one first-order, one second-order, and two third-order determinants. The corresponding *normal coordinates* have then the forms indicated in the second and last columns of Table II (see also Fig. 4). Those containing x coordinates for $\lambda\approx 0$ will correspond to optically active chain vibrations giving rise to parallel type bands, those containing y and z coordinates for $\lambda\approx\pi$ to perpendicular type bands.

There may also be end vibrations for frequencies near those found from (14) most probably for $\lambda\approx 0$, possibly for $\lambda\approx\pi$, or since $l=2$, possibly even for other values of λ, which could give rise either to parallel or to perpendicular type bands. The two zero frequencies for $\lambda=\pi$ correspond to translations of the whole molecule along and rotation about the y and z directions; the two for $\lambda=0$ to translation along and rotation about the axis (x direction).

V. Comparison of the Theory with the Experimental Results for $C_{11}H_{24}$

In order to test the above theory the infra-red spectrum of undecane, $C_{11}H_{24}$, has been measured in the region from 1 to 15μ. Undecane was selected because it has a chain long enough (nine CH_2 groups and two CH_3 groups) to make certain of its approximating an infinite chain, while it is still light enough to give a sufficient pressure of gas at fairly low temperatures.

The liquid undecane was vaporized by means of an oven surrounding the absorption cell. The spectrum was then measured on a Wadsworth-Littrow NaCl prism spectrometer of the type described by Strong and Randall.[13] The results are shown in Fig. 5, where the percentage of

TABLE I. *The infra-red absorption spectrum of undecane.*

Wave-Length μ	Frequency cm^{-1}	I	Wave-Length μ	Frequency cm^{-1}	I
1.11	9000	2	5.815	1720	2
1.183	8453	2	6.188	1616	1
1.446	6915	1	6.447	1551	3
1.780	5618	2	6.835	1463	9
1.950	5128	1	7.297	1370	8
2.305	4338	6	7.647	1308	5
2.410	4149	1	7.901	1266	3
2.668	3748	3	8.446	1184	5
3.397	2944	2	8.806	1136	3
3.600	2778	10	9.378	1066	8
4.310	2320	6	10.508	951.4	4
4.612	2168	2	11.023	907.2	8
4.875	2051	3	12.425	805.5	3
5.334	1875	3	13.310	751.3	6
5.535	1807	5	13.85	722.0	8
5.712	1751	3			

[13] Strong and Randall, Rev. Sci. Inst. **2**, 585 (1931).

absorption is plotted against the wave-length and frequency. The wave-lengths, frequencies, and estimated intensities of the vibration bands observed are given in Table I.

An attempt was made to measure the spectrum at a higher dispersion using a prism-grating spectrometer. However the complexities introduced by the rotational fine structure and by the overlapping of bands prevented this work from being of much value in the determination of the envelope structure. After measuring one of the four regions this work was abandoned.

In order to apply the theory to these results certain simplifications were made. It was assumed that the potential energy constants K_6, K_9, and K_{11}, are negligible and that K_8 and K_{10} are equal. The constants k, l, n, p, q, s, t, and u, were found by taking α and β each half the tetrahedral angle, i.e. $\alpha=\beta=55°$. The C–H distance, a, was taken to be 1.15A[14] and the C–C distance, b, to be 1.56A.[15] This gives the following values:

$c=2.8065$A, $d=2.2241$A, $f=3.1786$A,
$k=0.57551$, $l=0.42356$, $n=0.69957$, $p=0.91218$,
$q=0.33567$, $s=0.23503$, $t=0.80538$, $u=0.59274$.

Approximate values for K_1, K_4, and K_3, were found from the bands at 3000 cm^{-1}, 990 cm^{-1}, and 1600 cm^{-1}, which are found in all compounds of this type. The constant K_i is found by using the formula

$$\nu_i=(1/2\pi c)(K_i/\mu_i)^{\frac{1}{2}}, \tag{16}$$

where μ_i is the reduced mass of the vibrating group. These constants were used to make an assignment of the frequencies and then accurate values were found as follows, from (14) with $\lambda=0$ or $\lambda=\pi$,

K_8 and K_{10} from the parallel band at 1463 cm^{-1}, 0.46557×10^5 dynes/cm,
K_1 from the band at 2320 cm^{-1}, 2.19551×10^5 dynes/cm,
K_3 from the band at 2778 cm^{-1}, 1.04932×10^5 dynes/cm,
K_4 from the band at 907 cm^{-1}, 2.87614×10^5 dynes/cm.

Using these constants the values of the frequency were obtained for the cases $\lambda=0°$, 5°, 45°, 90°, 135°, 175°, and 180°. These values are given in Table II and are plotted in Fig. 6. There is little variation of the frequency with the phase except for those types of which the frequencies vanish for phases 0 and π.

We expect chain vibrations with the following frequencies to be optically active and to give rise to fundamental bands:

designation	$\nu_6(\pi\sigma)$	$\nu_4(\pi\sigma)$	$\nu_9(o\pi)$	$\nu_2(o\pi)$	$\nu_7(\pi\sigma)$	$\nu_5(\pi\sigma)$
frequency in cm^{-1}	385	1106	1354	1463	2320	2778

[14] Kistiakowsky, Phys. Rev. **45**, 4 (1934).
[15] Murison, Phil. Mag. **17**, 201 (1934).

TABLE II. *The roots of $D=0$.*

λ	0°	0°	5°	45°	90°	135°	175°	180°	180°
ν_1	$X+(x+x')$	0	75.72	456.80	423.10	229.08	0	0	$Z+(z+z')$
ν_4	$-\gamma_4'Z+\delta_4'(z+z')+\epsilon_4'(y-y')$	907.02	907.03	953.70	889.70	1076.59	1101.86	1105.65	$\gamma_4''\{\frac{6}{7}(z+z')-\frac{1}{7}Z\}+\epsilon_4''(y-y')$
ν_5	$\gamma_5'Z-\delta_5'(z+z')+\epsilon_5'(y-y')$	1038.32	1038.53	1062.10	1066.95	1115.97	1112.17	1106.71	$\alpha_5''X+\beta_5''(x+x')$
ν_2	$-\frac{1}{7}X+\frac{6}{7}(x+x')$	1463.00	1461.02	1360.60	1473.18	1398.94	1413.89	1416.03	$-\alpha_2''X+\beta_2''(x+x')$
ν_3	$\gamma_3'Z+\delta_3'(z+z')-\epsilon_3'(y-y')$	2751.94	2751.53	2756.48	2755.96	2770.44	2778.22	2778.00	$\gamma_3''\{\frac{6}{7}(z+z')-\frac{1}{7}Z\}-\epsilon_3''(y-y')$
ν_8	$\xi_8'Y+\zeta_8'(y+y')-\sigma_8'(z-z')$	0	19.32	172.25	267.90	151.61	0	0	$Y+(y+y')$
ν_6	$-\xi_6'Y+\zeta_6'(y+y')+\sigma_6'(z-z')$	604.20	603.13	585.65	513.50	399.23	385.30	385.21	$\xi_6''\{\frac{6}{7}(y+y')-\frac{1}{7}Y\}+\sigma_6''(z-z')$
ν_9	$x-x'$	1354.46	1354.57	1356.06	1359.67	1371.66	1354.88	1354.46	$x-x'$
ν_7	$\xi_7'Y-\zeta_7'(y+y')+\sigma_7'(z-z')$	2272.83	2272.78	2272.20	2276.30	2302.52	2319.75	2320.00	$\xi_7''\{\frac{6}{7}(y+y')-\frac{1}{7}Y\}-\sigma_7''(z-z')$

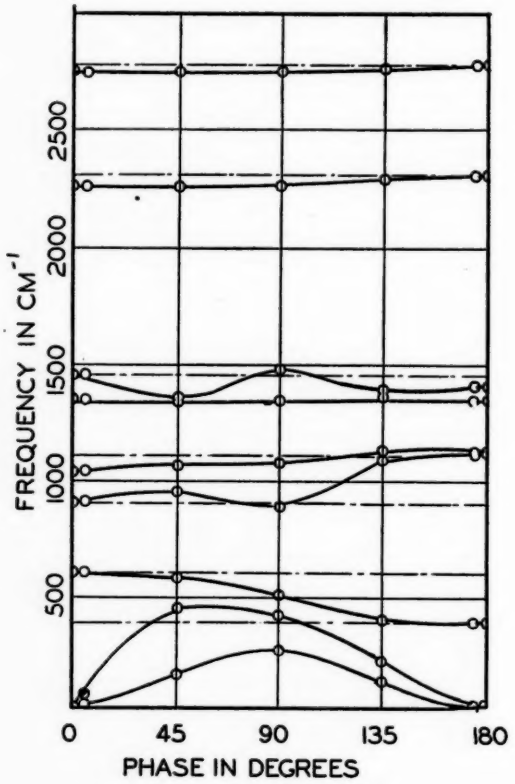

FIG. 6. The nine roots of $D=0$.

while end vibrations with the following frequencies may well exist, be optically active, and give fundamental bands:

designation	$\nu_6(o\sigma)$	$\nu_4(o\sigma)$	$\nu_5(o\sigma)$	$\nu_7(o\sigma)$	$\nu_3(o\sigma)$
frequency in cm^{-1}	604	907	1038	2273	2752

The number suffix in the above designations refers to the row of Table II and to Fig. 4, the first symbol in the parentheses gives the value of λ, either 0 or π, the second the type of band expected, either parallel, π, or perpendicular, σ.

As stated above the frequencies at 907, 1463, 2320, and 2778 cm^{-1}, were used to fix the force constants; the observed bands at 1066 and 1370 cm^{-1} are assumed to be those predicted at 1038 or 1106 and 1354 cm^{-1}. The envelope structure shows clearly that those at 1370 and 1463 cm^{-1} are of parallel type. The best comparison of the theory with experiment is found, however, in the consideration of the harmonic and combination bands. These bands are given in Table III and it is seen that, with the exception of three weak bands, all the bands are accounted for within five percent. In some cases more than one combination band seems to fit the observed frequency; wherever possible on the basis of intensity considerations, the most important band is indicated by an asterisk.

VI. CONCLUSIONS

The theory of the vibrations of long chain compounds as developed here seems capable of accounting completely for the infra-red spectrum of undecane, although the problem is incompletely solved because the end conditions have not been considered explicitly. The theory may be applied just as easily to the other straight chain hydrocarbons of the methane series. It is possible that it may also be applicable to the derivatives of the series, with modifications to take account of the added groups. A similar theory should explain the spectra of the cyclic hydrocarbons. The agreement of the observed and calculated results for undecane verifies the theory and substantiates the choice of dimensions and constants.

TABLE III. *Observed and calculated frequencies.*

Frequency, cm^{-1}				Frequency, cm^{-1}			
Obs.	Cal.	$\Delta\nu$	Designation	Obs.	Cal.	$\Delta\nu$	Designation
9000				1875	1876	− 1	$2\nu_6(\pi\sigma)+\nu_4(\pi\sigma)$
8433	8334	+99	$3\nu_3(\pi\sigma)$		*1848	+27	$\nu_6(\pi\sigma)+\nu_2(o\pi)$
6915	6960	−45	$3\nu_7(\pi\sigma)$	1807	*1814	− 7	$2\nu_4(o\sigma)$
	6910	+ 5	$2\nu_3(\pi\sigma)+\nu_9(o\pi)$		1812	− 5	$3\nu_6(o\sigma)$
5618	5556	+62	$2\nu_3(\pi\sigma)$		1808	− 1	$2\nu_6(\pi\sigma)+\nu_5(o\sigma)$
5128	5098	+30	$\nu_7(\pi\sigma)+\nu_3(\pi\sigma)$	1751	1739	+12	$\nu_6(\pi\sigma)+\nu_9(o\pi)$
4338	*4389	−51	$3\nu_2(o\pi)$	1720	1710	+10	$\nu_6(o\sigma)+\nu_4(\pi\sigma)$
	4280	+58	$2\nu_3(o\pi)+\nu_9(o\pi)$	1616	1642	−26	$\nu_6(o\sigma)+\nu_5(o\sigma)$
4149	4171	−22	$2\nu_9(o\pi)+\nu_2(o\pi)$	1551	1540	+11	$4\nu_6(\pi\sigma)$
	*4132	+17	$\nu_3(\pi\sigma)+\nu_9(o\pi)$	1463	1491	−28	$\nu_6(\pi\sigma)+\nu_4(\pi\sigma)$
3748	3816	−68	$\nu_5(o\sigma)+\nu_3(\pi\sigma)$		*1463	—	$\nu_2(o\pi)$
	*3783	−35	$\nu_2(o\pi)+\nu_7(\pi\sigma)$	1370	1374	− 4	$2\nu_6(\pi\sigma)+\nu_6(o\sigma)$
	3685	+63	$\nu_4(o\sigma)+\nu_3(\pi\sigma)$	1308	1354	−46	$\nu_9(o\pi)$
2944	*2926	+18	$2\nu_2(o\pi)$	1266	1292	−26	$\nu_4(o\sigma)+\nu_6(\pi\sigma)$
	2924	+20	$\nu_6(o\sigma)+\nu_7(\pi\sigma)$	1184	1208	−24	$2\nu_6(o\sigma)$
2778	2817	−39	$\nu_9(o\pi)+\nu_2(o\pi)$	1136	1155	−19	$3\nu_6(\pi\sigma)$
	*2778	—	$\nu_3(\pi\sigma)$	1066	*1106	−40	$\nu_4(\pi\sigma)$
	2721	+57	$3\nu_4(o\sigma)$		1038	+28	$\nu_5(o\sigma)$
2320	2370	−50	$\nu_4(o\sigma)+\nu_2(o\pi)$	951	989	−38	$\nu_6(\pi\sigma)+\nu_6(o\sigma)$
	*2320	—	$\nu_7(\pi\sigma)$	907	907	—	$\nu_4(o\sigma)$
	2314	+ 6	$2\nu_6(o\sigma)+\nu_4(\pi\sigma)$	805			
2168	2199	−31	$2\nu_4(o\sigma)+\nu_6(\pi\sigma)$	751	770	−19	$2\nu_6(\pi\sigma)$
	*2144	+24	$\nu_5(o\sigma)+\nu_4(\pi\sigma)$	722			
2051	2076	−25	$2\nu_5(o\sigma)$		604		$\nu_6(o\sigma)$
	2067	−16	$\nu_2(o\pi)+\nu_6(o\sigma)$		385		$\nu_6(\pi\sigma)$
	2013	+38	$\nu_4(o\sigma)+\nu_4(\pi\sigma)$				

Raman Spectra of Simple Ethers

FORREST F. CLEVELAND,* M. J. MURRAY,* HERSCHEL H. HANEY, AND JULIA SHACKELFORD,
Departments of Physics and Chemistry, Lynchburg College, Lynchburg, Virginia

(Received October 24, 1939)

Displacements, estimated intensities, and depolarization factors are listed for the main lines of diethyl ether, di-*n*-propyl ether, di-isopropyl ether, di-*n*-butyl ether, di-isobutyl ether, di-*n*-amyl ether, and di-isoamyl ether. All the frequencies in the 2900 cm^{-1} region are polarized, except the one near 2970 cm^{-1} which is, without exception, highly depolarized.

INTRODUCTION

WITH the exception of dimethyl and diethyl ethers, the Raman spectra of the simple ethers have not been subject to thorough investigation. High[1] reported data for the propyl and amyl ethers, but the data are obviously incomplete, probably due to the fact that he was interested in measuring the main lines for many related compounds rather than in a detailed study of any particular one. Since High apparently used unfiltered mercury light for excitation of the spectra, there also existed the possibility of inaccuracy in the data due to incorrect assignment of the exciting frequency. More recently, Cleveland and Murray[2] have published results obtained for di-*n*-butyl ether with a spectrograph having a rather low dispersion (40A/mm at 4500A). At the time the present investigation was begun, depolarization data were available only for dimethyl and diethyl ethers.

In view of this situation, it appeared worth while to undertake a systematic investigation of the simple ethyl, propyl, butyl and amyl ethers with the purpose of obtaining not only the displacements and estimated intensities, but also depolarization factors for the principal lines.

EXPERIMENTAL PROCEDURE

Light from a cylindrical Pyrex mercury arc[3] passes vertically upward through a filter solution contained in a glass tube (Wood's arrangement). The filter tube acts as a cylindrical lens and concentrates the light in a nearly parallel beam along the axis of the horizontal Raman tube. A plane mirror placed above the tube sends the light back through the liquid, thus nearly doubling the intensity of illumination. The wavelengths are measured by use of an iron comparison spectrum. The method used in the depolarization measurements and the characteristics of the spectrograph have been described elsewhere.[4]

The filters used were a solution of iodine in carbon tetrachloride when excitation was by Hg 4047A and an alcoholic solution of *p*-nitrotoluene and rhodamine 5 GDN Extra when excitation was by Hg 4358A. During the course of the investigation, it was found that the excellence of the filter used for isolating Hg 4358A made excitation by Hg 4047A superfluous. Consequently, excitation by Hg 4358A only was used for diethyl and di-isobutyl ethers.

TABLE I. *Raman spectrum of diethyl ether.*

PRESENT RESULTS			TABLES ANNUELLES*			PRESENT RESULTS			TABLES ANNUELLES*		
$\Delta\nu$ (cm^{-1})	I	ρ	$\Delta\nu$ (cm^{-1})	I	ρ	$\Delta\nu$ (cm^{-1})	I	ρ	$\Delta\nu$ (cm^{-1})	I	ρ
373	½	—	375	0	—	1272	2*b*	0.8	1275	2*b*	0.90
439	6	0.4	440	5	0.48	1452	6*b*		1453	5	0.89
496	½	—	497	1	—	1465	1	0.9	—	—	—
—	—	—	[544]	—	—	1480	½		—	—	—
830	2		—	—	—	2696	½	—	2694	1	—
842	4	0.4	843	8	0.29	2724	2	—	—	—	—
927	½	0.9	928	3*b*	0.61	2774	1	—	—	—	—
1035	1*b*	—	1033	3	—	2806	4	0.3	2805	5	—
1074	1	0.6	1080	0	—	2866	10*b*	0.3	2867	6*b*	0.30
1122	½	0.8	—	—	—	2898	3	—	—	—	—
1152	4*b*	0.4	1150	1	—	2935	10*b*	0.2	2932	10	0.20
						2979	8	0.9	2980	10	0.89

* M. Magat, *Tables Annuelles de Constantes et Données Numériques, Effet Raman* (Hermann & Cie., 1937), Volume XII, Chapter 26, page 37.

* Now at Armour Institute of Technology, Chicago Illinois.

[1] M. E. High, Phys. Rev. **38**, 1837 (1931).

[2] Forrest F. Cleveland and M. J. Murray, J. Chem. Phys. **5**, 752 (1937).

[3] Forrest F. Cleveland and M. J. Murray, Am. Phys. Teacher **5**, 271 (1937).

[4] Forrest F. Cleveland and M. J. Murray, J. Chem. Phys. **7**, 396 (1939).

All the ethers studied were carefully fractionated in a heated column using a high reflux ratio. Details regarding the samples used are as follows:

Diethyl ether. Dried over sodium. Boiling point, 34.2°–34.3°.

Di-n-propyl ether. Eastman product. Boiling point, 89.4°–89.6°.

Di-isopropyl ether. Eastman product. Boiling point, 67.5°–67.7°. Distilled over sodium.

Di-n-butyl ether. Eastman product. Boiling point 142°. Distilled over sodium.

Di-isobutyl ether. Synthesized from sodium isobutylate and isobutyl bromide. Boiling point 121°. (Product gave no action with sodium and showed a negative Beilstein test for halogen.)

Di-n-amyl ether. Eastman product. Boiling point, 68° at 12 mm pressure.

Di-isoamyl ether. Eastman product. Boiling point, 62° at 12 mm pressure.

TABLE II. *Raman spectra of propyl ethers.*

DI-NORMAL-					DI-ISO-				
PRESENT RESULTS			HIGH'S VALUES		PRESENT RESULTS			HIGH'S VALUES	
$\Delta\nu$ (cm^{-1})	I	ρ	$\Delta\nu$ (cm^{-1})	I	$\Delta\nu$ (cm^{-1})	I	ρ	$\Delta\nu$ (cm^{-1})	I
323	2	—	—	—	306	3	0.5	—	—
335	2	—	—	—					
408	4	0.6	—	—					
437	1	—	—	—					
478	2	—	—	—	492	4	0.1	—	—
852	2		—	—	794	6	0.2	791	6
870	2	0.6	874	2	848	1	0.8	848	2
890	3		—	—					
904	2		—	—	903	4	0.5	903	5
940	2*b*	0.8	—	—	930	2	0.9	930	1
989	1	—	—	—					
1027	2*b*	0.9	—	—					
1055	1*b*	—	—	—					
—	—	—	1091*	2					
1110	1*b*	—	—	—	1126	2*b*	0.7	—	—
1149	3	0.6	—	—	1158	2*b*	0.7	—	—
1243	2	—	—	—	1188	1*b*	—	—	—
1282	3	0.8	1282	3	1328	1	0.7	—	—
1298	1	—	—	—	1384	1	0.7	—	—
1433	4				1447	5			
1449	6	0.8	1446	4	1460	6	0.7	1453	8
1462	7				1476	2			
1482	4								
2737	2*b*	0.5	—	—	2721	1	—	—	—
2794	3*b*	0.4	—	—					
2839	2	—	—	—					
2854	8	0.3	2864	3	2874	7*b*	0.1	2872	9
2875	8								
2908	5	0.2	—	—	2919	8	0.1	2916	2
2935	10*b*		2931	3	2937	8		2929	9
2968	6	0.8	—	—	2976	10	0.9	2975	9
					—	—	—	3073†	1

* 1091(2)*kei* is probably 902*i*, 2858*k* and 1280*k*, respectively.
† 3073(1)*oq* is probably 485*k* and 2978*o*, respectively.

RESULTS

The results obtained for diethyl ether are given in Table I. The displacements appear in column one, estimated intensities in column two, and depolarization factors in column three. Columns four, five and six give for comparison the values listed in *Tables Annuelles.* Broad lines are designated by the letter *b* and data in regard to which there is some question are enclosed in brackets. The wider slit used in the depolarization measurements prevented resolution of some of the lines which were clearly resolved on the other plates. Such cases are indicated by joining the unresolved lines by a brace. Mercury lines (in angstroms) are referred to by letters in the

TABLE III. *Raman spectra of amyl ethers.*

DI-NORMAL-					DI-ISO-				
PRESENT RESULTS			HIGH'S VALUES		PRESENT RESULTS			HIGH'S VALUES	
$\Delta\nu$ (cm^{-1})	I	ρ	$\Delta\nu$ (cm^{-1})	I	$\Delta\nu$ (cm^{-1})	I	ρ	$\Delta\nu$ (cm^{-1})	I
310	1	—	—	—	421	1*b*	—	—	—
770	½*b*	—	764*	2	767	3	0.4	765	4
848	2	0.6	—	—	815	1	0.4	815	1
868	2		—	—	849	1		—	—
889	1	—	—	—	913	2*b*	0.6	908	1
907	1	—	—	—	953	2	0.7	950	3
					981	1		—	—
					996	1	0.8	—	—
1065	2*b*	0.7	—	—	1014	1		—	—
1116	2*b*	0.6	—	—	1128	3			
1148	2*b*	0.6	—	—	1139	3	0.6	1144	4
					1151	3			
					1170	3			
1203	1	—	—	—	1231	1	—	—	—
1295	2	0.8	1292	4	1301	3*b*	0.8	—	—
1306	2				1335	3*b*	0.8	—	—
1434	5								
1450	5	0.8	1447	7	1448	5			
1462	4				1463	5	0.7	1449	9
1483	3				1485	2			
2716	1	0.5	—	—	2763	1	0.4	—	—
2784	2	0.5	—	—	2797	1	0.5	—	—
2849	10	0.3	2853	5	2866	10	0.3	2862	7
2871	10				2904	5	0.4	2906	7
2904	8	0.4	2904	5	2932	5		—	—
2921	8	0.4	—	—	2953	6	0.8	2958	7
2941	8		—	—	2965	5			
2960	4	0.8	2957	5	—	—	—	3145†	½

* 764 may be due to the presence of di-isoamyl ether as an impurity.
† 3145*ko* is probably 2956*i* and 1444*m*, respectively.

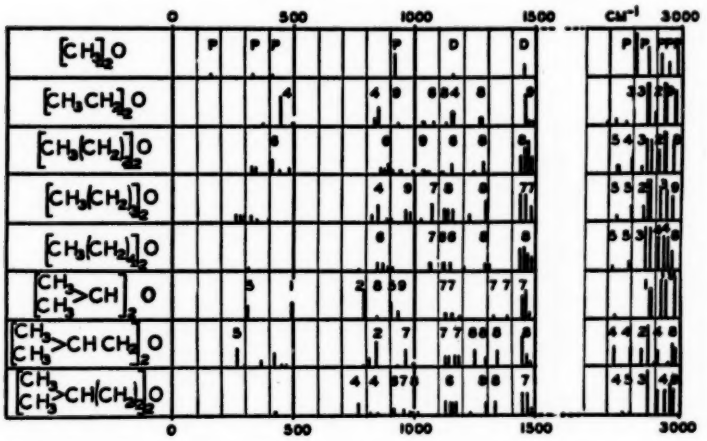

FIG. 1. Graphical summary of the Raman spectra of simple ethers, $R-O-R$.

tables, as follows:

$$e=4358,\quad f=4348,\quad k=4047,\quad i=4078,$$
$$m=3906,\quad o=3663,\quad \text{and}\quad q=3650.$$

The results obtained for the propyl and amyl ethers are compared with those reported by High[1] in Tables II and III. Table IV lists the results for the butyl ethers.

A graphical summary of the results for all the ethers concerned in this investigation is given in Fig. 1. The spectrum of dimethyl ether is included for sake of comparison. In this figure, the height of the line is proportional to its intensity and the depolarization factors are written near the lines. Decimal points have been omitted from the depolarization factors in order to simplify the diagram.

TABLE IV. *Raman spectra of butyl ethers.*

DI-NORMAL-			DI-ISO-			DI-NORMAL-			DI-ISO-		
$\Delta\nu$ (cm^{-1})	I	ρ	$\Delta\nu$ (cm^{-1})	I	ρ	$\Delta\nu$ (cm^{-1})	I	ρ	$\Delta\nu$ (cm^{-1})	I	ρ
262	2	—	263	4	0.5	1120	3		1123	3	
276	2	—				1137	3	0.8	1137	3	0.7
294	2	—	299	1	—	1156	3		1168	3	
319	2	—							1181	3	0.7
346	1	—	362	2	—	1228	2	—	1249	4	0.8
398	1	—	418	3	—	1300	5	0.8	1294	2	0.8
			450	1	—				1339	4	0.8
			467	1	—	1439	6	0.7	1448	7	
820	2	—	789	½	—	1459	6		1461	3	0.8
844	4	0.4	810	2	—	1484	3	0.7	1478	2	
882	1	—	836	6	0.2	2732	2	0.5	2718	3	0.4
900	1	—	930	½	—	2798	3	0.5	2793	3	0.4
961	3					2849	3	—	2837	3	—
979	2	0.9	958	4	0.7	2864	10		2866	10	0.2
1026	1	—	1001	1	—	2876	10	0.2	[2891]	1	—
1068	4	0.7				2912	8		2905	3	
						2941	8	0.3	2952	1	0.4
						2967	6	0.9	2963	4	
									2975	3	0.8

DISCUSSION OF RESULTS

The most intense lines in the Raman spectra of the simple ethers are those corresponding to the C−H vibration frequencies near 2900 cm^{-1}. The C−H deformation frequencies near 1450 cm^{-1} are also relatively strong and are highly depolarized. It is interesting to note that no lines appear between 500 and 700 cm^{-1}. This is true also for the aliphatic alcohols and for many aliphatic hydrocarbons.

Assuming that, to a first approximation, the methyl group in the ethers may be regarded as having a pyramidal structure independent of the remainder of the molecule, one would expect this group to have four frequencies: Two of these will be deformation frequencies, in one of which ($\delta_{\parallel}$) the change in electric moment is parallel to the symmetry axis, while in the other ($\delta_{\perp}$) the change in electric moment is perpendicular to the symmetry axis. The other two frequencies will be vibration frequencies in which the change in electric moment is parallel ($\nu_{\parallel}$) and perpendicular ($\nu_{\perp}$), respectively, to the symmetry axis. The former will be polarized, the latter depolarized.

$\nu_{\parallel}$ is believed to be the frequency near 2930 cm^{-1} which is polarized, while $\nu_{\perp}$ is believed to be the frequency near 2970 cm^{-1} which is depolarized. These assignments are in agreement

TABLE V. C−H *vibration frequencies.*

ETHER	$-CH_3$		$-CH_2-$?
	$\nu_{\parallel}$	$\nu_{\perp}$	$\nu_{\parallel}$
Diethyl	2935(10*b*).2	2979(8).9	2866(10*b*).3
Di-*n*-propyl	2935(10*b*).2	2968(6).8	*2865(8).3
Di-*n*-butyl	*2927(8).3	2967(6).9	*2870(10).2
Di-*n*-amyl	*2931(8).4	2960(4).8	*2860(10).3
Di-isopropyl	*2928(8).1	2976(10).9	2874(7*b*).1
Di-isobutyl	*2929(2).4	*2969(3).8	2866(10).2
Di-isoamyl	2932(5).4	*2959(5).8	2866(10).3

* Mean of the doublet, which is presumably due to Fermi resonance interaction.

with those made by Crawford for methylacetylene[5] and dimethylacetylene[6] and by Crawford, Avery and Linnett[7] for ethane.

The $-CH_2-$ group may be considered, roughly, as a triangular molecule with inner vibrations as follows: A polarized deformation frequency ($\delta_{\parallel}$) and two vibration frequencies, one strong and polarized ($\nu_{\parallel}$), the other weak and depolarized ($\nu_{\perp}$). The former ($\nu_{\parallel}$) may be the strong polarized frequency observed at 2866 cm^{-1}. On the other hand, this frequency appears in dimethyl ether,[8] methylacetylene, and dimethylacetylene which contain no methylene groups. It is assigned by Crawford *et al.*, in these cases, however, as an overtone of 1446 cm^{-1}. Only one depolarized frequency was observed, except for di-isobutyl and di-isoamyl ethers where the depolarized line appears double. It is conceivable that $\nu_{\perp}$ for the CH_2 group may coincide with $\nu_{\perp}$ for the CH_3 group or may be close to some other line and, being weak, not be observable as a depolarized line.

The values of the three frequencies, tentatively assigned above, are collected in Table V. The selection of doublets is somewhat arbitrary, especially in the case of the amyl ethers, but the constancy of the frequencies seems to justify the choice made. It should be noted that lines unresolved on the depolarization film and indicated by the braces in Tables I–IV are not necessarily those considered as resonance doublets in Table V.

ACKNOWLEDGMENTS

It is a pleasure to acknowledge grants in aid of this research program by the American Association for the Advancement of Science, Sigma Xi, and the Virginia Academy of Science.

[5] Bryce L. Crawford, Jr., J. Chem. Phys. **7**, 140 (1939).
[6] Bryce L. Crawford, Jr., J. Chem. Phys. **7**, 555 (1939).
[7] Bryce L. Crawford, Jr., William H. Avery and J. W. Linnett, J. Chem. Phys. **6**, 682 (1938).
[8] Bryce L. Crawford, Jr. and Lois Joyce, J. Chem. Phys. **7**, 307 (1939).

The Absorption Coefficient of Nitrogen Dioxide in the Visible Spectrum

J. K. Dixon
Physics Laboratory, Calco Chemical Division, American Cyanamid Company, Bound Brook, New Jersey
(Received October 30, 1939)

The absorption coefficient of nitrogen dioxide in the visible spectrum has been measured at pressures up to 70 mm Hg with a 40A spectrophotometer slit. Beer's law is obeyed in this region. The transmission as measured when using a tungsten source, is the same as that obtained with either a high or low pressure mercury arc, except at the 4339–4358A group of mercury lines, where the absorption coefficient was found to be 15 percent greater with the mercury source. The absorption coefficient curve obtained with either a 40A or 15A slit is essentially sinusoidal in appearance, the absorption maxima and minima generally differing by about 10 percent in intensity. The maxima are separated by 700 ± 100 cm^{-1}. They appear to be due, not to the ground state of the molecule, but to groups of excited levels which are uniformly separated.

Introduction

THE visible absorption spectrum of nitrogen dioxide has been studied in some detail in the past by a number of workers.[1] Curry and Herzberg[1] have described briefly some features of the numerous bands which extend from 8900A to the ultraviolet and presented an interpretation of some of these bands. Daniels and Holmes[2] reported measurements on the absorption coefficient at 4030 and 4359A in connection with similar measurements for several of the oxides of nitrogen. Since we have had occasion to measure the absorption coefficient at all wave-lengths in the visible spectrum with considerable accuracy, it has seemed desirable to record the values obtained and also to present several interesting features of the spectrum which hitherto do not appear to have been described.

Experimental Method

Nitrogen dioxide was generated by heating C.P. lead nitrate. The gas was dried by passing over phosphorous pentoxide and condensed in a suitable trap. The gas was freed of gaseous impurities by repeated freezing and evacuation. It was colorless on freezing.

Equipment for carrying out the work was constructed throughout of Pyrex glass. The supply of nitrogen dioxide was connected by means of capillary tubing and stopcocks to the oil pump, a one-liter storage flask, a source of dry carbon dioxide free air, a mercury manometer, an oil manometer, and an all-glass photometric absorption cell. The manometers, which were constructed of capillary tubing, were evacuated on one side.

The entire apparatus was mounted so that it could be moved as a unit, thus permitting placing of the glass absorption cell in position for measurement in a General Electric recording spectrophotometer.[3] The length of the cell was measured and found to be 5.01 ± 0.03 cm. Photometric measurements were made *versus* a similar cell of the same length filled with air. It was possible to check the operation of the machine by calibration for percentage transmission *versus* a clear glass filter and a gray glass filter.* The wave-length calibration was made with a mercury arc.

After generating and evacuating a supply of nitrogen dioxide in the trap, air was admitted to the storage flask to a definite pressure and nitrogen dioxide then allowed to enter from the trap to increase the pressure in the flask by some desired amount. The storage flask was shut off from the rest of the system, the latter evacuated and then filled to a measured pressure with the mixture. By leaving air in the capillary manometer, attack of the mercury and oil by nitrogen

[1] Curry and Herzberg, Nature **131**, 842 (1933); L. Harris, Proc. Nat. Acad. Sci. **14**, 693 (1928); Carwile, Astrophys. J. **67**, 184 (1928).
[2] Daniels and Holmes, J. Am. Chem. Soc. **56**, 630 (1934).
[3] Michaelson and Liebhafsky, Gen. Elec. Rev. **39**, 445 (1936).
* These filters had been checked against the National Bureau of Standards' filters.

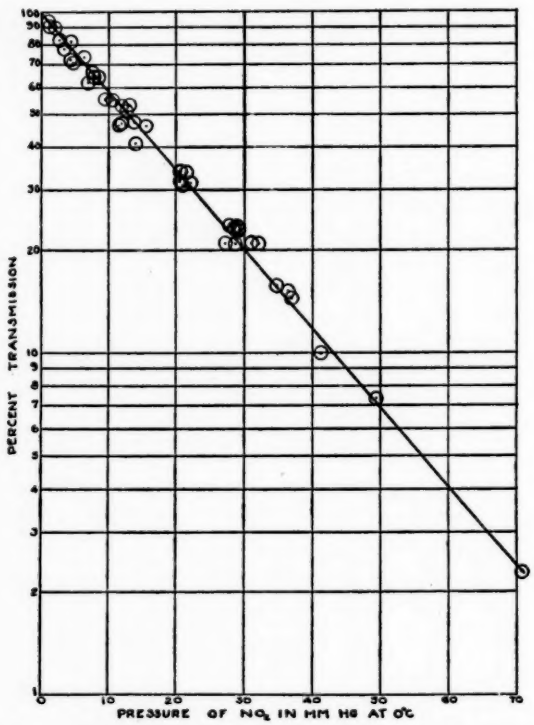

FIG. 1. Absorption of light by NO_2. Cell length 5.01 ± 0.03 cm tungsten source, wave-length 4850A, slit 40A.

dioxide was effectively eliminated. The temperatures of the absorption cell and storage flask were recorded. The entire visible range absorption curve of the gas in the absorption cell was then obtained. The storage flask and system were pumped down to a lower pressure and the same set of data was obtained again, thus permitting a number of measurements to be made at successively lower pressures on one mixture. In some of the later series of runs, no air was admitted to the system and nitrogen dioxide pressures were obtained from readings of the oil manometer alone.

In some cases, the order of addition of the air and nitrogen dioxide was reversed to reveal any errors of procedure, but no effect was observed.

Calculation of Results and Errors

Manometer readings were corrected to mm of mercury at 0°C.[4]

The pressure of nitrogen dioxide was calculated from the measured pressure, which was equivalent to the sum $NO_2+N_2O_4$, by using the equilibrium constants given by Verhoek and Daniels.[5] In the dilute concentrations employed, N_2O_4 was usually some 85 percent–95 percent dissociated, hence errors of ± 0.5°C in temperature measurement were negligible. Although no extreme precautions were taken to obtain exact equilibrium, it was possible to check the vapor pressure measurements of Giauque and Kemp,[6] in the range from 20 to 40 mm with an accuracy of ± 10 percent. In this connection, it should be noted that these workers did not report measurements below 20 mm, but it has been found that one may safely extrapolate their curve to probably 5 mm, thus supplementing the rather uncertain values in the literature.[7]

In the blue and green portions of the visible spectrum nitrogen dioxide transmitted only a few percent of the light at 70 mm pressure and more than 80 percent at less than 4 mm. It was difficult to measure the absolute percentage absorption to better than 1 percent, thus making the error of the order of 1 part in 10 for 10 percent absorption and proportionately less at higher absorption values. In order to illustrate the randomness of the results, the percentage transmission at 4850A has been plotted in Fig. 1 on a semi-log scale against pressure of NO_2 (reduced to mm of Hg at 0°C) for measurements in six different series of runs. It is believed that the results of different series of runs are in satisfactory agreement since the standard deviation of the logarithm of the transmission for the individual points from the line shown is only 0.035.[8]

Validity of Beer's law would require a straight line in Fig. 1. This type of curve appears to fit the data quite well since the computed estimate of standard deviation of the slope is 1.5 percent. The straight line may reasonably be extrapolated into the region from 90 percent to 100 percent transmission in order to establish the transmission with more accuracy than obtained by drawing the best curve through the experimental data in this region.*

[4] Int. Crit. Tab., Vol. I, p. 69.

[5] Verhoek and Daniels, J. Am. Chem. Soc. **53**, 1250 (1931).

[6] Giauque and Kemp, J. Chem. Phys. **6**, 40 (1938).

[7] Int. Crit. Tab., Vol. III, p. 207.

[8] P. R. Rider, *Statistical Methods* (John Wiley & Sons, 1939), Chap. IV.

* Some points below 10 mm pressure are omitted for purposes of clarity only. All points have been used in estimating errors quoted above.

It was also easily shown that Beer's law is valid at all wave-lengths as well as at 4850A. This was true with an error less than 5 percent in absorption coefficient at all wave-lengths provided the absorption was greater than 10 percent, below which figure photometric errors began to increase rapidly.

Experimental Results

The slope of the transmission curve at 4850A (Fig. 1) was used to establish the absorption coefficient at this wave-length. The General Electric spectrophotometer establishes the transmission relative to that at any one particular wave-length with considerable accuracy, hence the transmission values at all wave-lengths were easily determined by averaging a large number of curves and then comparing the absorption at any wave-length for the average curve with the value at 4850A. In the relation (percent transmission/100) $= t = 10^{-kpl}$

p = pressure of NO_2 corrected from the temperature of measurement to 0°C in mm of Hg.
l = cell length in cm.
k = absorption coefficient, mm $Hg^{-1} \times cm.^{-1}$.

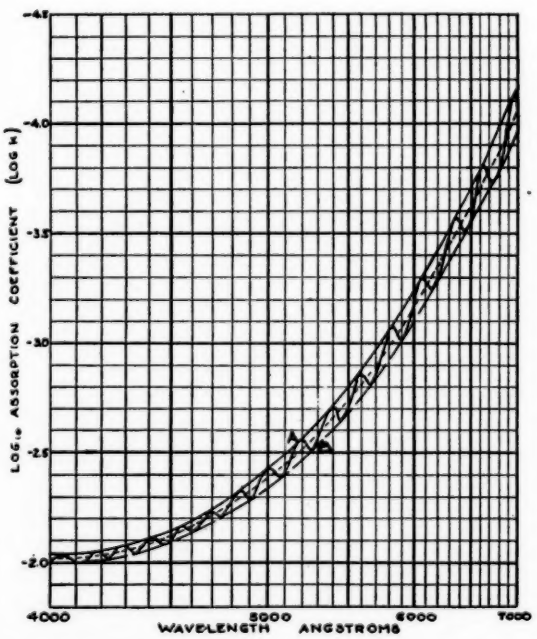

Fig. 2. Probable best value for absorption coefficient of NO_2. Slit 40A, percent transmission/100 $= t = 10^{-kpL}$, p in mm Hg: L in cm. k in 1/mm Hg×cm.

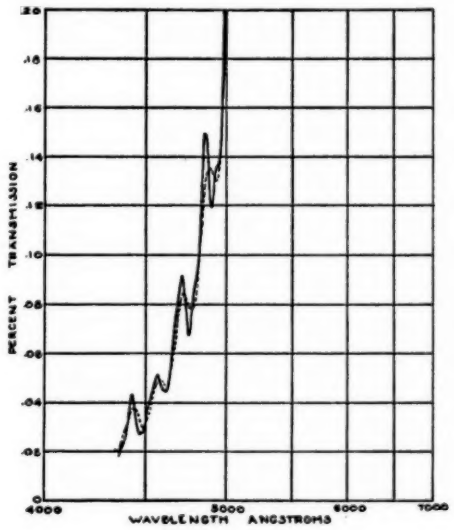

Fig. 3. Slit width effect. ———— slit 15A, - - - - - - slit 40A.

Values of $\log_{10} k$ are plotted against wave-length in Fig. 2.

The curve shown was obtained with a slit width equivalent to approximately 40A. When the slit width was decreased to approximately 15A, the vertical spread between the maxima and minima was doubled.

The appearance of the curve was not affected by fairly wide variations in the plotting speed or direction of plotting, nor was it changed by heating the gas to 85°C. It was also shown that the peaks and valleys were not due to fairly rapid time fluctuations since the transmission did not change with time.

Since the spectrophotometer can be operated so that it plots the percentage transmission with fivefold greater scale, it seems desirable to present a trace of actual absorption curves obtained by this method at two different slit widths; namely, about 40 and 15A. Fig. 3 records these absorption curves which give the percentage transmission *versus* wave-length in angstroms, and illustrates qualitatively how the maxima and minima were spread when the slit width was decreased. With the narrower slit width used in Fig. 3; namely, 15A, further fine structure in the bands begins to be evident and with a finer slit a large number of absorption bands were observed which were in agreement with those evident in

TABLE I. *Absorption coefficient of* NO_2.

WAVE-LENGTH, A	k (DANIELS & HOLMES)*	k (THIS WORK)*
4050 (mercury source)	0.00936	0.0093
(tungsten source)	—	0.0093
4359 (tungsten)	—	0.0085
4359 (mercury arc)	0.00833	—
4339–4359A (mercury arc)	—	0.0098

* (% transmission/100) $= 10^{-kpl}$ (see text).

photographs published in the literature.[9] With a slit of 40A the absorption coefficient curve is that which is shown in Fig. 2 (full line). For wider slits the absorption curve would approach the average (dotted curve). It is likely that in most photochemical or analytical work, this curve will be most useful.

Data available in the literature have been concerned chiefly with the absorption coefficients as measured with discrete line sources. In view of the known fine structure of the spectrum it is evident that agreement between different sources and slit widths should not be expected. However, it seemed of interest to establish the extent of this difference. A low pressure mercury source was first tried out in the spectrophotometer. Within the experimental accuracy of about ± 1 percent in the absorption coefficient, the absorption was the same as with the tungsten source at the wave-lengths of the 4050, 5460 and 5780A mercury lines. On the other hand at the 4339–4358A group, the absorption coefficient was 15 percent higher with the mercury arc than with the tungsten source. The same state of affairs existed on using a high pressure arc as source, for which source there is a broadening of the mercury lines (between which there is a strong continuum).[10]

These results are summarized in Table I.

The absorption coefficients shown in Fig. 2 may be utilized, with due regard to the effect of slit width, for a continuous source and for a mercury arc at its principal visible lines except for the group at 4339–4358A. In the latter case, it is suggested that a value of $k=0.0098$, as determined in this work, be employed. With the 4359A mercury line as source, it seems desirable to use $k=0.0083$, the value of Daniels. In cases where other sources with discrete spectra are employed it would be advisable to determine the absorption coefficient since otherwise there appears to be no certainty that the curve of Fig. 2 is applicable.

The absorption maxima differ on the average by 700 ± 100 cm^{-1} and those for the minima by the same amount. The average difference between adjacent maxima and minima are 250 ± 50 cm^{-1}. In view of the complexity of each peak or valley, it is not desirable to stress intensity relationships, but it is notable that for the curve of Fig. 2, the absorption coefficient at a peak such as A in Fig. 2 is approximately 90 percent of that at the valley B over the entire curve.

The ratio of absorption coefficients for any two adjacent absorption maxima in Fig. 2 is greater than 0.5. If the uniform difference of 700 cm^{-1} between any two bands is due to transitions from two adjacent ground state levels to a common upper vibration level, then the intensity ratio for two adjacent peaks can be calculated with aid of Boltzmann's law, assuming equal statistical weights, to be 0.03. Since the observed ratio is so much greater and, furthermore, because of the lack of any observable temperature coefficient, it is concluded that the constant differences which are observed are to be attributed to excited vibrational levels which tend to group themselves in such a way that the groups are separated by constant energy increments. Curry and Herzberg[1] stated that they were able to follow a series of bands in the visible, which were separated by 740 cm^{-1}. Very probably the band groups which have shown up in this work with a separation of 700 ± 100 cm^{-1} can be identified with their frequency difference. Although the absorption maxima are found to be fairly complex, the envelope of the bands gives the simple picture shown in Fig. 2 in which the maxima are regularly spaced. It also appears to be significant that the progression of band groups is such as to give a minimum of absorption roughly 250 cm^{-1} from the maximum and with an intensity 90 percent as great, for all peaks.

The advice and help of several members of the Physics Laboratory are gratefully acknowledged.

[9] Melvin and Wulf, J. Chem. Phys. **3**, 755 (1935).
[10] B. T. Barnes, J. Opt. Soc. Am. **27**, 83 (1937).

The Determination of Internuclear Distances and of Dissociation Energies from Force Constants

G. B. B. M. SUTHERLAND*
Pembroke College, Cambridge, England

(Received August 23, 1939)

With a view to obtaining the internuclear distances and dissociation energies of individual bonds in polyatomic molecules purely from a knowledge of force constants the consequences of assuming that the potential energy of any di-atom may be expressed in the form $V=-\alpha/r^m+\beta/r^n$ have been further investigated. In addition to giving a relation between internuclear distance and force constant of the form suggested empirically by Badger, this assumption leads to a relation between force constant (k_e), internuclear distance (r_e) and dissociation energy (D_e) of the form $D_e=(k_e r_e^2)/mn$. It is found that such a relation does exist between those quantities for series of diatomic molecules belonging to the same row in the periodic table, provided one uses an "effective" internuclear distance r_e-d_{ij}. This was also used by Badger in his relation of force constant to internuclear distance and the values of d_{ij} obtained by the two different methods are in reasonably good agreement. The values obtained for the product mn are 4, 6.2, 6.2 and 10.8 for the respective series LiH to FH, Li_2 to F_2, Na_2 to Cl_2 and K_2 to Br_2. For the hydrides it would seem that $-\alpha/r+\beta/r^4$ is the correct form with β varying along the series. It is also shown that this function leads to a relation between the shift in frequency $\delta\nu$ and the change in bond energy δD in the formation of a hydrogen bond.

IT has been clear for some time that unless some very striking advance is made in the direction of obtaining higher resolving power in the infra-red, the future application of vibration spectra to problems of molecular structure will be largely concerned with the interpretation and use of force constants derived from purely vibrational data. Indeed for complex molecules, even if the rotational fine structure of the bands could be obtained, the resulting information on the three principal moments of inertia would be of little value since the various internuclear distances could not be obtained and it is the internuclear distance which is now recognized as the most important characteristic of a chemical bond. For this reason the various attempts[1] which have recently been made to establish an empirical relation between the length of a bond and its force constant are of considerable interest and importance. The fact that a relation should exist at all between these two quantities for series of related di-atoms indicates that the potential energy curves must have certain common features. It was with this in view that the present author proposed[2] that the potential might be represented by a simple function of the form

$$V=-\frac{\alpha}{r^m}+\frac{\beta}{r^n}. \tag{1}$$

From such an assumption it is easy to derive that the following relations should hold between the equilibrium internuclear distance, (r_e) the force constant (k_e) and the dissociation energy (D_e):

$$k_e=\frac{m\alpha(n-m)}{r_e^{m+2}}=\frac{n\beta(n-m)}{r_e^{n+2}}, \tag{2}$$

$$D_e=\frac{k_e r_e^2}{mn}. \tag{3}$$

The purpose of the present paper is to investigate a little more fully the consequences of such an assumption and the relation of the above equations to the observed facts.

We have essentially two different empirical proposals for the connection between internuclear distance and force constant, that of Badger *viz.*

$$k_e=\frac{C_{ij}}{(r_e-d_{ij})^3} \tag{4}$$

and that of Douglas Clark, and Allen and

* Leverhulme Fellow.

[1] Badger, J. Chem. Phys. **2**, 128 (1934), **3**, 710 (1935); Douglas Clark, Phil. Mag. **18**, 459 (1934); D. Clark and J. L. Stoves, *ibid.* **22**, 1137 (1936), **27**, 389 (1939); Huggins, J. Chem. Phys. **3**, 473 (1935), **4**, 308 (1936).

[2] Sutherland, Proc. Ind. Acad. Sci. **8**, 341 (1938).

Longair *viz.*[3]

$$k_e=\frac{C_{ij}'}{Nr_e^6}. \qquad (5)$$

In order to correlate our theoretical relation (2) with one of these findings we must decide that either m or n is constant for a series of molecules made up from atoms in fixed rows of the periodic table. Remembering that n must be greater than m the most likely alternatives are $m=1$ or $n=4$. The former would give agreement with Badger's relation provided we write the potential function with an effective rather than a true internuclear distance. It would also imply that α and n are constant and that only β varies as we go from one member to another in the series of related molecules. The latter would give agreement with Clark's relation without the use of an effective

[3] The constant C_{ij} in both formulae takes different values according to the rows in the periodic table to which the atoms belong and d_{ij} in Badger's formula varies in a similar way. In the earlier papers quoted it will be found that Clark's relation is given in the form $\omega_e=C_{ij}'/\sqrt{Nr_e^3}$. Such a form is dynamically unsatisfactory and Dr. Clark informs the author that he has recently modified it to be essentially as given here. The symbol N is defined by Clark as the number of electrons in molecular rather than atomic orbitals. It is omitted by Allen and Longair.

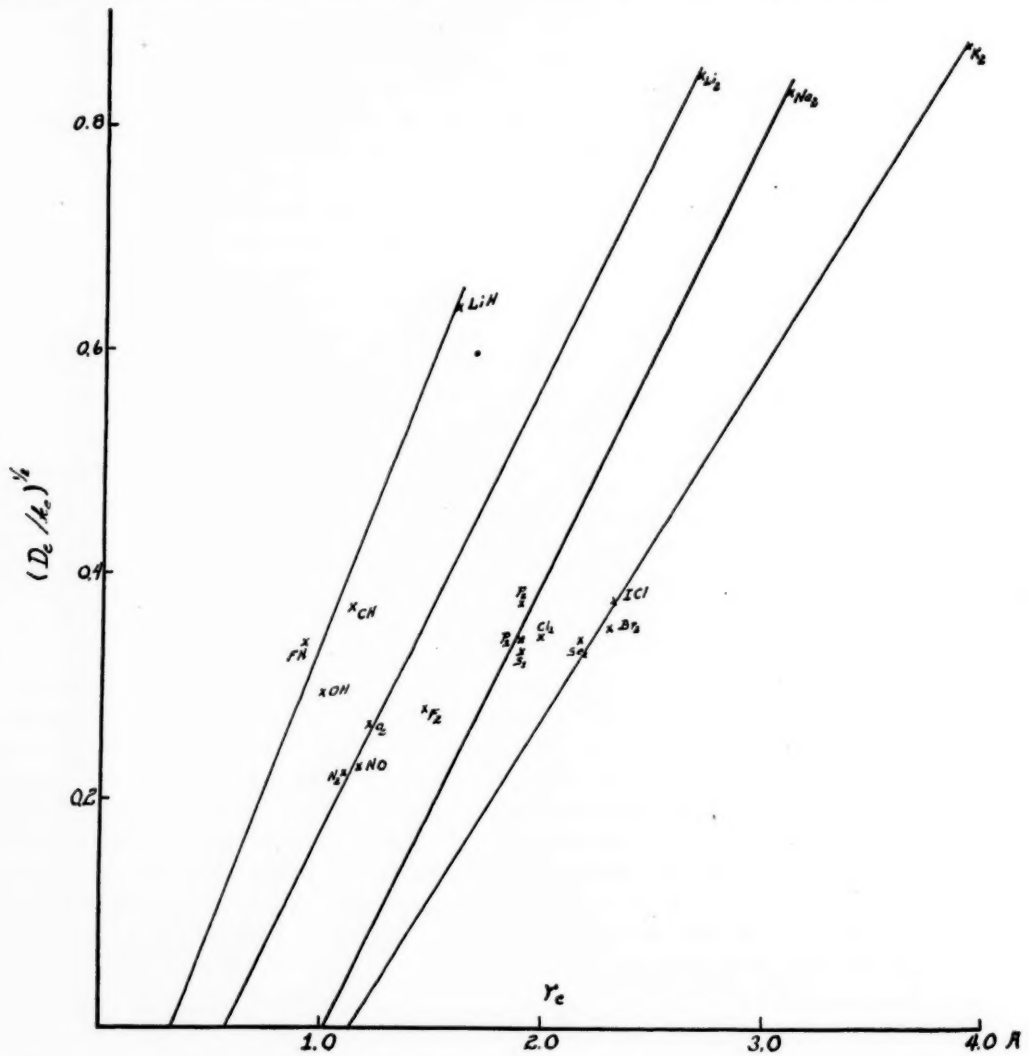

FIG. 1. Graph showing linear relation between $(D_e/k_e)^{\frac{1}{2}}$ and r_e for diatomic molecules in same row of the periodic table. Intercept on r_e axis gives d_{ij} and slope of the line gives $(mn)^{\frac{1}{2}}$ in the relation $D_e=k_e(r_e-d_{ij})^2/mn$.

internuclear distance but since N varies the only conclusion to be drawn regarding m, α and β is that α and either m or β or even both may vary in a related series.

In order to get further information on this point we examine what happens for a small variation in r_e. According to Badger's relation we should have

$$\frac{\delta r_e}{r_e - d_{ij}} = -\frac{1}{3}\frac{\delta k_e}{k_e},$$

while Clark's would give

$$\frac{\delta r_e}{r_e} = -\frac{1}{6}\frac{\delta k_e}{k_e}.$$

Now the C−H bond is slightly different in methane and in acetylene. In the former[4] $r_e = 1.093$A and $k_e = 4.9\times10^5$ dynes/cm while in the latter[5] we have $r_e = 1.057$ and $k_e = 5.9\times10^5$ dynes/cm. This gives

$$-\frac{\delta k_e}{k_e} = 17\%, \quad \frac{\delta r_e}{r_e} = 3.4\%, \quad \frac{\delta r_e}{r_e - d_{ij}} = 5\%.$$

It will be seen that these figures slightly favor Badger's form of the relation. Unfortunately there are no other reliable cases in which this test might be applied since it is extremely sensitive to minute variations in either the distance or the force constant but as data accumulate it should be possible to use it as a discriminant.

We consider next how the dissociation energy varies for a small variation in r_e. Thus we have from

$$D_e = -V_e = \frac{\alpha}{r_e^m}(1 - m/n), \quad \frac{\delta D_e}{\delta r_e} = \frac{-m\alpha(n-m)}{n r_e^{m+1}}.$$

But from (2)

$$\frac{\delta k_e}{\delta r_e} = -\frac{(m+2)m\alpha(n-m)}{r_e^{m+3}}$$

and so finally

$$\frac{\delta D_e}{D_e} = \frac{m}{m+2}\frac{\delta k_e}{k_e}. \tag{6}$$

By substituting for D_e and for k_e this relation may be thrown into the form

$$\delta D_e = B\frac{\delta\nu}{\nu^{(2-m)/(2+m)}}, \tag{7}$$

where

$$B = \frac{2}{n(m+2)}(4\mu\pi^2)^{m/(m+2)}[m\alpha(n-m)]^{2/(m+2)}.$$

In these calculations we have assumed that α is constant and β varies. It is fairly clear that the opposite assumption would have led to the relations

$$\frac{\delta D_e}{D_e} = \frac{n}{n+2}\frac{\delta k_e}{k_e} \quad \text{and} \quad \delta D_e = B'\frac{\delta\nu}{\nu^{(2-n)/(2+n)}}. \tag{8}$$

If now we substitute the most probable value for each case *viz.* $m=1$ and $n=4$ we obtain the alternative forms

$$\delta D_e = B\frac{\delta\nu}{\nu^{\frac{1}{3}}} \quad \text{and} \quad \delta D_e = B'\nu^{\frac{1}{3}}\delta\nu. \tag{9}$$

There is as yet too little data to test these equations. Badger and Bauer[6] have proposed the empirical relation

$$\delta D = B''\frac{\delta\nu}{\nu} \tag{10}$$

between the interaction energy and the frequency shift $\delta\nu$ when a hydrogen bond is formed. But until a relation has been established between the change in energy of the strong XH bond and the weak XH . . . Y bond has been established, we can make no use of Badger's suggestion.

We next consider the relation

$$D_e = \frac{k_e r_e^2}{mn}$$

and whether it is fulfilled for those diatomic molecules of which the dissociation energies have been accurately determined. Unfortunately there are remarkably few diatomic molecules for which D_e is accurately known and for polyatomic molecules the dissociation energies of particular bonds are still more uncertain. In Fig. 1 we have plotted $(D_e/k_e)^{\frac{1}{3}}$ against the internuclear dis-

[4] For distance, see Ginsburg and Barker, J. Chem. Phys. **3**, 668 (1935); for force constant, see Voge and Rosenthal, J. Chem. Phys. **4**, 137 (1936).

[5] For distance, see Herzberg, Patat and Verleger, Zeits. f. Physik **102**, 1 (1936); for force constant, see Colby, Phys. Rev. **47**, 388 (1935).

[6] Badger and Bauer, J. Chem. Phys. **5**, 839 (1937).

tance r_e and we should expect the points for molecules in which the two atoms come from the same row in the periodic table to lie on a straight line the slope of which should be $(mn)^{-\frac{1}{2}}$. If the relation is true as it stands then the straight lines should go through the origin but if one should use an effective internuclear distance then the intercept on the r_e axis will give that defect which has to be subtracted from the actual distance, *viz.* d_{ij} in Badger's notation. As far as the somewhat meager data go it would appear that an effective rather than a true internuclear distance should be used and we have drawn the lines through the points to find the d_{ij}'s and compare them with those used by Badger. The comparison is given in Table I which also records the values for the product mn deduced from the slopes of the lines. It should be added that the values of the dissociation energies of the alkali hydrides are not absolutely certain. The data employed have all been taken from Herzberg's recent compilation.[7] There is still some doubt about the dissociation energy of P_2 and so the points corresponding to the two alternative values have both been given.

It will be noticed that the greatest deviation from any of the lines occurs for F_2 and this results from the anomalously large internuclear distance which has been reported for this molecule from electron diffraction.[8] Chlorine is next worst but if the lower value for the dissociation energy of P_2 turns out to be correct, then the line would have to be redrawn and the deviation would be considerably reduced while the resulting value for d_{ij} would also be in better agreement with Badger's. It is interesting that the point for ICl falls on the Br_2 line. The values obtained for mn are all of a reasonable magnitude. In the case of the hydrides the excellent agreement with

TABLE I.

	Li_2	Na_2	K_2	LiH
d_{ij} (here)	0.57	1.02	1.13	0.34
d_{ij} (Badger)	0.68	1.18	1.35	0.335
mn	6.2	6.2	10.8	4

[7] *Molecular Spectra* (Prentice Hall, 1939).
[8] Brockway, J. Am. Chem. Soc. **60**, 1348 (1938).

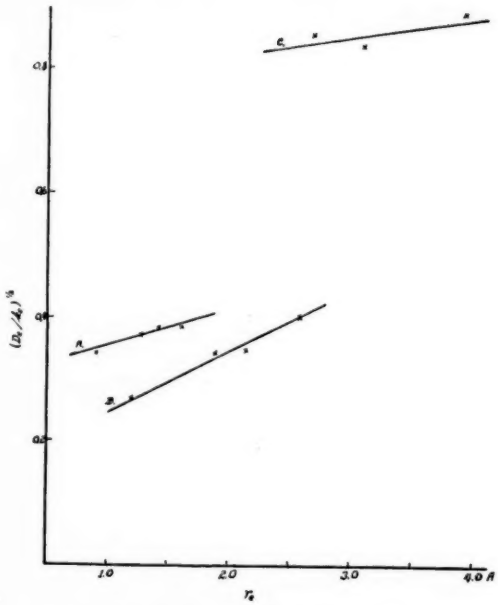

FIG. 2. Graph showing linear relation between $(D_e/k_e)^{\frac{1}{2}}$ and r_e for similar molecules. Line *A* refers to HF, HCl, HBr, HI; line *B* to O_2, S_2, Se_2, Te_2; and line *C* to Li_2, Na_2, K_2. A similar line can also be drawn for Cl_2, Br_2, and I_2 but F_2 does not lie on it.

Badger's d_{ij} would indicate that $m=1$ and $n=4$ gives a satisfactory representation.

Until more experimental data are available it is not possible to be sure how safe it will be to extrapolate or interpolate from the above results. This method should at least prove useful in giving first estimates of dissociation energies. Thus it should be noticed that satisfactory straight lines may also be drawn connecting related elements in the periodic table (Fig. 2) and also related hydrides. Although the reason for this is not yet clear on the above theory it can probably be used as an additional check in predicting dissociation energies. The extension of this to polyatomic molecules where it will find its greatest application will be discussed in a subsequent paper.

The author wishes to express his gratitude to the Trustees for a Leverhulme Fellowship during the tenure of which the above work was carried out. He also wishes to acknowledge the benefit of discussing these matters with Professors R. M. Badger and L. Pauling of the California Institute of Technology.

Exchange Reaction of Gaseous Bromine and Hydrogen Bromide

LAURENCE C. LIBERATORE AND EDWIN O. WIIG
Department of Chemistry, University of Rochester, Rochester, New York

(Received August 10, 1939)

The exchange reaction of bromine and radioactive hydrogen bromide in the gas phase has been found to fall just short of reaching equilibrium in two minutes. The very rapid rate of exchange would seem to be accounted for best by a chain reaction involving bromine atoms.

THE exchange reactions of halogens with their corresponding halides in aqueous solutions have been studied by several investigators.[1-4] In all cases exchange has been found to take place freely. Topley and Weiss[5] studied the exchange reaction of hydrogen bromide and bromine in carbon tetrachloride and found that equilibrium was reached in less than two minutes. The present gas phase measurements in the absence of water vapor were undertaken in the hope that the gaseous exchange might be somewhat slower which would permit us to make a kinetic study of the thermal and photochemical bromine-hydrogen bromide exchange. This hope was not realized since our experiments indicate that equilibrium is almost, but not quite, reached in two minutes. Nevertheless, our results may be of interest. Brezneva, Roginsky, and Schilinsky[6] allowed radioactive bromine and hydrogen bromide to remain in contact for fifteen minutes and found that equilibrium was established according to the masses of bromine in the two gases.

EXPERIMENTAL

Radioactive bromine was obtained by bombardment of selenium with protons in the Department of Physics cyclotron. The bombarded selenium was finely ground and placed in a bulb attached to an all glass system using a minimum number of stopcocks and comprising a mercury diffusion pump (backed by an oil pump), manometer, McLeod gage, reaction vessel, trains for preparing and purifying HBr and Br_2, etc. Pure, dry HBr gas was admitted to the selenium and the mixture heated to bring about exchange. In the first six runs this HBr, containing radiobromine, was distilled into the 600-cc spherical reaction bulb which already contained the desired pressure of bromine frozen down in a small side tube. After reading the HBr pressure on a phosphoric acid manometer the condensed bromine was quickly vaporized by placing alcohol at room temperature around the trap. To stop the reaction the two gases were condensed with liquid air. The time of reaction was taken from the moment bromine began to vaporize to the time when both gases were completely condensed. Obviously the actual time of reaction was somewhat less than this.

Following reaction, the pressure of the HBr was measured, keeping the Br_2 condensed, after which the HBr was completely absorbed in a tube containing aqueous NaOH. The Br_2 pressure was also measured, followed by freezing it down in another tube containing aqueous NaOH. This tube was sealed off, the cooling mixture removed and the bromine allowed to react. The bromine in each solution was completely precipitated as AgBr. The precipitate was filtered, dried, pressed into a disk about 15 mm in diameter, and the disk covered with Cellophane. The radioactivities of the two disks were measured on an ionization chamber and compared.

In runs 7–13 HBr at high pressure was quickly admitted to the bromine vapor in the reaction vessel. The gases were allowed to react for two minutes, frozen down and handled as before.

Run 13 was made in the presence of oxygen. Since the gases were very difficult to condense after reaction, as much of them as possible was condensed and the rest completely pumped off.

[1] Grosse and Agrusse, J. Am. Chem. Soc. **57**, 591 (1935).
[2] Long and Olson, J. Am. Chem. Soc. **58**, 2214 (1936).
[3] Hull, Shiflett and Lind, J. Am. Chem. Soc. **58**, 535 (1936).
[4] Dodson and Fowler, J. Am. Chem. Soc. **61**, 1215 (1939).
[5] Topley and Weiss, J. Chem. Soc. 912 (1936).
[6] Brezneva, Roginsky and Schilinsky, Acta Physicochim., U.R.S.S. **5**, 549 (1936).

The radioactivities were determined as before. In runs 10 to 12 the bulb B was filled with enough tubing to increase the surface exposed to the gases by a factor of seven.

In certain runs, as shown in the table, the radioactivity was measured on γ-rays, because it was thought that perhaps all the β-rays did not emerge from the disk. However, negligible differences were found in the ratios of the radioactivities of those samples which were measured both on β-rays and on γ-rays.

Results

In the exchange reaction

$$HBr^* + Br\text{-}Br \rightleftharpoons HBr + Br\text{-}Br^*,$$

the probability that the radioactive Br atom will appear in the Br_2 molecule in the forward reaction is twice the probability that it will appear in the HBr molecule in the reverse reaction. Therefore at equilibrium the radioactivity is distributed between the HBr and Br_2 in proportion to the number of Br atoms present, and if the Br_2 pressure is one-half that of the HBr, the radioactivities of the two resultant AgBr samples are the same. If the gases are not present in the ratio $2HBr : 1Br_2$, then at equilibrium the fraction of the total radioactivity due to HBr should be numerically equal to the fraction of the total number of Br atoms present as HBr.

The calculations in the last two columns of Table I were made as follows. The radioactivity of the HBr was calculated to what it would have been if the pressure of the HBr were twice that of the Br_2. This value was then used in calculating the total radioactivity and the fractions due to $BrBr^*$ and to HBr^*. If reaction has reached equilibrium, the result is a value of 0.5 for the fraction of the total radioactivity due to either Br_2 or HBr.

No change in the data could be detected in experiments in which the bromine and hydrogen bromide were allowed to remain frozen down, before analysis, for varying lengths of time up to an hour. This would seem to eliminate exchange in the solid state.

As can be seen from Table I, the thermal exchange is not quite complete in two minutes. The pressures stated are those obtained after reaction had occurred. In the experiments in which the gases were left mixed for 15–20 minutes the

Table I. *Summary of experimental data.*

Run No.	Type	Time min.	P_{HBr} mm	P_{Br_2} mm	$\frac{\text{Br as } Br_2}{\text{Total Br}}$	$\frac{\text{Radio. of } Br_2}{\text{Total Radio.}}$*	$\frac{\text{Radio. of } Br_2}{\text{Total Radio. for Mixture } 2HBr : 1Br_2}$
4	Photochemical-Unpacked	30	82	34	0.454	0.473	0.510
1		20	95	48	0.503	0.507	0.505
5		20	68	42.5	0.556	0.560	0.506
2	Thermal-Unpacked	65	111.5	42	0.429	0.465	0.535
6		15	95.5	55	0.535	0.530	0.496
3		2	79	52	0.468	0.490	0.423
7		2	47	35	0.598	0.538	0.423
8		2	66	48	0.593	0.517	0.424
9		2	93	50	0.518	0.483	0.465
13	Thermal-Unpacked+O_2	2	90	48	0.516		0.450
10	Thermal-Packed	2	61	52	0.630	0.565	0.432
11		2	69	38.5	0.528		0.466
12		2	69.5	38	0.523		0.458

* Radioactivity measurements in 4, 5, 6, 8, 10, 11, 12, 13 made on gamma-rays.

radioactivity in the Br_2 is just that required for equilibrium. In the 65-minute experiment the Br_2 is somewhat more radioactive than expected; this effect is apparently real and not due to experimental error, but needs to be checked. The reaction appears to be homogeneous as there is no effect observed in packing the bulb with Pyrex tubing. The experiments indicated as photochemical were carried out in broad daylight; those marked "thermal" in a semi-darkened room with the reaction vessel completely covered.

Since Br^{80} decomposes to give krypton, the radioactive hydrogen bromide would dissociate into a hydrogen atom plus krypton. Later considerations show that the effect of these hydrogen atoms is small and, as might be expected, any influence of the added oxygen in experiment 13 would not be apparent.

The total number of radioactive bromine atoms present can be estimated. A number of workers[7, 8] have shown that radioactive Br^{80} having a half-life of 4.5 hours emits almost pure gamma-rays. These gamma-rays cause internal conversion of electrons in the bromine atom so that an electron is removed, forming a radioactive bromide ion with a half-life of 18 minutes. This bromide ion changes to krypton with the loss of a beta-particle. Of the above particles only the beta-particle causes a current in the ionization chamber, along with the beta-particle emitted by radioactive Br^{82} (half-life 32 hours). In calculating the total number of radioactive atoms present at the time of reaction, the amount of each isomer present must be calculated. A sample calculation follows.

At time of measuring, activity Br^{80} = activity Br^{82} (from half-lives)

Ionization chamber sensitivity = 100 β's per sec. per cm deflection (from standard U source)

Sixty-five percent β's due to Br^{80} get through sample
Eighty-five percent β's due to Br^{82} get through sample
} Estimated for sample 1 mm thick.

Or, 66.5 β's per sec. per cm deflection due to Br^{82} emitted in sample and

66.5 β's per sec. per cm deflection due to Br^{80} emitted in sample.

Deflection = 263 cm (Total radioactivity)

$$N(Br^{80}) = -\frac{dN}{dt}\cdot\frac{1}{\lambda} = \frac{66.5\times 3600\times 4.5}{0.693}\times 263 = 4.0\times 10^8$$

at time of measuring. This gives, by the decay law,

5×10^8 radioactive Br^{80} atoms at time of reaction.

Similarly, $N(Br^{82}) = 2.96\times 10^9$ at time of reaction.

Total $N(Br^{80}+Br^{82}) = 3.46\times 10^9$ at time of reaction.

There are two ion pair producing processes occurring in the reaction vessel: (1) ionization by β-particles and (2) ionization by the internal conversion electron ejected by the γ-ray. Because of its much smaller energy any effect of the recoil ion may be neglected.

The number of ion pairs due to beta-particles was calculated from the ionization chamber deflections as follows (the internal conversion electrons do not reach the ionization chamber). The energy of the beta-particles is rather low (2 Mev), so that the number of ion pairs formed per centimeter in air is about 50 [9] at normal temperature and pressure. The number of ion pairs formed was assumed to be proportional to the atomic number of the gas present. Thus the number of ion pairs formed in the reaction bulb is

$$50\times\frac{\text{pressure}}{760}\times\frac{\text{temp.}}{273}\times\frac{\text{atomic No. Br}}{\text{atomic No. air}}\times\frac{3}{4}\times\text{No. }\beta\text{'s per cm deflection}\times\text{deflection in cm}\times\text{radius of bulb}\times\text{time of reaction in seconds.}$$

The three-fourths factor is used because three-fourths of the atoms are bromine, the rest being hydrogen.

$$N = 50\times\frac{131}{760}\times\frac{300}{273}\times\frac{35}{8}\times 133\times 263\times 5\times 120 = 6.5\times 10^8 \text{ ion pairs}$$

[7] Segrè, Halford and Seaborg, Phys. Rev. **55**, 321 (1939).
[8] DeVault and Libby, Phys. Rev. **55**, 322 (1939).
[9] Rutherford, Chadwick and Ellis, *Radiation from Radioactive Substances* (Cambridge University Press, London, 1930).

formed by the beta-particles from Br^{80} and Br^{82} in the vessel in two minutes.

The number of ion pairs produced by the internal conversion electrons may also be calculated. According to measurements just completed by Valley[10] these internal conversion electrons have an average energy of about 40,000 ev and are about 75 percent emitted. This gives an average energy of 30,000 ev available and assuming about 30 ev per ion pair, we have an average of 1000 ion pairs per disintegration of Br^{80} (4.5 hr.). From the concentration of Br^{80} and the decay law the number of disintegrations in two minutes is 2.5×10^6, which gives 2.5×10^9 ion pairs.

The total number of ion pairs produced in the vessel in the two minutes the gases are mixed is thus 3.15×10^9.

Discussion

The data may be summarized as follows: the thermal exchange is unaffected by increasing the surface sevenfold; equilibrium is not quite reached in two minutes; in an average experiment of this duration there are present *ca.* 3.5×10^9 radioactive Br atoms; the total number of ion pairs formed in the vessel during this time is 3.15×10^9.

Two mechanisms have been suggested to account for radiochemical reactions, *viz.*, the cluster theory of Lind[11] and the primary formation of atoms and ions followed by thermal reactions (Eyring, Hirschfelder and Taylor[12]).

For the sake of simplicity let us assume a cluster of only three molecules (one of these being a positive or negative ion) as represented by

$$HBr^*+HBr+Br_2 \rightleftharpoons \begin{pmatrix} HBr^* \\ HBr \end{pmatrix} Br_2 \rightleftharpoons BrBr^*+2HBr.$$

When such a cluster breaks up due to neutralization of the charge (by a cluster of opposite charge or by an ion or electron) the probability of the cluster yielding BrBr* is equal to that of giving HBr*. If every ion pair forms such a cluster and *each contains a radioactive atom*, then 1.6×10^9 "tagged" atoms should appear in the Br_2 and actually at equilibrium 1.8×10^9 "tagged" atoms do appear. However, the probability of finding a Br* atom in the cluster is given by the ratio of the number of Br* atoms present to the total number of HBr molecules present or $(3.5\times10^9)/(3.2\times10^{21})=1\times10^{-12}$. The rate of the exchange reaction is thus about 10^{12} times as great as such a simple cluster would predict. Obviously, no adjustment of the composition of the cluster can begin to account for this large difference.

The rapidity of the exchange would seem to require a chain mechanism. Chain reactions would readily be initiated by the hydrogen and bromine atoms formed as a result of the neutralization of the ion pairs. These effects will be approximately the same as discussed in detail for α-particles by Eyring, Hirschfelder and Taylor.[12] The primary process in the case of α-particles consists of (1) excitation of molecules leading to a rupture into atoms and (2) a primary ionization. The latter is followed by secondary processes which lead finally to atoms. Thus an α-particle, passing through Br_2 and HBr forms by ionization processes, according to these authors, about 6 Br atoms and 2–3 H plus 3 Br atoms, respectively. To these must be added dissociation without ionization. Similarly, for β-particles, we may expect from each ion pair several Br or H atoms or both. The modified cluster theory of Lind and Livingston,[13, 14] in which the cluster, after recombination of the positive and negative ions with the liberation of the energy of ionization, is thought of as a small isolated volume of gas momentarily at high temperature, might lead to a dissociation into atoms. The source of the atoms does not affect our consideration of the exchange reaction, except as it affects the number of atoms produced.

The molecular species present are HBr, Br_2, HBr*, and BrBr*, the ratio of the first two to the last two being of the order of 10^{12}. Consequently any "tagged" atoms produced as a *direct*

[10] We are indebted to Dr. George E. Valley of the Department of Physics for supplying us with these unpublished data.

[11] S. C. Lind, *The Chemical Effects of Alpha Particles and Electrons* (Chemical Catalog Co., New York, 1928).

[12] Eyring, Hirschfelder and Taylor, J. Chem. Phys. **4** 479, 570 (1936).

[13] Livingston and Lind, J. Am. Chem. Soc. **58**, 612 (1936).

[14] Earl F. Ogg, J. Phys. Chem. **43**, 399 (1939).

result of the various dissociation processes can be neglected. Hydrogen atoms can play no role except to furnish Br atoms, since the only reactions which H can undergo are

$$H+Br_2 \rightarrow HBr+Br$$
$$H+HBr \rightarrow H_2+Br$$
and also $$H+BrH \rightarrow HBr+H,$$

which would have no net effect.

The only reactions in which Br atoms can participate are

$$Br+BrBr' \rightarrow BrBr+Br'$$
$$Br+HBr' \rightarrow HBr+Br',$$

the superscripts being used simply to differentiate between two atoms. These exchange reactions might well be expected to have only small or negligible energies of activation. The only effect then of a collision of a Br atom with ordinary Br_2 or HBr is to pass a Br atom along. Collision of Br with a molecule containing a "tagged" atom may result in exchange as

$$Br+HBr^* \rightarrow BrH+Br^*$$
and $$Br+BrBr^* \rightarrow BrBr+Br^*.$$

The reverse reactions would also occur. Gas phase recombination of atoms at the pressures used would be small, the atoms eventually disappearing at the walls.

Equilibrium may be looked upon as being attained by setting free all the Br* atoms, after which the equilibrium distribution would be instantly attained by collision of Br* with HBr and Br_2. This would require at least 3.5×10^{21} collisions of bromine atoms with HBr in two minutes, since the total number of HBr* is 3.5×10^{9}, and the ratio of HBr/HBr* is 1×10^{12}. This corresponds to 5×10^{16} collisions of Br and HBr per cc per second and assumes that exchange occurs at every collision.

Aside from negligible thermal effects, there are four processes occurring which may result in the formation of atoms: (1) decomposition and ionization by the γ-rays emitted, (2) liberation of an atom when radioactive disintegration with the ejection of a β-particle occurs, e.g.,

$$HBr^* \rightarrow H+Kr+\beta$$
or $$BrBr^* \rightarrow Br+Kr+\beta,$$

(3) neutralization of the ion pairs produced by (a) the internal conversion electrons and (b) the β-particles and (4) excitation of molecules by the β-particle. The first two are negligible compared to (3) and (4), as is also any effect of the recoil ion.

We shall assume an average of 6 Br atoms produced per ion pair (Eyring, Hirschfelder and Taylor estimate 6 Br in Br_2 and 2–3 H+3 Br in HBr produced per ion pair from α-particles). Since about equal amounts of the β-particle energy go into ionization and excitation, an average total of 12 Br atoms should be formed per ion pair by both ionization and excitation processes. This corresponds to about 8×10^{9} Br atoms formed in the 600-cc reaction vessel in the two-minute period by the β-particles. Similarly, assuming 6 Br atoms per ion pair, the 2.5×10^{9} ion pairs produced by the internal conversion electrons yield 1.5×10^{10} Br atoms. All three processes thus yield 2.3×10^{10} Br atoms in two minutes or an average concentration over this period of 1.15×10^{10} Br atoms in 600 cc. Assuming this concentration of Br atoms and a collision diameter of 3A, the number of collisions of Br and HBr per cc per sec. is 1.2×10^{16}. This is in surprisingly good agreement with the minimum number of collisions required, *viz.*, 5×10^{16} cc^{-1} $sec.^{-1}$.

Two assumptions, which are certainly only approximations, have been made: that for the exchange reactions of Br with HBr and Br_2 the energy of activation is zero and that practically no Br atoms are lost by recombination. The inclusion of these factors would make the agreement worse, which may mean that the estimates of the number of Br atoms produced by the various processes is too small or that the collision diameter is too small, or both. The chain suggested might also involve ions instead of Br atoms. This contribution should be small, however, since the number of ions produced is smaller than the number of Br atoms and the rate of recombination of the former much greater than that of the latter.

A possible alternative explanation that suggests itself is that exchange occurs through the reaction

$$BrBr+HBr^* \rightarrow BrBr^*+HBr.$$

However, calculation of the number of such collisions at the walls indicates that the heterogeneous reaction could have an energy of activa-

tion not greater than 3 kcal. while for the homogeneous reaction the energy of activation must be less than 15 kcal. to account for the observed rate. Both values seem far too low. The wall reaction also seems unlikely because no effect of increased surface was observed.

We wish to express our thanks to Professor L. A. DuBridge and his associates in the Department of Physics for supplying us with radioactive bromine, permitting us the use of their ionization chambers, and for many stimulating discussions and suggestions.

FEBRUARY, 1940 JOURNAL OF CHEMICAL PHYSICS VOLUME 8

Spectroscopic Evidence for Hydrogen Bonds: Comparison of Proton-Attracting Properties of Liquids. II

WALTER GORDY* AND SPENCER C. STANFORD†
Mendenhall Laboratory of Physics, Ohio State University, Columbus, Ohio
(Received November 11, 1939)

Forty-two different organic liquids are rated according to their proton-attracting power by comparing the strength of the hydrogen bonds which they form with heavy methyl alcohol. The classes of liquids studied are: aldehydes, ketones, esters, ethers and amines. The amount of perturbation which the different solvents cause in the OD vibrational band of the CH_3OD is taken as a measure of the strength of the deuterium bridges formed with the CH_3OD. The study is a continuation of a previous work in which twenty-six similar liquids were studied, and the results agree with those of the former study in showing that according to proton-attracting power the different classes are in the order: esters<aldehydes and ketones<ethers <amines. From the study it is possible to observe the effects of unsaturation, substitution, and other structural variations on the electron donor power of the O or N atom to which the OD group forms a bond. It is shown that the strength of the deuterium bonds formed with CH_3OD bears a close relation to the basicities of the solvents, to their solubilities for other proton donor solutes, and to their reactivity with other compounds. There appears to be no correlation between the dipole moments of the solvents and the strengths of the bonds formed with the CH_3OD.

INTRODUCTION

THE present paper is a continuation of the spectroscopic comparison of the power of different proton acceptor solvents to form hydrogen bonds with a common proton donor solute.[1] These studies should assist in the prediction of many important properties of solvents because the power of the solvents to form hydrogen bonds with a proton donor group is largely conditioned by its tendency to donate an electron pair. According to the modern conception of a base as a proton acceptor, or electron pair donor,[2] the ability of a solvent to form hydrogen bonds with a proton donor would depend upon its strength as a base. Hence this application of infra-red spectroscopy offers a new and direct method for comparing the intrinsic strength of bases. The recent comprehensive studies of Zellhoefer, Copley and Marvel[3] on solubility of haloforms in electron donor solvents enable us to compare solvent power with the shift of the OD band. The remarkable agreement between the amount of perturbation brought about in the OD band and the solubility in the solvent suggest that abnormal solubilities depend to a marked extent on the electron donor power or the ability to form a complex with the solute.

In the previous paper it was shown that according to proton-attracting power the different classes of liquids are in the order: nitro compounds<esters<aldehydes and ketones<ethers <amines. In the present work a more extensive study of the different classes is made. In general

* Department of Physics, Mary Hardin-Baylor College, Belton, Texas.
† Department of Chemistry, The College of Wooster, Wooster, Ohio.
[1] W. Gordy, J. Chem. Phys. **7**, 93 (1939).
[2] K. W. Sherk, J. Chem. Educ. **13**, 358 (1936); J. N. Bronsted, Chem. Rev. **5**, 23 (1928).
[3] M. J. Copley, G. F. Zellhoefer and C. S. Marvel, J. Am. Chem. Soc. **60**, 1337, 2666, 2714 (1938).

the results bear out the conclusion previously reached, although the wider survey reveals many interesting variations depending upon the structure of the individual members of each class.

Experimental Procedure

The resolving instrument is the same as that described in the previous paper.[1] As in the earlier work on CH_3OD solutions a 1 molar solution was found to be most satisfactory. For concentrations much more dilute than this the thickness of the cell required is such that the general absorption and harmonic bands of the solvent decrease the accuracy of the results. On the other hand, for a more concentrated solution a smaller percentage of the alcohol molecules would be linked to the solvent. This, too, would tend to make the results uncertain. It was found that more reliable results could be had for most of the solutions by using a slightly thicker cell than was used before. Consequently a thickness of 0.008 cm was used instead of 0.006 cm. The curves given in the figures represent the ratio of transmission of the solution to that of an approximately equal thickness of the pure solvent.

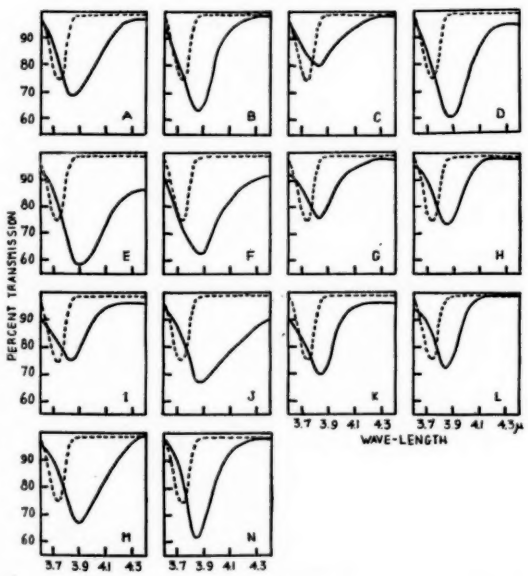

FIG. 1. Effects of solvent on the OD band of CH_3OD. Broken line, 0.1 M (t=0.32 cm) CH_3OD in benzene. Solid line, 1 M (t=0.008 cm) CH_3OD in: A. m-tolualdehyde; B. cinnamic aldehyde; C. furfural; D. citral; E. heptaldehyde; F. 2 ethyl butraldehyde; G. methyl iso-butyl ketone; H. di-iso-butyl ketone; I. methyl amyl ketone; J. mesityl oxide; K. acetophenone; L. p-methyl acetophenone; M. cyclohexanone; N. fenchone.

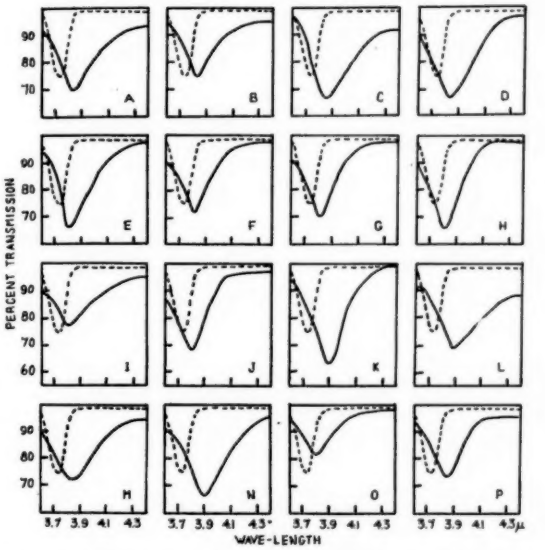

FIG. 2. Effects of solvent on the OD band of CH_3OD. Broken line, 0.1 M (t=0.32 cm) CH_3OD in benzene. Solid line, 1 M (t=0.008 cm) CH_3OD in: A. iso-amyl formate; B. ethyl chloroacetate; C. γ-bromopropyl acetate; D. phenyl acetate; E. furfuryl acetate; F. methyl benzoate; G. benzyl benzoate; H. n-butyl pthalate; I. diethyl oxalate; J. ethyl carbonate; K. n-butyl phosphate; L. ethyl n-butyl ether; M. $\beta\beta'$ dichloroethyl ether; N. dibenzyl ether; O. phenetole; P. epichlorohydrin.

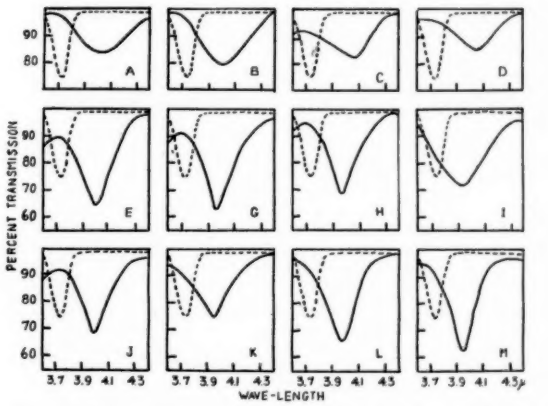

FIG. 3. Effects of solvent on the OD band of CH_3OD. Broken line, 0.1 M (t=0.32 cm) CH_3OD in benzene. Solid line, 1 M (t=0.008 cm) CH_3OD in: A. diamyl amine; B. triamyl amine; C. benzylamine; D. dibenzylamine; E. aniline; F. o-chloroaniline; G. m-chloroaniline; H. dimethyl aniline; I. o-toluidine; J. ethyl o-toluidine; K. methylanthranilate; L. pyrrole.

The bands are fairly sharp and the minima easily determined for all the compounds except the aliphatic amines and quinoline. Here the experimental difficulties are increased by over-

TABLE I. CH_3OD *solutions.*

SOLVENT	POSITION OF OD BAND		SHIFT FROM MONOMOLECULAR BAND IN BENZENE SOLUTION	
	μ	cm^{-1}	$\Delta\mu$	$\Delta\nu$
*Benzene C_6H_6	3.73	2681		
*Pure liquid CH_3OD	4.01	2494	0.28	187
*Nitrobenzene $C_6H_5NO_2$	3.77	2653	0.04	28
Aldehydes				
*Benzaldehyde $C_6H_5 \cdot CH : O$	3.85	2597	0.12	84
m-tolualdehyde $CH_3 \cdot C_6H_4 \cdot CHO$	3.85	2597	0.12	84
Cinnamic aldehyde $C_6H_5CH : CH \cdot CH : O$	3.86	2591	0.13	90
Furfural $C_4H_3O \cdot CH : O$	3.83	2611	0.10	70
Citral $(CH_3)_2C : CH \cdot CH_2 \cdot C(CH_3) : CH \cdot CHO$	3.88	2577	0.15	104
Heptaldehyde $CH_3(CH_2)_5 \cdot CHO$	3.90	2564	0.17	117
2 ethyl butraldehyde $(C_2H_5)_2 \cdot CH \cdot CHO$	3.88	2577	0.15	104
**n*-butraldehyde $C_2H_5 \cdot CH_2 \cdot CHO$	3.90	2564	0.17	117
Ketones				
*Methyl ethyl ketone $CH_3 \cdot CO \cdot C_2H_5$	3.84	2604	0.11	77
*Acetone $CH_3 \cdot CO \cdot CH_3$	3.87	2584	0.14	97
Methyl iso-butyl ketone $CH_3 \cdot CO \cdot C_4H_9$	3.84	2604	0.11	77
Di-iso-butyl ketone $(C_4H_9)_2CO$	3.85	2597	0.12	84
Methyl amyl ketone $C_5H_{11} \cdot CO \cdot CH_3$	3.84	2604	0.11	77
Mesityl oxide $(CH_3)_2C : CH \cdot CO \cdot CH_3$	3.87	2584	0.14	97
Acetophenone $C_6H_5 \cdot CO \cdot CH_3$	3.84	2604	0.11	77
p-methyl acetophenone $CH_3 \cdot C_6H_4 \cdot COCH_3$	3.84	2604	0.11	77
Cyclohexanone $CH_2(CH_2)_4 \cdot CO$	3.90	2564	0.17	117
Fenchone $C_{10}H_{16}O$	3.85	2597	0.12	84
Esters				
*Ethyl acetate $CH_3CO_2 \cdot C_2H_5$	3.85	2597	0.12	84
*Amyl acetate $CH_3CO_2 \cdot C_5H_{11}$	3.86	2591	0.13	90
Iso-amyl formate $HCO_2 \cdot C_5H_{11}$	3.83	2611	0.10	70
Ethyl chloroacetate $Cl \cdot CH_2 \cdot CO_2C_2H_5$	3.83	2611	0.10	70
γ-bromo-propyl acetate $CH_3 \cdot CO_2C_3H_6Br$	3.85	2597	0.12	84
Phenyl acetate $CH_3CO_2C_6H_5$	3.84	2604	0.11	77
Furfuryl acetate $CH_3CO_2 \cdot C_4H_3O$	3.82	2618	0.09	63
Methyl benzoate $C_6H_5CO_2 \cdot CH_3$	3.82	2618	0.09	63
Benzyl benzoate $C_6H_5CO_2 \cdot CH_2 \cdot C_6H_5$	3.82	2618	0.09	63
n-butyl pthalate $C_6H_4(CO_2C_4H_9)_2$	3.82	2618	0.09	63
Diethyl oxalate $(CO_2C_2H_5)_2$	3.82	2618	0.09	63
Ethyl carbonate $CO(OC_2H_5)_2$	3.80	2632	0.07	49
n-butyl phosphate $PO(OC_4H_9)_3$	3.90	2564	0.17	117
Ethers				
*Diethyl ether $(C_2H_5)_2O$	3.92	2551	0.19	130
Ethyl *n*-butyl ether $C_2H_5 \cdot O \cdot C_4H_9$	3.90	2564	0.17	117
*Iso-propyl ether $(CH_3)_2 \cdot CH_2O$	3.91	2558	0.18	123
**n*-butyl ether $(C_4H_9)_2O$	3.89	2571	0.16	110
$\beta\beta'$ dichloroethyl ether $(Cl \cdot CH_2 \cdot CH_2)_2O$	3.85	2597	0.12	84
Dibenzyl ether $(C_6H_5CH_2)_2O$	3.90	2564	0.17	117
Phenetole $C_2H_5O \cdot C_6H_5$	3.81	2624	0.08	57
*Dioxan $CH_2OCH_2CH_2OCH_2$	3.87	2584	0.14	97
Epichlorohydrin $O \cdot CH_2 \cdot CH \cdot CH_2Cl$	3.88	2577	0.15	104
Amines				
Diamyl amine $(C_5H_{11})_2NH$	4.02	2488	0.29	193
Triamyl amine $(C_5H_{11})_3N$	4.00	2500	0.27	181
Benzyl amine $C_6H_5CH_2 \cdot NH_2$	4.07	2457	0.34	224
Dibenzylamine $(C_6H_5CH_2)_2NH$	4.05	2469	0.32	212
*Pyridine C_5H_5N	4.00	2500	0.27	181
**a*-picoline $CH_3 \cdot C_5H_4N$	4.02	2488	0.29	193
*Piperidine $CH_2(CH_2)_4NH$	4.10	2439	0.37	242
Aniline $C_6H_5 \cdot NH_2$	4.00	2500	0.27	181
o-chloroaniline $Cl \cdot C_6H_4 \cdot NH_2$	3.96	2525	0.23	156
m-chloroaniline $Cl \cdot C_6H_4 \cdot NH_2$	3.97	2519	0.24	162
Dimethyl aniline $(CH_3)_2N \cdot C_6H_5$	3.94	2538	0.21	143
o-toluidine $CH_3 \cdot C_6H_4 \cdot NH_2$	3.99	2506	0.26	175
Ethyl *o*-toluidine $CH_3 \cdot C_6H_4 \cdot NH \cdot C_2H_5$	3.95	2532	0.22	149
Methylanthranilate $NH_2 \cdot C_6H_4 \cdot CO_2CH_3$	3.97	2519	0.24	162
Pyrrole $(CH : CH)_2NH$	3.96	2525	0.23	156

* Repeated from previous paper, J. Chem. Phys. 7, 93 (1939).

lapping of the intense CH absorption of the solvent and by the broadness and shallowness of the band.

DISCUSSION OF RESULTS

The transmission curves for aldehydes and ketones are given in Fig. 1; for esters and ethers, in Fig. 2; for amines, in Fig. 3. With each of these curves is given a curve for CH_3OD in an inert solvent, benzene (0.1 molar solution; cell thickness, 0.32 cm). The positions of the minima in these bands, with the shift from the position of the monomolecular band in the benzene solution are listed in Table I. Although there is considerable variation in the perturbation of the OD absorption made by the different members of each class, the classes themselves show noticeable unlikeness to each other. For example, the shifts produced by the esters are consistently lower than those produced by the aldehydes and ketones, which are about the same. For the most part, the ethers cause greater shift than the aldehydes and ketones; and the amines greater than the ethers.

Effects of unsaturation

The cases studied do not permit a direct comparison to ascertain the effect of an aliphatic double bond. Citral produces a slightly smaller shift in the OD band than does heptaldehyde, the saturated aldehyde most nearly like it of those studied. Cinnamic aldehyde has two carbon atoms between the carbonyl group and the benzene ring. For this reason it may be expected to behave more nearly like an aliphatic than an aromatic aldehyde. The fact that it produces a smaller shift than do the aliphatic aldehydes may be a result of its unsaturation. As these cases are not conclusive we expect to make further study of the aliphatic double bond.

A comparison of the shift produced by pyridine with that produced by the similar but fully hydrogenated compound, piperidine, shows that the effect of unsaturation here is to decrease appreciably the proton-attracting power of the nitrogen. This result is in agreement with the lower basicity constant of pyridine as compared with that of piperidine.

In general the effect of the attachment of a ring containing double bonds is to decrease the

perturbation produced on the OD band. As would be expected the effects are less pronounced the further the unsaturated ring is removed from the atom involved in hydrogen bond formation. Furfural, for example, causes less shift than any of the other aldehydes studied, while benzaldehyde and *m*-tolualdehyde produce slightly less shift than the aliphatic aldehydes.

Effects of substitution

The effect of the substitution of a chlorine for a hydrogen may be seen by comparing diethyl ether with dichloroethyl ether:

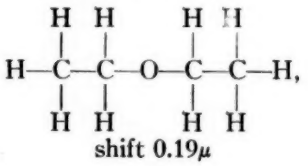

shift 0.19μ

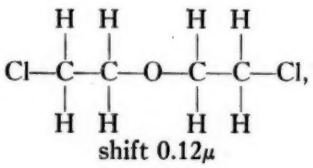

shift 0.12μ

also by comparing ethyl acetate (shift 0.12μ) with ethyl chloroacetate (shift 0.10μ), and aniline (shift 0.27μ) with *o*-chloroaniline (shift 0.23μ) or *m*-chloroaniline (shift 0.24μ). The influence of the strongly electronegative chlorine is transmitted through the carbons to the oxygen or nitrogen and results in a decrease of the effective negative charge on the electron donor atom. In this connection it should be mentioned that the chlorine atoms in chloroform are believed to make the CH group sufficiently acidic to share its proton in hydrogen bonding.[4]

The substitution of a phenyl group for an ethyl group causes a very marked decrease in the electron donor power of the ether oxygen. This may be seen by comparing diethyl ether with phenetole:

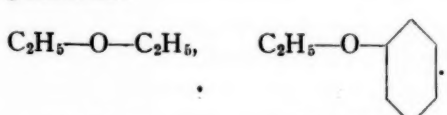

shift 0.19μ shift 0.08μ

[4] S. Glasstone, Trans. Faraday Soc. **23**, 200 (1936); W. Gordy, J. Chem. Phys. **7**, 163 (1939).

On the other hand, the influence of the phenyl group in decreasing the electron donor power of the oxygen is practically nullified when a carbon is placed between the phenyl group and the electron donor atom. Compare methyl ether with acetophenone:

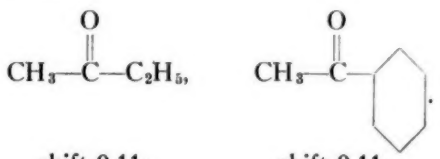

shift 0.11μ shift 0.11μ

There is very little difference in the shifts caused by ethyl acetate and phenyl acetate:

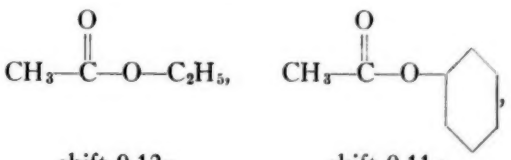

shift 0.12μ shift 0.11μ

a fact which probably indicates that the bonding is to the carbonyl oxygen of the acetate, which is somewhat removed from the phenyl group.

Similarly, a benzyl when substituted for an ethyl group has only a slight effect as compared with a phenyl group. Compare diethyl ether (shift 0.19μ) with dibenzyl ether (shift 0.17μ). That a phenyl group decreases the effective negative charge of the electron donor atom much more than does a benzyl group may be seen by a comparison of aniline (shift 0.27μ) with benzyl amine (shift 0.34μ). This result is in complete accord with other physical data. For example, phenol is much more acidic—less basic—than benzyl alcohol.

To compare a furyl group with a methyl group, notice ethyl acetate and furfuryl acetate:

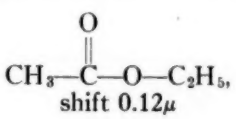

shift 0.12μ

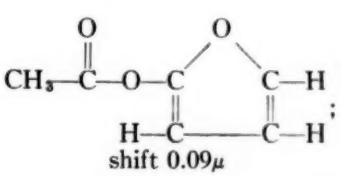

shift 0.09μ

to compare it with a phenyl group, notice furfural

(shift 0.10μ) and benzaldehyde (shift 0.12μ). The effect of the furyl ring was mentioned above in the discussion of unsaturation.

The shift produced by benzaldehyde is the same as that produced by *m*-tolualdehyde; and that produced by acetophenone as that by *p*-methyl acetophenone. These cases suggest that the substitution of a methyl group for a hydrogen has little if any effect. In these cases, however, the substitution is remote from the atom to which the OD is bonded. Naturally the most pronounced effect takes place when a hydrogen joined directly to the electron donor atom is replaced by a methyl group. Compare aniline (shift 0.27μ) with dimethyl aniline (shift 0.21μ). From the latter example it would seem that the substitution of a methyl group for a hydrogen tends to decrease the electron donor power of the aniline nitrogen. Yet *a*-picoline, in which a methyl group is attached to a carbon adjacent to the nitrogen in the pyridine ring, causes a slightly greater shift (0.29μ) in the OD band than does pyridine (shift 0.27μ). The large difference in the effects of aniline and dimethyl aniline may be due to unlikenesses in the steric hindrance of the methyl group and the hydrogen rather than to unlikenesses in their effect on the electron donor power of the nitrogen.

As a class the esters, with two oxygens linked to the same carbon, cause less effects upon the OD band than do the ketones, with one oxygen linked to the carbon. Diethyl carbonate, with its three oxygens linked to one carbon, produces a smaller shift than do the other esters. Phosphorous when joined to the electron donor atom appreciably increases its power to attract a proton. *n*-butyl phosphate causes a much greater shift (0.17μ) than any of the other esters. We may compare, for example, ethyl carbonate and *n*-butyl phosphate:

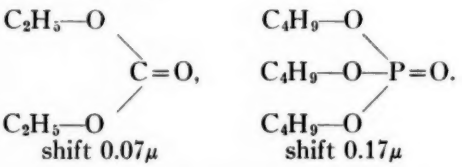

The pronounced variation here is probably not entirely due to the differences in the groups attached to the carbon and phosphorus but at least partly to differences in the electro-negativity of these two atoms. From other data[5] carbon is known to be more electro-negative than phosphorus.

TABLE II. *Comparison of dipole moment of solvent with shift in* OD *band.*

SOLVENT	DIPOLE MOMENT $\times 10^{18}$ e.s.u.	SHIFT IN OD BAND $\Delta\mu$
Bromobenzene	1.71	0
Nitrobenzene	4.23	0.04
Benzaldehyde	2.75	0.12
Acetone	2.9	0.14
Acetophenone	3.0	0.11
Ethyl acetate	1.8	0.12
Amyl acetate	1.9	0.13
Diethyl ether	1.15	0.19
Dioxan	0.4	0.14
Pyridine	2.2	0.27
Aniline	1.55	0.27
Dimethyl aniline	1.58	0.21
Pyrrole	1.8	0.23
Methyl cyanide	3.2	0.09
Benzyl cyanide	3.8	0.11

Other structural effects

From a comparison of the shift caused by dioxan with that caused by ethyl, propyl and butyl ethers, it would seem that a cyclic ether is not as effective an electron donor solvent as is an open chain ether. This is borne out, but to a less degree, by epichlorohydrin. Except for cyclohexanone,

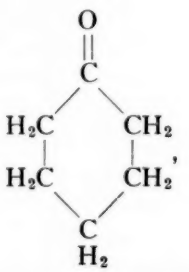

there is not much variation among the different ketones. It produces a considerably greater shift than do the other ketones. Piperidine, the amine which is structurally similar to this compound, correspondingly produces a large shift of the OD band as compared with the other amines. Fenchone, with the carbon of its carbonyl group forming part of a ring structure, causes about the same shift as the ordinary ketones.

The nitrogen in the pyrrole ring has an electron donor power equivalent to that of the least

[5] L. Pauling, *The Nature of the Chemical Bond* (Cornell University Press, 1939), p. 60.

effective of the aromatic amines. Compare, for instance, the shift produced by pyrrole (0.23μ) with that produced by *o*-chloroaniline (0.23μ).

Comparison with Other Physical Properties

Dipole moment of solvent

In Table II we have arranged a comparison of the dipole moments of several typical solvents with the shifts of the OD band which they produce. There seems to be little if any relation between the two. Nitrobenzene, which has the largest dipole moment of any of the solvents studied, produces the smallest shift of any except bromobenzene, while dioxan, with the smallest dipole moment of any of those listed, causes a shift of 0.14μ. Both pyridine (dipole moment 2.2) and aniline (dipole moment 1.55) produce a shift of 0.27μ. Considered as a class ethers have much lower dipole moments than ketones and aldehydes, yet they produce greater shifts of the OD band. Similarly, the amines, with lower dipole moments than the ketones, in general cause greater shifts than any of the other compounds studied. The nitriles and nitro compounds, with the highest dipole moments, produce relatively small shifts. This comparison indicates that the complex formation here is not due simply to dipole attraction, and that the tendency of a solvent to acquire protons from a hydroxyl group bears little relation to the dipole moment of the solvent.

Basicity constants

Few of the aromatic amines absorb appreciably in the region of 4μ, so that it is possible to make reasonably accurate measurements on the OD band for CH_3OD solutions in these solvents. Also for most of them the band is sufficiently sharp and symmetrical for its center to be located without difficulty. In Fig. 4 we have plotted basicity constants against shifts of the OD band for ten aromatic amines and one aliphatic amine. The other amines for which basicity constants are available in the literature have bands so complex and shallow, or so affected by intense absorption of the solvent, that determination of the centers is uncertain. Because the basicity constants used are for water solutions they represent essentially the measure of the ability

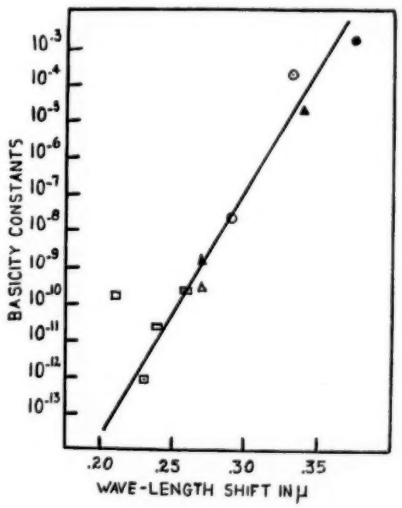

FIG. 4. Relation of basicity constant of solvent to shift in OD band. □ dimethyl aniline; ⊡ *o*-chloroaniline; ▭ *m*-chloroaniline; ⊡ *o*-toluidine; △ aniline; ◬ pyridine; ○ *a*-picoline; ⊙ tributylamine; ▲ benzylamine; ● piperidine.

of a base to capture a proton from water. Except in certain cases where difference in steric hindrance may cause slight variations—for example, repulsion of the methyl groups of dimethyl aniline for the CH_3OD may explain why the point for this solvent lies off the curve—we see no reason why the tendency of different solvents to capture protons from water, as indicated by their basicity constants, should not vary in the same way as their tendency to capture protons from an hydroxyl group of alcohol, as in either case it would be conditioned by the electron donor power of the solvent. The shift of the OD band made by these different solvents is the measure of the weakening of the binding force of the hydroxyl group and is, therefore a measure of the tendency of the base to capture the hydroxyl proton. Assuming the linear relationships suggested in Fig. 4, we may obtain by extrapolation basicity constants for the oxygenated solvents recorded in Table I. This method gives the following values for K_b: nitrobenzene, 4×10^{-25}; benzaldehyde, 8×10^{-20}; acetone, 2×10^{-18}; acetophenone, 1×10^{-20}; ethyl acetate, 8×10^{-20}; isopropyl ether, 9×10^{-16}.

Solubility

In their studies of the solubility of monofluorodichloromethane ($CHCl_2F$) in electron donor

TABLE III. *Relation of solubility to shift in* OD *band.*

SOLVENT	SOLUBILITY OF $CHCl_2F$ MOLE/FR.	SHIFT IN OD BAND $\Delta\mu$
Nitrobenzene	0.360	0.04
Benzaldehyde	0.436	0.12
Furfural	0.367	0.10
Heptaldehyde	0.519	0.17
Cyclohexanone	0.548	0.17
Furfuryl acetate	0.438	0.09
Diethyl oxalate	0.556	0.09
$\beta\beta'$ dichloroethyl ether	0.451	0.12
Dioxan	0.479	0.14
Phenetole	0.425	0.08
Aniline	0.258	0.27
Dimethyl aniline	0.425	0.21

solvents, Zellhoefer, Copley and Marvel,[3a] investigated many of the same solvents which are used in this study. They interpreted the solubilities which they found to be in excess of Raoult's law as being due largely to hydrogen bonding between the $CHCl_2F$ and the solvents. In Table III we have arranged a comparison of their data on solubilities of $CHCl_2F$ in 12 different solvents with our data on the shifts which these same solvents produce on the OD band of CH_3OD. For most of these solvents the correlation is remarkable, and is strong evidence that the interpretation of Zellhoefer, Copley and Marvel is correct. For diethyl oxalate the solubility obtained (0.556) is larger than that which the small shift of 0.09μ would seem to indicate. In this molecule, however, there are two carbonyl groups with the possibility of two molecules of $CHCl_2F$ tying to one molecule of the solvent. This possibility could, we believe, explain the lack of correlation in this case. The solubility of $CHCl_2F$ in aniline (mole fr. 0.258) is less than the ideal solubility predicted by Raoult's law (mole fr. 0.381), whereas this solvent brings about a rather large shift (0.27μ) in the OD band. Here the NH→N hydrogen bonds between the aniline molecules[6] are probably stronger than the CH→N bonds which would be formed with the $CHCl_2F$. On the contrary, OD→N bonds formed between CH_3OD and aniline would probably be stronger than the hydrogen bridges linking the aniline molecules. Thus the marked difference in data on solubility and shift is additional evidence that the proton donor power of the groups studied is in the order: CH < NH < OH.[7] As pointed out in the discussion of the relation of shifts to basicity constants, CH_3OD does not form as strong a bond with dimethyl aniline as one would predict from its basicity constant. It was suggested that this may be due to differences in steric hindrance of this solvent for water and methyl alcohol. The solubility of $CHCl_2F$ in dimethyl aniline, lower than would be predicted from the shift which the solvent produces on the OD band of CH_3OD, may be caused by a difference in steric hindrance of the dimethyl aniline for the $CHCl_2F$ and the CH_3OD.

Although they did not use the identical phosphate, they found, in agreement with our data, that a phosphate forms much stronger bonds than other esters. Other points of agreement are: that the chlorines in $\beta\beta'$ dichloroethyl ether decrease the electron donor power of the ether oxygen; that a cyclic ether has a weaker electron donor power than an ordinary ether; that a phenyl group attached to an oxygen or nitrogen atom markedly decreases its electron donor power; that the effect of unsaturation is to decrease the electron donor power slightly; and that in their power to donate electrons the classes of oxygenated solvents studied are in the order: nitro compounds < esters < aldehydes and ketones < ethers.[8] There seems to be one major point of disagreement: these observers state that the basicity of the amine solutions in water apparently is not related to the donor properties of the nitrogen in forming hydrogen bridges, whereas in our measurements there is a close correlation with the donor properties of the nitrogen in forming hydrogen bridges.

Chemical reactivity

Conant and Bartlett[9] have compared the rates of semi-carbazone formation for some aldehydes and ketones. The general reaction which they studied may be illustrated by the reaction with acetone:

$$(CH_3)_2CO + NH_2NHCONH_2 \rightleftharpoons (CH_3)_2C{=}NNCONH_2 + H_2O.$$

[6] W. Gordy, J. Chem. Phys. **7**, 167 (1939).

[7] N. V. Sidgwick, *The Covalent Link in Chemistry* (Cornell University Press, 1933), p. 166.

[8] See also, M. J. Copley and C. E. Holley, Jr., J. Am. Chem. Soc. **61**, 1599 (1939).

[9] Conant and Bartlett, J. Am. Chem. Soc. **54**, 2881 (1932); Conant, Ind. Eng. Chem. **24**, 466 (1932).

Only four of the eight carbonyl compounds studied by these observers were included in the present study. Fortunately they are ones which show rather wide variations. The results of Conant and Bartlett are compared with ours in Table IV. In Fig. 5 we have plotted OD shift against log k_2. Although there are too few cases for generalization, the comparison suggests an interesting relation. Also, in agreement with our data, these observers found furfural to be least reactive of all the aldehydes studied, and cyclohexanone to be most reactive of all the ketones studied.

Though steric effects undoubtedly cause considerable variation in certain cases, the most important factor in determining the relative strengths of the deuterium bonds which these different solvents form with CH_3OD is probably the effective negative charge on the electron donor atom, or its readiness to donate its electrons. Thus the close relation existing between amount of shift of the OD band produced by the various solvents and their basicities, solubilities and reactivities with certain other compounds is not surprising. Indeed all organic molecules may be broadly classified as electron acceptors or electron donors—i.e., all their chemical properties are in some way affected by their ability to accept or donate electrons. The method employed here in estimating this important property is more direct and far less laborious than many other types of measurement used for this purpose.

TABLE IV. *Comparison of reaction rate of semi-carbazone formation of aldehydes and ketones with shift in* OD *band.*

	Velocity Constants of Semi-carbazone Formation⇌Hydrolysis		Shift in OD Band
	k_2	$k_1 \times 10^5$	$\Delta\mu$
Furfural	0.73	0.55	0.10
Benzaldehyde	2.05	0.62	0.12
Acetone	6.02	1800.00	0.14
Cyclohexanone	36.00	7600.00	0.17

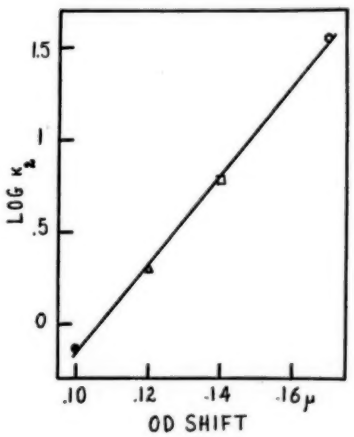

FIG. 5. Plot of OD shift against log k_2 of semi-carbazone formation: ● furfural; △ benzaldehyde; □ acetone; ○ cyclohexanone.

ACKNOWLEDGMENTS

The authors are indebted to Dr. H. H. Nielsen and Dr. Alpheus W. Smith for the use of their equipment and material and for their constant interest in this work; to Dr. W. G. France, of the Department of Chemistry, Ohio State University, for the use of his fluorite plates; to Dr. R. I. Grady and Dr. J. W. Chittum, of the Department of Chemistry, The College of Wooster, to Dr. W. R. Brode, of the Department of Chemistry, Ohio State University, and to Dr. H. P. Lankelma, of the Department of Chemistry, Western Reserve University, for some of the chemicals; and to Vida Miller Gordy for her assistance in preparing the manuscript. They also wish to acknowledge a very helpful talk with Dr. G. B. B. M. Sutherland, of Cambridge University.

Adsorption Isotherms for Mobile Monolayers

WILLIAM BAND
Physics Department, Yenching University, Peiping, China
(Received October 3, 1939)

A three-dimensional gas is pictured in contact with a liquid, forming at the interface a mobile monolayer. The density of the monolayer is maintained in equilibrium with the pressure of the gas. An equation is deduced giving as a function of temperature, the gas pressure which is just sufficient to initiate condensation in the monolayer. The only physical parameters involved in the relationship are the mass of the molecule and the heat of evaporation per molecule from the completely clustered monolayer. The fatty acids which exhibit monolayers with negligible external gas pressures, must have heats of evaporation greater than about 100×10^{-14} erg. Molecules as small as 20 atomic mass units and heats of evaporation less than about 75×10^{-14} erg should require pressures of the order of 10^{-2} atmosphere. An adsorption isotherm equation is found for monolayer concentrations less than the saturation value. Its form is similar but not identical with Langmuir's isotherm for immobile monolayers.

INTRODUCTION

FOWLER[1] has succeeded in deducing Langmuir's isotherm equation for monolayers in which the molecules are adsorbed at definite locations on a solid surface. Using the results recently found[2] for mobile monolayers on liquid surfaces, it is now possible to apply Fowler's general arguments to this case. The results are: first, an equation giving as a function of temperature, the minimum pressure of gas required to maintain the monolayer in its condensed state; and secondly, the pressure of the gas as a function of the corresponding concentration of the unsaturated monolayer, at any temperature —in other words the adsorption isotherm for the mobile monolayer.

There do not yet appear to be any data requiring detailed interpretation by such formulae; actual mobile monolayers being produced without the aid of any three-dimensional gas in contact with the liquid. This means merely that the equilibrium gas pressure is unmeasurably small with existing technique; it does not mean that in future mobile monolayers may not be produced which require an appreciable pressure of gas for their maintenance.

[1] Fowler, *Statistical Mechanics* (Cambridge University, 1936), second edition, §21.53.

[2] Band, "Statistical Mechanics of Condensation Phenomena in Mobile Monolayers," J. Chem. Phys. **8**, 116 (1940).

GENERAL THEORY

Let the complete assembly contain X molecules and possess total energy E. Consider an example of the assembly in which M of the molecules are attached in the monolayer, and $N=X-M$ are in the gas. The analysis must find the example, specified by M, for which the number of complexions is a maximum.[3]

Write $f_s(z)$ for the partition function of a single cluster of type s in the monolayer, and $g(z)$ for the partition function of a molecule in the gas. Write x_1 for the variable corresponding to the selection of a state in the monolayer, and x_2 for the selector variable corresponding to the gaseous state.

Then the number of complexions corresponding to a particular assignment of energy E_g in the gas and E_m in the monolayer will be, in the example considered, the product of the coefficient of $x_1{}^M z^E m$ in $\exp\{\sum_s x_1{}^s f_s(z)\}$ and the coefficient of $x_2{}^M z^E g$ in $\exp\{x_2 g(z)\}$. To include all possible assignments of energy, will require the coefficient of z^E, $E=E_m+E_g$, in the product of the two expressions. This leads to the integral expression for the total number:

$$C_N=1/(2\pi i)^3\int\int\int\frac{dx_1dx_2dz}{x_1{}^{M+1}x_2{}^{N+1}z^{E+1}}\times\exp\{x_2g(z)\}\cdot\exp\{\Sigma_s x_1{}^s f_s(z)\}. \quad (1)$$

[3] Fowler, reference 1, §5.4, uses a similar argument in the study of equilibrium between a crystal and its vapor.

Using, without rigorous proof, the theorem of Darwin and Fowler, reference 1, §2.42; it then follows that:

$$\ln C_N = \sum_s \lambda_1^s f_s(\zeta) + \lambda_2 g(\zeta) - M \ln \lambda_1 - N \ln \lambda_2 - E \ln \zeta, \quad (2)$$

where λ_1, λ_2, ζ are the unique roots of the equations:

$$\partial/\partial\zeta \ln C_N = \sum_s \lambda_1^s \partial/\partial\zeta f_s(\zeta) + \lambda_2 \partial/\partial\zeta g(\zeta) - E/\zeta = 0, \quad (3)$$

$$\partial/\partial\lambda_1 \ln C_N = \sum_s s\lambda_1^{s-1} f_s(\zeta) - M/\lambda_1 = 0, \quad (4)$$

$$\partial/\partial\lambda_2 \ln C_N = g(\zeta) - N/\lambda_2 = 0. \quad (5)$$

The example with largest C_N will be that in which N is adjusted to give

$$\partial/\partial N \ln C_N = 0. \quad (6)$$

Since $M = X - N$, and X is not varied, this means that

$$\ln \lambda_1 - \ln \lambda_2 = 0,$$

or

$$\lambda_1 = \lambda_2 = \lambda \text{ say}. \quad (7)$$

Eqs. (3)–(5) then become:

$$E = \sum_s \zeta \lambda^s \partial/\partial\zeta f_s(\zeta) + \zeta\lambda \partial/\partial\zeta g(\zeta), \quad (8)$$

$$M = \sum_s s\lambda^s f_s(\zeta), \quad (9)$$

$$N = \lambda g(\zeta). \quad (10)$$

From these equations the law of "mass action" follows by elimination of λ between (9) and (10):

$$M/N = \sum_s s f_s(\zeta) N^{s-1} [g(\zeta)]^{-s}. \quad (11)$$

From this equation either concentration, monolayer or gas, can be found in terms of the other under equilibrium conditions. The usual argument, from (8), gives the familiar relation between the parameter ζ and the absolute temperature:

$$\zeta = \exp(-1/kT).$$

Minimum Gas Pressure for Condensed Monolayer

Making use of the arguments employed before,[4] the partition function for the monolayer cluster type s is:

$$f_s(T) = s^2 A (1-\beta_s)/\rho \exp(\phi_s - \phi_1 - sW)/kT. \quad (12)$$

[4] Reference 2, Eqs. (1), (2), and (8)–(11).

For the meaning of ρ see reference 2, Eq. (19). The energy of a cluster of type s is $sW - \phi_s$, the term ϕ_1 occurs in (12) to cancel a similar term in ρ. Classically

$$g(T) = (2\pi mkT)^{\frac{1}{2}} V h^{-3}, \quad (13)$$

where V is the volume of the gas. The internal vibratory states of the molecules have been omitted from (12) and (13) because, if they are assumed unaffected by adsorption, they will cancel from Eq. (11). This last equation now becomes:

$$(M/A)/(N/V) = \sum_s s^3(1-\beta_s)/\rho \times \exp(\phi_s - \phi_1 - W)/kT \times h^3(2\pi mkT)^{-\frac{3}{2}} \times \{(N/V)h^3 \exp(-W/kT)(2\pi mkT)^{-\frac{3}{2}}\}^{(s-1)}. \quad (14)$$

The critical value of this expansion occurs when

$$(N/V) = (N/V)_c = (2\pi mkT)^{\frac{1}{2}} h^{-3} \exp(W/kT). \quad (15)$$

The critical sum corresponding to substitution of (15) into (14) gives the result:

$$(M/A)_c = (1/\rho) \sum_s s^3(1-\beta_s) \exp(\phi_s - \phi_1)/kT. \quad (16)$$

This equation gives information concerning the monolayer condensation, and should agree with the result of the previous work.[2] To prove this, note that (16) gives

$$(M/A)_c \rho/(1-\beta_1) = \sum_s s^3(1-\beta_s)/(1-\beta_1) \times \exp(\phi_s - \phi_1)/kT \quad (17)$$

$$= 1 + \sum_s{}' s^3(1-\beta_s)/(1-\beta_1) \exp(\phi_s - \phi_1)/kT = 1 + \sigma^*, \quad (18)$$

in the notation of reference 2, Eq. (23). But (18) is identical with Eqs. (20) and (22) of the paper quoted, showing that the results are the same.

Equation (15) above leads to the desired relation between the critical gas pressure and the temperature at which the monolayer is to be maintained in the saturated state. Assuming that the gas pressure is so low that it obeys the perfect gas law, it will follow at once from (15) that

$$P = (2\pi m)^{\frac{1}{2}} h^{-3} (kT)^{5/2} \exp(W/kT). \quad (19)$$

Again from reference 2, Eq. (9), it will be seen that the quantity W means the negative heat of

evaporation from the completely clustered monolayer; it is remarkable that this is the only physical parameter, except for the mass m, upon which the minimum gas pressure depends as a function of T. The equation is of course valid only for temperatures below the critical point for the phase change in the monolayer.

The Adsorption Isotherm

It is usual to define the concentration of an immobile monolayer as the ratio between the actual number of sites occupied by adatoms, and the total number of sites. Here the relative concentration of a mobile monolayer at any given temperature will be defined as the ratio of the actual number of adsorbed molecules to the number required to produce saturation at that temperature. Note that this is not the ratio to the number in the condensed state; this part of the theory does not cover conditions in the monolayer after condensation has set in.

Write for the relative condensation

$$\theta=(M/A)/(M/A)_c, \tag{20}$$

and use (18) to deduce that

$$\theta=(M/A)\rho/\{(1+\sigma^*)(1-\beta_1)\}. \tag{21}$$

Then (14) gives

$$\theta=\{(\psi)^s/(1+\sigma^*)\}\sum_s s^3(1-\beta_s)/(1-\beta_1) \times\exp\,(\phi_s-\phi_1)/kT, \tag{22}$$

where

$$\psi=(N/V)/(N/V)_c. \tag{23}$$

This series converges for $\psi<1$. It can always be made to converge as rapidly as desired by taking ψ small enough; which means physically taking conditions far enough from saturation. Assume conditions such that it is enough to take only the first two terms of the series, and write approximately:

$$\theta(1+\sigma)=\psi+8\psi^2\exp\,(\phi_2-\phi_1)/kT. \tag{24}$$

Since far enough from saturation the β_s can all be neglected, these terms have been omitted from (24), and σ written for σ^*, see reference 2, Eq. (27).

In actual cases $(\phi_2-\phi_1)/kT$ is about negative 3, so Eq. (24) can be written approximately

$$\theta(1+\sigma)=\psi/(1-\alpha\psi) \tag{25}$$

or

$$\psi=(1+\sigma)\theta/\{1+\alpha(1+\sigma)\theta\}, \tag{26}$$

where

$$\alpha=8\exp\,(\phi_2-\phi_1)/kT. \tag{27}$$

To express these in physical terms, note the definition (23) and the value (15) of $(N/V)_c$, then writing $N/V=P/kT$, (26) becomes:

$$P=A\theta(1+\sigma)/\{1+\alpha\theta(1+\sigma)\}, \tag{28}$$

where

$$A=(2\pi m)^{\frac{3}{2}}h^{-3}(kT)^{5/2}\exp\,(W/kT) \tag{29}$$

has the same value as the constant in Langmuir's isotherm, namely

$$P=A\theta/(1-\theta). \tag{30}$$

Eq. (28) is in the form of an adsorption isotherm also, but differs slightly from Langmuir's, (30), not only in mathematical form, but physically because of the different meaning of θ.

Numerical Predictions

In practice the fatty acids form mobile monolayers under conditions where gas pressures are negligibly small. From (19) this means that the (negative) value of W must be relatively large. A simple calculation shows that for molecules with mass greater than about 200 units, values of $-W$ greater than about 100×10^{-14} erg will suffice to make the minimum pressure P less than 10^{-4} atmosphere, when T is around 300°K. For pressures to reach as high as 10^{-2} atmosphere at room temperatures presumably smaller molecules will be required, say around 20 mass units, and in this case $-W$ will have to be smaller than about 75×10^{-14} erg.

Even in this case a condensed monolayer will be possible only if the critical point temperature for the phase change is above the range considered, and this can hardly be determined in advance.

The dependence of P as a function of W is thus quite sharp. Should suitable substances be found and the required technique be developed for producing monolayers and dealing with the equilibrium here discussed, Eq. (19) should provide a very useful method of analysis.

The Entropy of Long Chain Compounds in the Gaseous State*

MAURICE L. HUGGINS
Kodak Research Laboratories, Rochester, New York
(Received October 28, 1939)

Equations are derived for the entropy of long chain compounds in the gaseous state at 25°C. (1) The *translational entropy*, computed classically, varies with chain length according to the relation $S_t = a + b \ln n$. (2) *The entropy of rotation of the molecule as a whole*, calculated statistically, assuming either a ball-like molecule or absolutely random kinking, is also linear with respect to $\ln n$. (3) The *entropy of internal vibrations*, assumed (following Pitzer) to be an additive function of contributions associated with the various types of bonds and bond angles present, obeys the equation $S_{iv} = a + bn$. (4) The *entropy of internal randomness*, for randomly-kinked molecules with no rotation, with hindered rotation, or with completely free rotation, is likewise linear in n. The equation deduced for *long* chain paraffins, containing but one adjustable constant (connected with the degree of hindrance of the rotation about the C−C bonds) agrees quite well with values deduced from specific heat data for *short* chain paraffins.

INTRODUCTION

MANY of the properties of high polymers and other substances consisting of very long molecular chains depend to a large extent on the entropy. A knowledge of the dependence of the entropy on the state, composition and chain length is, therefore, of prime importance. As a step in this direction, this paper deals with the dependence on chain length and composition of the entropy in the gaseous state of long chain compounds which may be assumed to be kinked in a random or nearly random manner.

The total entropy may be considered to be equal to the sum of (1) the translational entropy, S_t, (2) the entropy of internal vibrations, S_v, (3) the entropy of external rotation—that is, of rotation of the molecule as a whole—S_{er}, and (4) the entropy of internal randomness, S_{ir}, due to alternative orientations and more-or-less free rotation and oscillation about the interatomic bonds.

THE TRANSLATIONAL ENTROPY

The molal translational entropy of a dilute gas is given[1, 2] by the equation

$$S_t = R \ln \frac{V}{N}\left(\frac{2\pi mkT}{h^2}\right)^{3/2} e^{5/2}, \qquad (1)$$

in which R is the gas constant per mole, in calories per degree, V is the molal volume, m is the mass of one molecule, T is the absolute temperature, k is the Boltzmann constant, h is Planck's constant, and e is the base of natural logarithms.

Into this equation one substitutes for the volume

$$V = \frac{R'T}{P}, \qquad (2)$$

where R' is the gas constant per mole in cc—atmos. per degree and P is the pressure in atmospheres, and for the mass

$$m = m_0 n = \frac{M_0 n}{N}, \qquad (3)$$

where m_0 is the mass of one of the n "submolecules" in each molecule and M_0 is the sum of the atomic weights of the atoms in the submolecule. (For a long paraffin chain, $(CH_2)_n$, M_0 is 14.03.)

One thus obtains the equation

$$S_t = R \ln \left[\frac{R'(2\pi k)^{3/2} e^{5/2}}{h^3 N^{5/2}} \cdot \frac{T^{5/2}}{P} \cdot M_0^{3/2} n^{3/2}\right]. \qquad (4)$$

At 298.1°K and 1 atmosphere, this reduces to

$$S_t = 26.0 + \tfrac{3}{2} R \ln M_0 + \tfrac{3}{2} R \ln n. \qquad (5)$$

---

* Contribution No. 692 from the Kodak Research Laboratories. Much of the material in this article was presented in a paper before the Division of Physical and Inorganic Chemistry at the Milwaukee Meeting of the American Chemical Society, September 7, 1938.

[1] G. N. Lewis and J. E. Mayer, Proc. Nat. Acad. Sci. **15**, 208 (1929).

[2] W. F. Giauque, J. Am. Chem. Soc. **52**, 4808 (1930).

For a long paraffin chain,

$$S_t = 33.8 + \tfrac{3}{2}R \ln n. \qquad (6)$$

The Vibrational Entropy

If the vibrational frequencies are known, the vibrational entropy can be calculated in the usual way[2, 3] as the sum of Einstein functions. In the absence of the direct experimental frequencies, one may assume a uniform frequency for each C−H bond, another for each C−C bond, another for each H−C−H bond angle, etc. For a long paraffin chain, tentatively adopting Pitzer's[4] frequency assignments, the entropy contributions given in the last column of Table I are calculated. Unfortunately, the lowest frequencies, which are most important for this purpose, are least well known. The calculated S_v may therefore be considerably in error.

For long chain molecules in general, one may put

$$S_v = k_v' + k_v n, \qquad (7)$$

computing rough values of k_v and k_v' as in Table I, if the requisite fundamental data are obtainable.

The Entropy of Rotation of the Molecule as a Whole

The entropy associated with rotation of a mole of rigid molecules, all alike, is given by the following equation:[5–7]

$$S_{er} = R \ln \left[\frac{1}{\pi\sigma} \left(\frac{8\pi^3 keT}{h^2} \right)^{\frac{3}{2}} (I_X I_Y I_Z)^{\frac{1}{2}} \right]. \qquad (8)$$

Table I. *Rough calculation of the vibrational entropy for normal paraffin hydrocarbons.*

Type	Number	Frequency	S_v (298°K)
CH	$2n+2$	3000 cm^{-1}	0.000
HCH	$n+4$	1440	$.064+0.016n$
CC	$n-1$	1000	$-.092+.092n$
HCC	$3n-2$	950	$-.226+.339n$
CCC	$n-2$	320	$-2.628+1.314n$
		Total	$S_v = -2.88+1.76n$

[3] L. S. Kassel, Chem. Rev. **18**, 277 (1936).
[4] K. S. Pitzer, J. Chem. Phys. **5**, 473 (1937).
[5] J. E. Mayer, S. Brunauer and M. G. Mayer, J. Am. Chem. Soc. **55**, 37 (1933).
[6] J. O. Halford, J. Chem. Phys. **2**, 694 (1934).
[7] M. L. Eidinoff and J. G. Aston, J. Chem. Phys. **3**, 379 (1935).

Here σ is the symmetry number, which is unity for kinked long chain molecules, and I_X, I_Y and I_Z are the moments of inertia of the molecule about mutually perpendicular X, Y and Z axes through the center of gravity.

Randomly-kinked molecules will, in general, not have the same moments of inertia. Hence, one must average, as follows:

$$S_{er} = R \ln \left[\frac{1}{\pi} \left(\frac{8\pi^3 keT}{h^2} \right)^{\frac{1}{2}} \right] + \frac{R}{2} \langle \ln (I_X I_Y I_Z) \rangle_{Av} \qquad (9)$$

$$= 284.5 + \frac{R}{2} \langle \ln (I_X I_Y I_Z) \rangle_{Av} \text{ at } 298°\text{K}. \qquad (10)$$

Although the individual moments, I_X, etc., of the molecules in a given sample of gas doubtless vary considerably from the average moments, $\bar{I}_X$, etc., the moment products, $I_X \cdot I_Y \cdot I_Z$, would be expected to be much more closely bunched around the average moment product. Likewise, the logarithms of the moment products, $\ln (I_X \cdot I_Y \cdot I_Z)$, would be expected to be closely bunched around the average, $\langle \ln (I_X \cdot I_Y \cdot I_Z) \rangle_{Av}$. The following approximation, therefore, introduces but little error.

$$\langle \ln (I_X \cdot I_Y \cdot I_Z) \rangle_{Av} = \ln \langle (I_X \cdot I_Y \cdot I_Z) \rangle_{Av}. \qquad (11)$$

Another justification for the use of this approximation is the fact that, on the average, randomly-kinked molecules are not very elongated. Kuhn[8] has shown that the root-mean-square length of the straight line between the first and the last atoms is only $\sqrt{6}$ times the root-mean-square distance of the middle atom from this straight line. (See Eqs. (16) and (19) below.)

Moreover, it seems likely, as Langmuir[9] has pointed out, that the van der Waals attractions between different parts of the molecular chain cause the molecule, in the gaseous state, to coil up into a roughly spherical ball. If so, the three moments of inertia of a given molecule are nearly equal to each other and to the moments of all the other molecules. Eq. (11) is then a very good approximation.

[8] W. Kuhn, Kolloid Zeits. **68**, 2 (1934).
[9] I. Langmuir, in *Colloid Chemistry*, edited by Jerome Alexander (Chemical Catalogue Co., New York, 1926), Vol. I, p. 525.

Two calculations of S_{er} will be made: one for spherical molecules having a uniform density equal to the density the substances would have in the liquid state at that temperature; the other for symmetrical "average" molecules, all alike, having dimensions equal to the root-mean-square dimensions calculated on the assumption of absolutely random kinking. The actual value of S_{er} would be expected to be between these two results.

For spherical molecules of uniform density ρ and radius r,

$$\bar{I}_X=\bar{I}_Y=\bar{I}_Z=\tfrac{2}{5}mr^2 \tag{12}$$

and

$$\rho=\frac{m}{(4/3)\pi r^3}. \tag{13}$$

Eliminating r from these equations, using Eq. (3), and substituting into Eq. (11), leads to the relation

$$\langle \ln (I_X I_Y I_Z)\rangle_{Av}=-5.62+\ln\left(\frac{M_0{}^5 n^5}{N^5\rho^2}\right). \tag{14}$$

For a long paraffin chain, giving ρ the value 0.78 g/cc,

$$\langle \ln (I_X I_Y I_Z)\rangle_{Av}=-265.7+5\ln n. \tag{15}$$

For large, randomly-kinked chain molecules, the mean square of the distance between the first atom and the ith atom is given, except for very small values of i, by the relation[8, 10, 11]

$$\langle R_i{}^2\rangle_{Av}=B_\infty l^2 i, \tag{16}$$

where l is the distance ($1.54\cdot 10^{-8}$ cm for a paraffin chain) between neighboring atoms in the chain and B_∞ is related to the angle α between each bond in the chain and the extension of either of the two adjacent bonds by the relation

$$B_\infty=\frac{1+\cos\alpha}{1-\cos\alpha}. \tag{17}$$

For "tetrahedral" angles,

$$B_\infty=2. \tag{18}$$

The mean square of the distance between the ith atom and the straight line joining the end atoms of a randomly-kinked chain is given (see Appendix) by the equation

$$\langle r_i{}^2\rangle_{Av}=\tfrac{2}{3}B_\infty l^2\left(i-\frac{i^2}{n}\right), \tag{19}$$

except when i is small.

The calculation of moments of inertia is now made for a symmetrical molecule, having $R_i{}^2$ and $r_i{}^2$ values equal to the averages in Eqs. (16) and (19), relative to mutually perpendicular X', Y', and Z axes through one end atom, the Z axis passing also through the other end atom. These moments of inertia are given by the equations

$$I_{X'}=m_0(\sum y_i{}^2+\sum z_i{}^2), \tag{20}$$

$$I_{Y'}=m_0(\sum x_i{}^2+\sum z_i{}^2), \tag{21}$$

and

$$I_Z=m_0(\sum x_i{}^2+\sum y_i{}^2). \tag{22}$$

Now,

$$\sum x_i{}^2=\sum y_i{}^2=\tfrac{1}{2}\sum r_i{}^2=\tfrac{1}{3}B_\infty l^2\left(\sum i-\frac{1}{n}\sum i^2\right) \tag{23}$$

and

$$\sum z_i{}^2=\sum(R_i{}^2-r_i{}^2)=\tfrac{1}{3}B_\infty l^2\left(\sum i+\frac{2}{n}\sum i^2\right). \tag{24}$$

For large i,

$$\sum_1^n i=\frac{n^2}{2} \tag{25}$$

and

$$\sum_1^n i^2=\frac{n^3}{3}. \tag{26}$$

Substituting, one obtains

$$I_{X'}=I_{Y'}=\frac{4}{9}B_\infty m_0 l^2 n^2 \tag{27}$$

and

$$I_Z=\frac{1}{9}B_\infty m_0 l^2 n^2. \tag{28}$$

The center of gravity of this hypothetical symmetrical molecule is on the Z axis, midway between the two end atoms. The moments of inertia about X and Y axes through this point are obtained by subtraction from $I_{X'}$ and $I_{Y'}$ of the product of the mass of the molecule by the square of the distance between the X and X'

[10] H. Eyring, Phys. Rev. **39**, 746 (1932).
[11] E. Guth and H. Mark, Monatsh. f. Chem. **65**, 94 (1934).

(or Y and Y') axes:

$$I_X = I_Y = I_{X'} = \frac{1}{4} B_\infty m_0 l^2 n^2 = \frac{7}{36} B_\infty m_0 l^2 n^2. \quad (29)$$

It is reasonable to assume that moments of inertia calculated according to Eqs. (28) and (29) are fairly close approximations to the average moments for randomly-kinked molecules. Substituting in Eq. (11) gives

$$\langle \ln (I_X I_Y I_Z) \rangle_{Av} = -5.47 + 3 \ln \left(\frac{B_\infty M_0 l^2 n^2}{N} \right). \quad (30)$$

For a long paraffin chain,

$$\langle \ln (I_X I_Y I_Z) \rangle_{Av} = -267.6 + 6 \ln n. \quad (31)$$

In general, the center of gravity of a randomly-kinked molecule is, of course, not exactly at the midpoint of the straight line joining the end atoms. The average moments of inertia about axes through the actual centers of gravity are, therefore, different from those just deduced. To correct for this, a statistical calculation has been made of the average squares of the coordinates of the center of gravity, relative to the origin at the midpoint of the line joining the end atoms, with the following results:

$$\overline{x_0^2} = \overline{y_0^2} \approx 0.034 B_\infty l^2 \quad (32)$$

$$\bar{z}_0^2 \approx 0.0033 B_\infty l^2 n. \quad (33)$$

Since the decrease in $\langle \ln (I_X I_Y I_Z) \rangle_{Av}$ due to this correction is very small (less than 0.1), the details of this calculation are not reproduced.

Possibly more important is the neglect in the above treatment of any allowance for the finite sizes of the atoms. It was assumed that *all* orientations (consistent with a constant bond angle) of each bond relative to an adjacent bond are possible. Actually, some are blocked, because of the large repulsions between atoms when their centers approach each other too closely. As a result, the molecules are, on the average, somewhat more extended—less closely packed—than if truly randomly kinked.[12] For a first approximation, one may assume a slightly larger "effective" angle between adjacent bonds (a smaller "effective" α) and hence a larger "effective" B_∞ and a larger coefficient of $\ln n$ in Eq. (31).

This correction may be important for molecules in the liquid state, but in the gaseous state it is probably more than balanced by the correction due to the van der Waals attractions within the molecule. As a comparison of Eqs. (15) and (31) shows, these attractions tend to decrease the coefficient of $\ln n$.

The difference between Eq. (15) and Eq. (31) is relatively small and unimportant for the present purpose. The former is probably more nearly correct.

Substituting Eqs. (14) and (30) into Eq. (10), one now obtains at 298°K

$$S_{cr} = 7 + \frac{5}{2} R \ln M_0 - R \ln \rho + \frac{5}{2} R \ln n \quad (34)$$

on the assumption of spherical molecules, and

$$S_{cr} = 116 + \frac{3}{2} R \ln (B_\infty M_0 l^2) + 3R \ln n, \quad (35)$$

assuming random-kinking. Using Eqs. (15) and (31), for large paraffin chain molecules, these equations reduce to

$$S_{cr} = 21 + \frac{5}{2} R \ln n \quad (36)$$

and

$$S_{cr} = 23 + 3R \ln n. \quad (37)$$

Entropy of Internal Randomness

One must still take account of the entropy due to alternative orientations, rotations and oscillations around the bonds within the molecules. This entropy contribution would be expected to be a linear function of n:

$$S_{ir} = k_{ir}' + k_{ir} n. \quad (38)$$

The constants must depend on the flexibility of the chain and so on the size and shape of the energy humps resisting free rotation.

For the hypothetical case of rigid molecules, with three equally probable orientations around each bond,

$$S_{ir} = R \ln 3^{n-3} = -6 + 2.18n. \quad (39)$$

For the opposite extreme—the hypothetical case of absolutely free rotation about each bond

[12] L. Laskowski and R. E. Burk, J. Chem. Phys. 7, 465 (1939).

—a theoretical calculation has been made, yielding

$$S_{ir} = -123 - \frac{3}{2}R \ln (B_\infty M_0 l^2) + \left[36 + \frac{R}{2} \ln (TB_\infty M_0 l^2)\right] n. \quad (40)$$

For normal paraffin chains at 298°K, (*if* there were free rotation)

$$S_{ir} = -26 + 9n. \quad (41)$$

Since the method of derivation is quite complex and involves certain somewhat questionable approximations, it will not be described here. The writer believes, however, that the results obtained are not far from correct.

For actual chains, in which the rotations are known to be considerably restricted, one would expect constants intermediate between those of Eq. (39) and those of Eq. (40)—or Eq. (41) for paraffins.

According to Eqs. (39) and (41), the simple relation

$$k_{ir}' = -3k_{ir} \quad (42)$$

holds approximately for hypothetical paraffin-like chains, in which either free rotation or no rotation is assumed. Making the reasonable assumption that it also holds for actual paraffins, in which the rotation is hindered, one obtains

$$S_{ir} = -3k_{ir} + k_{ir} n. \quad (43)$$

This should be a sufficiently good approximation, for very long chains at least. (Although, from theoretical considerations, deviations from Eqs. (39), (41) and (43) of the order of magnitude of, say, 15 units would not be surprising; such deviations would be of importance only for short chains.)

The Total Entropy

Adding together Eqs. (5), (7), (34) and (43), the total entropy at 298°K and 1 atmos. of a ball-like molecule is

$$S = 33 + k_v' + k_{ir}' + R \ln \left(\frac{M_0^4}{\rho}\right) + 4R \ln n + (k_v + k_{ir}) n. \quad (44)$$

For a randomly-kinked molecule, using Eq. (35) instead of Eq. (34):

$$S = 142 + k_v' + k_{ir}' + 3R \ln (M_0 B_\infty^{\frac{1}{2}} l) + \frac{9}{2}R \ln n + (k_v + k_{ir}) n. \quad (45)$$

These sums reduce, for long chain paraffins, to

$$S = 52 - 3k_{ir} + 8 \ln n + (1.8 + k_{ir}) n \quad (46)$$

and

$$S = 54 - 3k_{ir} + 9 \ln n + (1.8 + k_{ir}) n, \quad (47)$$

respectively.

Although these equations have been derived for chain molecules in which n is large, and would be expected to be inaccurate for short chains, a comparison with the values which have previously been deduced for the simplest normal paraffins is of interest. Such a comparison is shown in Fig. 1, in which the solid line represents Eq. (46), with k_{ir} given the arbitrary value 6.2. The values for the individual points, listed in Table II, were obtained largely from specific heat data.

The values given for the last four compounds were computed from the $S_{298}°$ values given by Parks,[16] using estimates of the heats of vaporization kindly furnished by Rossini,[17] and vapor pressure data from Landolt-Börnstein's *Tabellen*, interpolated and extrapolated to 25°C.

For comparison, curves for rigid chains and for absolutely free rotation, calculated on the assumption of spherical molecules rather than

TABLE II. *Entropies of gaseous normal paraffin hydrocarbons at 25°C.*

FORMULA	S^0_{298}	REFERENCE
CH_4	44.60±0.0	4
C_2H_6	54.85± .2	13
C_3H_8	64.7 ± .3	14
C_4H_{10}	75.8 ± .8	15
C_5H_{12}	82	
C_7H_{16}	102	
C_8H_{18}	111	
$C_{12}H_{26}$	147	

[13] R. K. Witt and J. D. Kemp, J. Am. Chem. Soc. **59**, 273 (1937).
[14] J. D. Kemp and C. J. Egan, J. Am. Chem. Soc. **60**, 1521 (1938).
[15] G. S. Parks, C. H. Shomate, W. D. Kennedy and B. L. Crawford, Jr., J. Chem. Phys. **5**, 359 (1937). This value "probably errs on the side of being a trifle high."
[16] G. S. Parks, Chem. Rev. **18**, 325 (1936).
[17] F. D. Rossini, private communication.

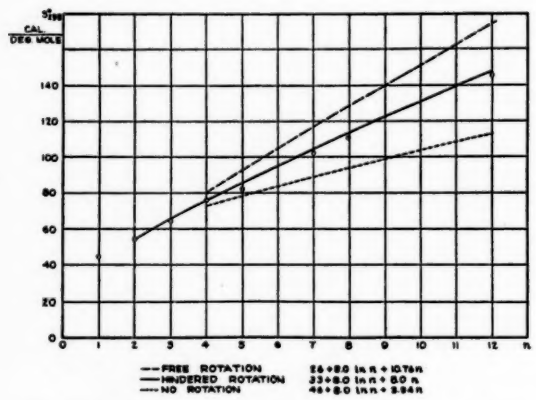

FIG. 1. Comparison of curves representing equations for the entropy of normal paraffin hydrocarbons (derived on the assumption of long chains) with previously calculated values for short chain paraffins. – – – – – Free rotation, $26+8.0 \ln n+10.76n$. ———— Hindered rotation, $33+8.0 \ln n+8.0n$. - - - - - No rotation, $46+8.0 \ln n+3.94n$.

for completely random kinking, are also shown in Fig. 1.

From the agreement shown in the figure one would seem to be justified in using equations of the form of Eq. (46), with appropriate changes of the constants, to deduce approximate entropy values for very long chain compounds in the gaseous state.

APPENDIX

Derivation of equations for the average distance and average square of the distance between the *i*th atom in a randomly-kinked chain and the straight line joining the end atoms

Kuhn[8] has derived the equations for the middle atom of the chain. His procedure, suitably generalized, is followed here.

For any value of the bond angle other than 90° or 180°, the directions of any two bonds are independent of each other, provided they are separated by a sufficient number of intervening bonds. Let the whole chain be divided into N segments, each large enough so that the straight lines connecting the end atoms of each segment are independent of each other as regards direction. Let the average length of the projection of one of these N straight lines on one of these mutually perpendicular axes X, Y and Z be called b. On the average, each segment adds or subtracts a length b to the projection of the chain on each of these axes.

Taking the origin of coordinates at one end of the chain, let the Z axis pass through the other end also. Consider the x coordinates of the atom at the end of the jth segment. Let P_+ be the number of positive values of b and P_- the number of negative values of b between the origin and this atom. Then

$$P_+ + P_- = j. \tag{48}$$

Defining a number p by the relation

$$P_+ - P_- = 2p, \tag{49}$$

one deduces

$$P_+ = j/2 + p \tag{50}$$

and

$$P_- = j/2 - p. \tag{51}$$

For the part of the chain between the atom being considered and the end ($j=N$), similarly:

$$P_+' - P_-' = -2p, \tag{52}$$

$$P_+' + P_-' = N - j, \tag{53}$$

$$P_+' = N/2 - j/2 - p, \tag{54}$$

$$P_-' = N/2 - j/2 + p. \tag{55}$$

The probability of having P_+ additions and P_- subtractions in the first part of the chain and P_+' additions and P_-' subtractions in the second part is

$$W_{P_+P_+'} = K \frac{j!}{P_+!P_-!} \cdot \frac{(N-j)!}{P_+'!P_-'!}. \tag{56}$$

Substituting Eqs. (50), (51), (54) and (55) and using Stirling's approximation for the factorials, one obtains

$$W_{P_+P_+'} = \frac{K \cdot 2^{j+1} \cdot 2^{N-j+1}}{2\pi j^{\frac{1}{2}}(N-j)^{\frac{1}{2}} \left(1+\frac{2p}{j}\right)^{j/2+p+\frac{1}{2}} \left(1-\frac{2p}{j}\right)^{j/2-p+\frac{1}{2}} \left(1+\frac{2p}{N-j}\right)^{N/2-j/2+p+\frac{1}{2}} \left(1-\frac{2p}{N-j}\right)^{N/2-j/2-p+\frac{1}{2}}}. \tag{57}$$

Taking logarithms, expanding ln $(1+2p/j)$, etc., dropping terms which are negligible for large j or large $(N-j)$, and taking the antilogarithm of the result, the following equation is obtained:

$$W_{P_+P_+'}=K' \exp\left(-\frac{2p^2N}{j(N-j)}\right). \quad (58)$$

From the relation

$$\int_{-\infty}^{\infty} W_{P_+P_+'}dp=1, \quad (59)$$

one deduces

$$K'=\left(\frac{2N}{\pi j(N-j)}\right)^{\frac{1}{2}}. \quad (60)$$

Substituting this and also

$$p=x/2b \quad (61)$$

and

$$dp=dx/2b \quad (62)$$

into Eq. (58), there results:

$$W_x dx=\frac{1}{2b}\left(\frac{2N}{\pi j(N-j)}\right)^{\frac{1}{2}} \times\exp\left(-\frac{Nx^2}{2b^2j(N-j)}\right)dx. \quad (63)$$

Similarly,

$$W_y dy=\frac{1}{2b}\left(\frac{2N}{\pi j(N-j)}\right)^{\frac{1}{2}} \times\exp\left(-\frac{Ny^2}{2b^2j(N-j)}\right)dy. \quad (64)$$

For a given pair of x and y values,

$$W_x W_y dxdy=\frac{N}{2\pi b^2 j(N-j)} \times\exp\left(-\frac{N(x^2+y^2)}{2b^2j(N-j)}\right)dxdy. \quad (65)$$

The distance r of the atom being considered from the Z axis is given by the equation

$$r^2=x^2+y^2. \quad (66)$$

Hence,

$$W_r dr=\frac{N}{b^2j(N-j)} \exp\left(-\frac{Nr^2}{2b^2j(N-j)}\right)rdr. \quad (67)$$

Averaging,

$$\bar{r}=\int_0^{\infty} W_r r dr=b\left(\frac{\pi j(N-j)}{2N}\right)^{\frac{1}{2}} \quad (68)$$

and

$$\overline{r^2}=\int_0^{\infty} W_r r^2 dr=\frac{2b^2j(N-j)}{N}. \quad (69)$$

One now introduces the proportionality

$$j/N=i/n \quad (70)$$

and the relation

$$b^2N=B_\infty l^2 n/3, \quad (71)$$

obtained by Kuhn[8] from a comparison of his statistical equation for R^2 with the equation derived for this quantity by Eyring.[10] Substitution into Eqs. (68) and (69) gives

$$\bar{r}=\left[\frac{\pi}{6}B_\infty l^2 i\left(1-\frac{i}{n}\right)\right]^{\frac{1}{2}} \quad (72)$$

and

$$\overline{r^2}=\frac{2}{3}B_\infty l^2 i\left(1-\frac{i}{n}\right). \quad (73)$$

This last equation is identical with Eq. (19) above.

Directed Valence*

GEORGE E. KIMBALL
Department of Chemistry, Columbia University, New York, New York

(Received October 19, 1939)

The problem of directed valence is treated from a group theory point of view. A method is developed by which the possibility of formation of covalent bonds in any spatial arrangement from a given electron configuration can be tested. The same method also determines the possibilities of double and triple bond formation. Previous results in the field of directed valence are extended to cover all possible configurations from two to eight *s*, *p*, or *d* electrons, and the possibilities of double bond formation in each case. A number of examples are discussed.

INTRODUCTION

PROBLEMS of directed valence, like most problems of molecular structure, can be attacked by either of two methods: the method of localized electron pairs (Heitler-London) or the method of molecular orbitals (Hund-Mulliken). While it is now realized[1] that these methods are but different starting approximations to the same final solution, each has its advantages in obtaining qualitative results. Theories of directed valence based on the methods of localized pairs have been developed by Slater[2] and Pauling[3] and extended by Hultgren.[4] The method of molecular orbitals has been developed principally by Hund[5] and Mulliken.[6] These methods have been compared extensively by Van Vleck and Sherman.[1]

In the previous papers no attempt has been made to discover *all* the possible stable electron groups which lead to directed valence bonds, nor have the possibilities of double bond formation been completely explored. In the present paper both of these deficiencies in the theory have been removed.

METHOD

Pauling's method consists of finding linear combinations of *s*, *p*, and *d* orbitals which differ from each other only in direction. Thus he has found combinations which are directed toward the corners of a tetrahedron, others directed toward the corners of a square, and others directed toward the corners of an octohedron. Electrons occupying these new orbitals can then resonate with unpaired electrons occupying orbitals of other atoms lying in the directions of these new orbitals and so form covalent bonds with these atoms. The further these orbitals project in the direction of the surrounding atoms, the stronger should be the resulting bonds.

In order to construct such sets of orbitals, it is most convenient to make use of group theory. Each set of equivalent directed valence orbitals has a characteristic symmetry group. If the operations of this group are performed on the orbitals, a representation, which is usually reducible, is generated. By means of the character table of the group[7] this representation, which we shall call the σ representation, can be reduced to its component irreducible representations. The *s*, *p*, and *d* orbitals of the atom also form representations of the group, and can also be divided into sets which form irreducible representations.[8]

Let us refer to the set of equivalent valence orbitals as the set $\mathfrak{S}$. If the transformation which reduces this set is T, then the set $T\mathfrak{S}$ can be broken up into subsets, each of which forms a basis for one of the irreducible representations of the symmetry group of $\mathfrak{S}$.

$$T\mathfrak{S}=\sum a_i\mathfrak{S}_i, \qquad (1)$$

* Presented at the Boston meeting of the American Chemical Society, September 15, 1939. Publication assisted by the Ernest Kempton Adams Fund for Physical Research of Columbia University.

[1] Van Vleck and Sherman, Rev. Mod. Phys. **7**, 167 (1935).
[2] Slater, Phys. Rev. **37**, 841 (1931).
[3] Pauling, J. Am. Chem. Soc. **53**, 1367, 3225 (1931).
[4] Hultgren, Phys. Rev. **40**, 891 (1932).
[5] Hund, Zeits. f. Physik **73**, 1 (1931); **73**, 565 (1931); **74**, 429 (1932).
[6] Mulliken, Phys. Rev. **40**, 55 (1932); **41**, 49 (1932); **41**, 751 (1932); **43**, 279 (1933).
[7] For the group theoretical methods used here see Wigner, *Gruppentheorie* (Vieweg, Braunschweig, 1931); Weyl, *Theory of Groups and Quantum Mechanics* (tr. Robertson) (Methuen, London, 1931); Van der Waerden, *Gruppentheoretische Methoden in der Quantenmechanik* (Springer, Berlin, 1932).
[8] Bethe, Ann. d. Physik (5) **3**, 133 (1929).

where $\mathfrak{S}_i$ belongs to the ith irreducible representation. If we let $\mathfrak{R}$ be the set of available orbitals of the atom, these may always be chosen so that they fall into subsets each of which is a basis for one of the irreducible representations:

$$\mathfrak{R}=\sum b_i\mathfrak{R}_i. \tag{2}$$

If each of the coefficients b_i in (2) is equal to or greater than the corresponding a_i in (1), we may form the new subset $\mathfrak{R}'$, given by

$$\mathfrak{R}'=\sum a_i\mathfrak{R}_i, \tag{3}$$

in which each orbital transforms in exactly the same way as the corresponding orbital in (1). If we now apply the inverse transformation T^{-1} to this set we obtain a set of orbitals $T^{-1}\mathfrak{R}'$ which must have exactly the symmetry properties of the desired set $\mathfrak{S}$.

To illustrate this process, consider the set $\mathfrak{S}=\sigma_1+\sigma_2+\sigma_3$ consisting of three valence orbitals lying in a plane and making equal angles of 120° with each other. If the atom in question has available s, p, and d orbitals, the set $\mathfrak{R}$ consists of the nine orbitals s, p_x, p_y, p_z, d_z, d_{xz}, d_{yz}, d_{xy}, d_{x+y}. The symmetry group of $\mathfrak{S}$ is D_{3h}, and the set $\mathfrak{S}$ may be reduced by the transformation

$$\begin{aligned}\sigma_1'&=1/\sqrt{3}(\sigma_1+\sigma_2+\sigma_3)\\ \sigma_2'&=1/\sqrt{6}(2\sigma_1-\sigma_2-\sigma_3)\\ \sigma_3'&=1/\sqrt{2}(\sigma_2-\sigma_3).\end{aligned} \tag{3}$$

Of these orbitals, σ_1' belongs to the representation[9] A_1' while σ_2' and σ_3' belong to E'. Hence we find for (1)

$$\mathfrak{S}=A_1'+E'. \tag{4}$$

TABLE I. *Character table for trigonal orbitals.*

D_{3h}	E	σh	$2C_3$	$2S_3$	$3C_2$	$3\sigma v$
A_1'	1	1	1	1	1	1
A_2'	1	1	1	1	−1	−1
A_1''	1	−1	1	−1	1	−1
A_2''	1	−1	1	−1	−1	1
E'	2	2	−1	−1	0	0
E''	2	−2	−1	1	0	0
s	1	1	1	1	1	1
p	3	1	0	−2	−1	1
d	5	1	−1	1	1	1
σ	3	3	0	0	1	1
π	6	0	0	0	−2	0

[9] The notation used here is that of Mulliken, Phys. Rev. **43**, 279 (1933).

The set $\mathfrak{R}$ is already reduced, for s and d_z belong to A_1', p_z to A_2'', the pairs p_x, p_y and d_{xy}, $-d_{x+y}$ to E', and the pair d_{xz}, d_{yz} to E''. Hence (2) becomes

$$\mathfrak{R}=2A_1'+A_2''+E'+E''. \tag{5}$$

Since the coefficients in (5) are each not less than the corresponding coefficient in (4), the desired directed orbitals are possible. In fact, since we have a choice between s and d_z for the orbital

TABLE II. *Reduction table for trigonal orbitals.*

D_{3h}	A_1'	A_1''	A_2'	A_2''	E'	E''
s	1	0	0	0	0	0
p	0	0	0	1	1	0
d	1	0	0	0	1	1
σ	1	0	0	0	1	0
π	0	0	1	1	1	1

belonging to A_1', we may construct two different sets of directed orbitals. If we choose for $\mathfrak{R}'$ the set

$$\mathfrak{R}'=s+p_x+p_y \tag{6}$$

and apply the inverse transformation

$$\begin{aligned}\sigma_1&=\frac{1}{\sqrt{3}}\sigma_1'+\frac{2}{\sqrt{6}}\sigma_2',\\ \sigma_2&=\frac{1}{\sqrt{3}}\sigma_1'-\frac{1}{\sqrt{6}}\sigma_2'+\frac{1}{\sqrt{2}}\sigma_3',\\ \sigma_3&=\frac{1}{\sqrt{3}}\sigma_1'-\frac{1}{\sqrt{6}}\sigma_2'-\frac{1}{\sqrt{2}}\sigma_3',\end{aligned} \tag{7}$$

we obtain Pauling's trigonal orbitals

$$\begin{aligned}\sigma_1&=\frac{1}{\sqrt{3}}s+\frac{2}{\sqrt{6}}p_x,\\ \sigma_2&=\frac{1}{\sqrt{3}}s-\frac{1}{\sqrt{6}}p_x+\frac{1}{\sqrt{2}}p_y,\\ \sigma_3&=\frac{1}{\sqrt{3}}s-\frac{1}{\sqrt{6}}p_x-\frac{1}{\sqrt{2}}p_y.\end{aligned} \tag{8}$$

On the other hand, this theory shows that we can everywhere replace s by d_z, or in fact by any linear combination $\alpha s+\beta d_z$ provided $\alpha^2+\beta^2=1$. Similarly p_x and p_y can be replaced by d_{xy} and d_{x+y}.

It is not necessary, however, to carry out the actual determination of T and the reduction of $\mathfrak{S}$ and $\mathfrak{R}$ to decide whether or not a given set of directed orbitals is obtainable from given atomic orbitals, for the coefficients a_i and b_i can be obtained very simply from the character tables of $\mathfrak{S}$ and $\mathfrak{R}$. The transformation matrices of the σ representation can be written down and the trace of each gives the character for the corresponding element of the group. The characters for $\mathfrak{R}$ are easily found by the method of Bethe.[8] We can thus construct a character table for the representations based on $\mathfrak{S}$ and $\mathfrak{R}$. We also can enter in the same table the characters for the irreducible representations, as given for example by Mulliken.[9] Such a character table for the plane trigonal case we have been considering is shown in Table I. By means of the orthogonality theorems for group characters, the coefficients a_i and b_i can easily be found. These are entered in a second table, to which I shall refer as the reduction table. The reduction table for our trigonal case is shown in Table II. Comparing the coefficients a_i (given in the row marked σ) with the coefficients b_i (given in the rows marked s, p, and d) we see immediately that the trigonal orbitals require one orbital which may be either s or d, and two p orbitals (remembering that the representation E' is of degree two) or two d orbitals. Hence the possible valence configurations are sp^2, dp^2, sd^2, and d^3.

It is interesting to note that the method of molecular orbitals leads to identical results, but by a rather different route. In this method we consider first the set of orbitals on the atoms surrounding the central atom. If this set consists of orbitals symmetrical about the line joining each external atom to the central atom, then these external orbitals form a basis for a representation of the symmetry group which is identical with the σ representation. The reduction of this representation then corresponds to the resonance of these external orbitals among themselves. The formation of molecular orbitals then takes place by the interaction between these reduced external orbitals and the orbitals of the central atom. This interaction can only take place, however, between orbitals belonging to the same representation. Hence, to obtain a set of molecular orbitals equal in number to the number of external atoms, it is necessary that each of the reduced external orbitals be matched with an orbital from the set $\mathfrak{R}$ which belongs to the same representation. The condition for this is again that $b_i \geqslant a_i$, so that the same result is reached as before.

The possibilities of double or triple bond formation are most easily discussed in terms of molecular orbitals. The principal type of multiple bond consists of two parts: first, a pair of electrons in an orbital symmetrical about the axis of the bond; and second, one or more pairs of electrons in orbitals which are not symmetrical about the axis. The first pair of electrons form a bond which differs in no way from the ordinary single, or σ, bond. The other pairs are ordinarily in orbitals which are antisymmetric with respect to a plane passed through the axis. They may be regarded as formed by the interaction of two p orbitals, one on each atom, with axes parallel to each other and perpendicular to the axis of the bond. We shall refer to orbitals of this type as π orbitals.

In a polyatomic molecule, consisting of a central atom and a number of external atoms bound to it, bonds of this type may also be formed. As far as the external atoms are concerned, the condition for the formation of π bonds is the presence of p orbitals at right angles to the bond axes. These p orbitals, however, will resonate among themselves to form new orbitals which are bases of irreducible representations of the symmetry group of the molecule. This reduction can be carried out in the same way as the reduction of the σ representation. We first determine the representation generated by the p orbitals of the external atoms. Since there are two such p orbitals per external atom, this representation, which will be referred to as the π representation, will have a degree twice that of the σ representation. The characters of this representation are then computed, and entered in the character table. This has been done for the case of a plane trigonal molecule in Table I. The component irreducible representations are found as before, and entered in the reduction table.

The condition for the formation of a π bond is now that there be an orbital of the central atom belonging to the same representation as one of

TABLE III. *Resolution table for linear bonds.*

$D_{\infty h}$	Σ_g^+	Σ_u^+	Π_g	Π_u	Δ_g	Δ_u
s	1	0	0	0	0	0
p	0	1	0	1	0	0
d	1	0	1	0	1	0
σ	1	1	0	0	0	0
π	0	0	1	1	0	0

TABLE IV. *Resolution table for angular bonds.*

C_{2v}	A_1	A_2	B_1	B_2
s	1	0	0	0
p	1	0	1	1
d	2	1	1	1
σ	1	0	0	1
π	1	1	1	1

the irreducible components of the π representation. Since this molecule is already supposed to be held together by σ bonds, it is not necessary that all of the irreducible components of the π representation be matched by orbitals of the central atom. However, unless at least half of the irreducible components of the π representation are so matched, it will be impossible to localize the π bonds, and the resulting molecule will be of the type ordinarily written with resonating double bonds.

Thus in the plane trigonal case, Table II shows that π bond formation is possible through the p orbital belonging to $A_2''(p_z)$, the d orbitals belonging to $E''(d_{xz},d_{yz})$ or through the two orbitals belonging to E' which are not used in forming the original σ bonds. Since, however, the σ bonds are probably formed by a mixture of both the p and the d E' orbitals, these last two π bonds are probably weaker than the others. In general we shall divide the π bonds into two classes, calling them "strong" if they belong to representations not used in σ bond formation, and "weak" if they belong to those representations already used in σ bond formation.

Because of the "resonating" character of π bonds, it is usually difficult to form a mental picture of them. In this trigonal case which we have been discussing, we may imagine the p_z orbital of the central atom to interact in turn with the p_z orbitals of the external atoms. If the orbitals d_{xz} and d_{yz} are available, these may be combined with p_z, in the same way that p_x and p_y can be combined with s, to form three directed π orbitals. No such simple picture, however, seems to be available for the π bonds formed by d_{xy} and d_{x+y}.

It should be noted that this method does not predict directly the type of bond arrangement formed by any given electron configuration. Instead it merely tells whether or not a given arrangement is possible. In many cases it is found that several arrangements are possible for a single configuration of electrons. In these cases the relative stability of the various arrangements must be decided by other methods, such as Pauling's "strength" criterion, or consideration of the repulsions between nonbonded atoms.

RESULTS

The results of these calculations are most conveniently arranged according to the coordination number of the central atom. For the sake of completeness all of the results, including those previously obtained by Pauling, Hultgren and others, are contained in the following summary.

Coordination number 2

If the central atom forms bonds with two external atoms only two arrangements of the bonds are possible: a linear arrangement (group $D_{\infty h}$) and an angular one (group C_{2v}). The resolution tables for these are given in Tables III and IV. The configurations sp and dp can lead to either arrangement. The linear arrangement, however, is favored by both the repulsive forces and the possibilities for double bond formation and is therefore the stable arrangement for these configurations. The configurations ds, d^2 and p^2 on the other hand must be angular.

In the linear arrangement two p and two d orbitals are available for double bond formation, while in the angular arrangement only two strong π bonds are possible, one of which must be through a d orbital, the other of which may be formed by either a d or a p orbital. The other two possible π bonds are weakened by the fact that their orbitals belong to representations already used by the σ bonds.

The angular nature of the p^2 bonds in such molecules as H_2O and H_2S is well known, and need not be discussed further. As examples of double bond formation in molecules having this

TABLE V. *Resolution table for trigonal pyramid bonds.*

C_{3v}	A_1	A_2	E
s	1	0	0
p	1	0	1
d	1	0	2
σ	1	0	1
π	1	1	2

TABLE VI. *Resolution table for three unsymmetrical bonds in a plane.*

C_{2v}	A_1	B_2	B_1	B_2
s	1	0	0	0
p	1	0	1	1
d	2	1	1	1
σ	2	0	1	0
π	1	1	2	2

primary valence structure the nitroso compounds are typical. The prototype of these compounds is the nitrite ion NO_2^-. In this ion each oxygen atom is joined to the nitrogen by a σ bond involving one of the p orbitals of the nitrogen. In addition to these bonds, however, there is a π bond which belongs to the representation B_1 and cannot be localized. Its component orbitals are the p_x orbital of the nitrogen atom and the normalized sum of the p_x orbitals of the two oxygen atoms. The remaining parts of the oxygen p orbitals are occupied by unshared pairs of electrons. Because of the distributed character of the π bond no single valence bond picture can be drawn for this molecule, but only the resonating pair

In the true nitroso compounds RNO, and also in the nitrosyl halides ClNO, etc., the situation is very similar. The lack of complete symmetry does not change any of the essential features of the structure of these molecules. In these cases, however, the difference in electro-negativity between oxygen and the atom or group R may cause ionic structures to play an important role. Pauling has suggested for example that in ClNO the important structures are

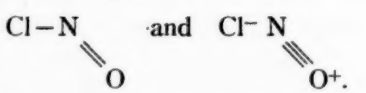

The bond formation in both these structures is in accord with the present theory.

Examples of the linear configuration are found in the ions of the $Ag(NH_3)_2^+$ type and those of the I_3^- type. In $Ag(NH_3)_2^+$ the configuration is certainly sp. In I_3^- and its relatives it is not certain whether the promotion of one of the $5p$ electrons of the central atom is to the $5d$ or $6s$ orbital, but in either case the resulting configuration (ps or pd) should give the observed linear arrangement.

The effect of double bond formation is shown clearly by CO_2 and SO_2. In CO_2 the valence configuration of the carbon is sp^3. The primary structure of σ bonds is sp, which requires the molecule to be linear. The other two p orbitals form the two π bonds. In SO_2, on the other hand, the primary bonds are certainly formed by two p orbitals, thus producing angular arrangement. The customary way of writing the structure of this molecule,

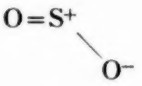

(analogous to NO_2^-) is quite possible, since the π bond can be formed by the third p orbital of the sulfur, but the structure

is also possible and probably as important as the first. In this structure one of the d orbitals of the sulfur acts as an acceptor for one of the electron pairs of the oxygen. It should be noted that the formation of two double bonds by an atom does not require the linear arrangement.

Coordination number 3

For this number of σ bonds three arrangements are important: the plane trigonal arrangement (group D_{3h}) already discussed, the trigonal pyramid (group C_{3v}), and an unsymmetrical plane arrangement with two of the bond angles equal, but not equal to the third (group C_{2v}). The resolution tables for the last two are given in Tables V and VI. As has already been shown, the plane arrangement is stable for the configurations sp^2, sd^2, dp^2, and d^3. (The pyramidal configuration is

also possible, but less stable because of repulsive forces. Such cases will simply be omitted in the future.) The configurations p^3 and d^2p are therefore the only ones leading to a pyramidal structure.[10] The configuration dsp leads to the unsymmetrical plane arrangement.

The possibilities of double bond formation in the plane trigonal arrangement have already been discussed. In the pyramidal arrangement no strong double bonds are possible, although weak π bonds are possible with d orbitals. Thus the sulfite ion, for example, is restricted to the structure

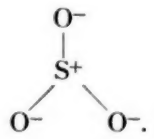

It is interesting to contrast this structure with that of SO_3. The most easily removed pair of electrons in $SO_3^=$ is the pair of $3s$ electrons in the sulfur atom. If these are removed, however, one of the $3p$ pairs forming a σ bond falls to the $3s$ level, thus making the valence configuration sp^2 and the molecule plane. The vacated $3p$ orbital is then filled by an unshared pair from the oxygen atoms to give a π bond. Two more unshared pairs of electrons from the oxygen atoms may interact with the $3d$ orbitals thus forming two more π bonds, which are somewhat weaker than the first. The SO_3 molecule has therefore three comparatively strong double bonds, while the $SO_3^=$ ion has only weak double bonds, if any at all. It is this lack of stabilizing double bonds which gives $SO_3^=$ its relative instability.

The remaining configuration, dsp, should give rise to three bonds in a plane forming two right angles. No examples of molecules of this configuration are known. This is hardly surprising, however, in view of the instability of this arrangement compared to the others. If molecules of this arrangement are to be found at all they would be complex ions of the transition elements. For example, if the ion $Ni(NH_3)_3^{++}$ existed it would be of this structure.

TABLE VII. *Reduction table for tetrahedral bonds.*

T_d	A_1	A_2	E	T_1	T_2
s	1	0	0	0	0
p	0	0	0	0	1
d	0	0	1	0	1
σ	1	0	0	0	1
π	0	0	1	1	1

TABLE VIII. *Reduction table for tetragonal plane bonds.*

D_{4h}	A_{1g}	A_{1u}	A_{2g}	A_{2u}	B_{1g}	B_{1u}	B_{2g}	B_{2u}	E_g	E_u
s	1	0	0	0	0	0	0	0	0	0
p	0	0	0	1	0	0	0	0	0	1
d	1	0	0	0	1	0	1	0	1	0
σ	1	0	0	0	0	0	1	0	0	1
π	0	0	1	1	1	1	0	0	1	1

[10] The bond angles of 90° in this structure are not predicted by the reduction table alone, but can be easily found by the process of forming the actual orbitals as shown in the second section.

Coordination number 4

With a coordination number of four there are three arrangements which need consideration. The reduction tables for these are given in Tables VII, VIII, IX and X. Table VII is for the regular tetrahedral arrangement of the bonds. It is easily seen that the configurations sp^3 and d^3s lead to this arrangement. For double bond formation there remain two d orbitals which can form strong π bonds and two other d orbitals (if the σ bonds are sp^3) or two p orbitals (if the σ bonds are d^3s) which can form weaker π bonds. These possibilities of double bond formation are in accord with Pauling's suggestion that the structure of ions of the type XO_4 should be written with double bonds. Thus for the sulfate ion the primary σ structure arises from the configuration sp^3, but two of the unshared pairs of the O^- ions can be donated to the vacant d

TABLE IX. *Reduction table for tetragonal pyramidal bonds.*

C_{4v}	A_1	A_2	B_1	B_2	E
s	1	0	0	0	0
p	1	0	0	0	1
d	1	0	1	1	1
σ	1	0	0	1	1
π	1	1	1	1	2

TABLE X. *Reduction table for irregular tetrahedral bonds.*

C_{3v}	A_1	A_2	E
s	1	0	0
p	1	0	1
d	1	0	2
σ	2	0	1
π	1	1	3

orbitals of the sulfur atom, thus giving the structure

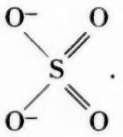

It must, however, be doubtful that two further π bonds are formed to give the structure

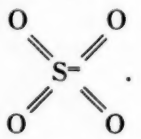

The situation in such molecules as $SiCl_4$ is similar.

From Table VIII it is seen that tetragonal planar (square) bonds are possible with configurations dsp^2 and d^2p^2. Beside the primary bonds, four strong π bonds are possible, using one p and three d orbitals. In $Ni(CN)_4^{=}$, for example, the primary valence configuration of the Ni is dsp^2, so that the structure

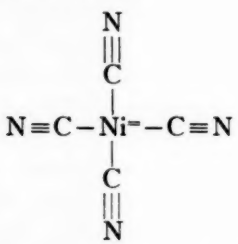

is one possible structure for this ion. By a shift of one of the π pairs forming the C−N triple bond to the nitrogen, however, the carbon atom is left with an empty orbital, which can accept an electron pair donated by the nickel atom. In this way three π bonds can be formed between the nickel and carbon. At the same time one of the triple bond π pairs can shift in the opposite direction and be donated by the carbon to the empty p orbital of the nickel. These shifts would lead to the structure

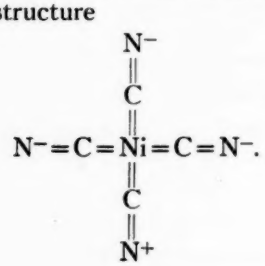

This structure affords an interesting contrast with that of $Ni(CO)_4$, in which one more pair of electrons must be accommodated. This pair occupies the d orbital of the nickel, thus pushing the valence configuration up to sp^3 and making the molecule tetrahedral. There are then only two π bonds possible, and the structure is

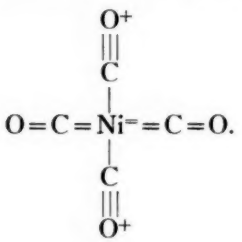

The configuration d^2p^2 is found in such ions as ICl_4^-, which are known to be plane.

From Table IX it appears that the configurations dp^3 and d^3p can lead to a tetragonal pyramid structure, while from Table X it appears that the "irregular tetrahedron" is also possible for these same configurations and also for the configuration d^2sp. By "irregular tetrahedron" is meant a structure in which three of the bonds are directed to the corners of an equilateral triangle and the fourth along the line perpendicular to the triangle at its center. The central atom is not necessarily located at the center of the triangle, but it is probably somewhat above it in the direction of the fourth bond. The choice between these two structures in the cases of the configurations dp^3 and d^3p is very close, with the advantage somewhat on the side of the irregular tetrahedron. The configuration d^4 can only have the pyramidal structure.

Examples of these configurations are rare. In the tetrahalides of the sulfur family we have the configuration p^3d produced by the promotion of one of the p electrons of the central atom to a d orbital. Unfortunately the spatial arrangements of these molecules are unknown. The other two configurations seem to be unstable. Such ions as $Fe(NH_3)_4^{++}$ and $Fe(CN)_4^{=}$ would have the configuration d^2sp, but do not seem to exist, which is perhaps some indication of this instability.

Coordination number 5

For this coordination number four bond arrangements are possible. In Table XI is given the

TABLE XI. *Reduction table for trigonal bipyramidal bonds.*

D_{3h}	A_1'	A_1''	A_2'	A_2''	E'	E''
s	1	0	0	0	0	0
p	0	0	0	1	1	0
d	1	0	0	0	1	1
σ	2	0	0	1	1	0
π	0	1	0	1	2	2

reduction table for a trigonal bipyramid, which is seen to be stable for the configurations dsp^3 and d^3sp. In Table XII the bonds are directed from the center to the corners of a square pyramid. This is the arrangement expected for the configurations d^2sp^2, d^4s, d^2p^3, and d^4p. Table XIII is for the case of five bonds in a plane, directed toward the corners of a regular pentagon, the arrangement for the configuration d^3p^2, and Table XIV is for the case of five bonds directed along the slant edges of a pentagonal pyramid, the arrangement for the configuration d^5.

In PCl_5 and other molecules of this type, the pentavalent state is formed by the promotion of an s electron to the vacant d shell. The valence configuration is therefore dsp^3 and the bipyramidal structure is to be expected, in agreement with the results of electron diffraction studies. Table XI shows that two of the remaining d orbitals are capable of forming strong π bonds; the other two, two weak π bonds by accepting pairs of electrons. Neglecting weak bonds, the structure of PCl_5 is best written

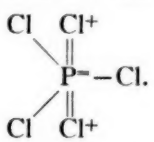

In the molecule $Fe(CO)_5$ the valence configuration is again dsp^3, and the bipyramidal structure is to be expected. Here π bonds can be formed by donation of pairs of d electrons from the iron through the carbon to the oxygens, as in $Ni(CO)_4$, giving the structure

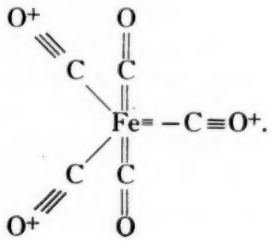

TABLE XII. *Reduction table for five tetragonal pyramidal bonds.*

C_{4v}	A_1	A_2	B_1	B_2	E
s	1	0	0	0	0
p	1	0	0	0	1
d	1	0	1	1	1
σ	2	0	0	1	1
π	1	1	1	1	3

TABLE XIII. *Reduction table for pentagonal plane bonds.*

D_{5h}	A_1'	A_1''	A_2'	A_2''	E_1'	E_1''	E_2'	E_2''
s	1	0	0	0	0	0	0	0
p	0	1	0	0	1	0	0	0
d	1	0	0	0	0	1	1	0
σ	1	0	0	0	1	0	1	0
π	0	1	1	0	1	1	1	1

TABLE XIV. *Reduction table for pentagonal pyramidal bonds.*

C_{5v}	A_1	A_2	E_1	E_2
s	1	0	0	0
p	1	0	1	0
d	1	0	1	0
σ	1	0	1	1
π	1	1	2	2

In IF_5, however, the valence configuration is p^3d^2, and the molecule should have the square pyramid structure. Here again two strong π bonds can be formed by donations of pairs of electrons from the F to the I, so that the structure may be

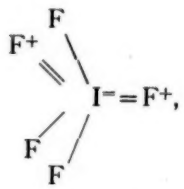

but the high electro-negativity of fluorine makes the existence of the double bonds doubtful. The spatial configuration of this molecule has not yet been determined experimentally.

The pentagonal configurations crowd the atoms so much that they must be unstable.

Coordination number 6

Six bonds may be arranged symmetrically in space in three ways: to the corners of a regular octahedron, to those of a trigonal prism, or to those of a trigonal antiprism (an octahedron stretched or compressed along one of the tri-

TABLE XV. *Reduction table for octahedral bonds.*

O_h	A_{1g}	A_{1u}	A_{2g}	A_{2u}	E_g	E_u	T_{1g}	T_{1u}	T_{2g}	T_{2u}
s	1	0	0	0	0	0	0	0	0	0
p	0	0	0	0	0	0	0	1	0	0
d	0	0	0	0	1	0	0	0	1	0
σ	1	0	0	0	1	0	0	1	0	0
π	0	0	0	0	0	0	1	1	1	1

TABLE XVI. *Reduction table for trigonal prismatic bonds.*

D_{3h}	A_1'	A_1''	A_2'	A_2''	E'	E''
s	1	0	0	0	0	0
p	0	0	0	1	1	0
d	1	0	0	0	1	1
σ	1	0	0	1	1	1
π	1	1	1	1	2	2

TABLE XVII. *Reduction table for trigonal antiprismatic bonds.*

D_{3d}	A_{1g}	A_{1u}	A_{2g}	A_{2u}	E_g	E_u
s	1	0	0	0	0	0
p	0	0	0	1	0	1
d	1	0	0	0	2	0
σ	1	0	0	1	1	1
π	1	1	1	1	2	2

gonal axes). The reduction tables for these possibilities are given in Tables XV, XVI, and XVII.

Table XV shows that octahedral bonds are formed by the configuration d^2sp^3 and no other. The commonness of this arrangement is therefore due to the fact that the configuration d^2sp^3 is the usual configuration of six valence electrons, rather than any particular virtue of the octahedral arrangement. This configuration arises both in the 6-coordinated ions of the transition elements, and in the molecules of the SF_6 type in which one s and one p electron are promoted to the next higher d level. Table XV also shows that all three remaining d orbitals are capable of forming strong π bonds. In the ferrocyanide ion $Fe(CN)_6^{-4}$, these d orbitals can donate their pairs of electrons to the nitrogen atoms, giving Pauling's structure

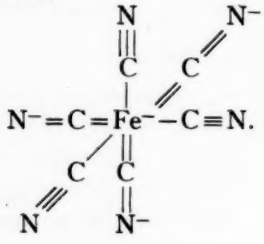

If SF_6 the remaining d orbitals are empty, and can accept pairs of electron from the fluorine atoms, giving the structure

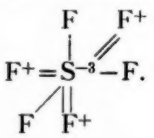

It is this structure which accounts for the great resistance of SF_6 to hydrolysis. It has been suggested by Sidgwick[11] that the hydrolysis of halides takes place either by their accepting a pair of electrons from the oxygen of a water molecule, with subsequent decomposition, or by donation of an unshared pair on the central atom to a hydrogen atom, with loss of hypohalous acid. With the usual single bonded structure of SF_6, the first mechanism is possible, and one would expect the hydrolysis to take place easily. With the double bonded structure, however, all of the electrons in the outer shell of the sulfur are taking part in bond formation, so that one should expect the same inertness as that displayed by CCl_4. It is interesting to note that SeF_6 is like SF_6, but TeF_6 is easily hydrolyzed. This must be due to the possibility of the Te atom's accepting a pair of oxygen electrons in the vacant $4f$ orbital.

In MoS_2 and WS_2 in the crystalline form the valence configuration is d^4sp and the arrangement is prismatic, as Hultgren[4] has pointed out. Table XVI indicates that the two empty p orbitals of the metal atom cannot form strong π bonds to the sulfur atoms. The configuration d^5p should also lead to the prismatic arrangement, but no examples are known.

The cases of the ions $SeBr_6^{-2}$ and $SbBr_6^{-3}$ are interesting in that the configuration in each of these should be p^3d^3. This configuration should lead to the antiprismatic arrangement, i.e., the octahedral symmetry should not be perfect. If, however, the unshared pair of s electrons is promoted to a d orbital, and one of the valence pairs slips into its place, the configuration will be the octahedral d^2sp^3. The deciding factor here may be the possibility of double bond formation offered by the octahedral but not by the antiprismatic arrangement.

[11] Sidgwick, *The Electronic Theory of Valency* (Oxford, 1927), p. 157.

The configurations d^3sp^2, d^5s and d^4p^2 do not permit any arrangement in which all of the bonds are equivalent. While the configuration d^3sp^2 might form bonds of a mixed type, e.g., the tetrahedral d^3s+the angular p^2, the bonds will be weak, and the configuration unstable. Molecules which might be expected to have this arrangement, e.g., $Fe(CN)_6^{-3}$, rearrange the electrons to obtain the more stable d^2sp^3 configuration. In $Fe(CN)_6^{-3}$ for example, the odd electron, which normally should occupy a $4p$ orbital, instead goes to a $3d$ orbital making the third $4p$ orbital available for the formation of octahedral bonds.

Coordination number 7

The coordination number 7 is extremely rare. The fact that it appears only in the heavier atoms, such as Zr, Cb, I, and Ta, leads one to suspect that for stability f electrons are necessary, although it is possible that the determining factor is ion size. Two arrangements of seven bonds have been observed:[12] the ZrF_7^{-3} structure, which may be obtained from the octahedron by adding an atom at the center of one face; and the TaF_7^{-2} structure, which may be obtained from the trigonal prism by adding an atom at the center of one of the square faces. The reduction tables for these two arrangements are given in Tables XVIII and XIX.

From Table XVIII we see that if no f orbitals are involved, the ZrF_7^{-3} type bonds can arise from the configurations d^3sp^3 and d^5sp. The configuration expected for ZrF_7^{-3} is d^5sp, so that it is not necessary to appeal to the f orbitals to form these bonds. This, however, does not preclude the possibility that f orbitals are used to strengthen the bonds.

Table XIX shows that the TaF_7^{-2} structure is possible with the configurations d^3sp^3, d^4sp^2, d^5sp, d^4p^3 and d^5p^2. The ion TaF_7^{-2} itself is isoelectronic with ZrF_7^{-3}, so that it is difficult to understand why it should prefer its structure to that of ZrF_7^{-3}. It is quite possible that the bonds in all the 7-coordinated molecules are so ionic that the

TABLE XVIII. *Reduction table for ZrF_7^{-3} type bonds.*

C_{2v}	A_1	A_2	E
s	1	0	0
p	1	0	1
d	1	0	2
f	2	1	2
σ	3	0	2
π	2	2	5

TABLE XIX. *Reduction table for TaF_7^{-2} type bonds.*

C_{2v}	A_1	A_2	B_1	B_2
s	1	0	0	0
p	1	0	1	1
d	2	1	1	1
f	2	1	2	2
σ	3	1	2	1
π	3	3	4	4

[12] Hampson and Pauling, J. Am. Chem. Soc. **60**, 2702 (1938); Hoard, J. Am. Chem. Soc. **61**, 1252 (1939).

TABLE XX. *Reduction table for cubic bonds.*

O_h	A_{1g}	A_{1u}	A_{2g}	A_{2u}	E_g	E_u	T_{1g}	T_{1u}	T_{2g}	T_{2u}
s	1	0	0	0	0	0	0	0	0	0
p	0	0	0	0	0	0	0	1	0	0
d	0	0	0	0	1	0	0	0	1	0
f	0	0	0	1	0	0	0	1	0	1
σ	1	0	0	1	0	0	0	1	1	0
π	0	0	0	0	0	0	1	1	1	1

TABLE XXI. *Reduction table for tetragonal antiprismatic bonds.*

D_{4d}	A_{1g}	A_{1u}	A_{2g}	A_{2u}	E_1	E_2	E_3
s	1	0	0	0	0	0	0
p	0	0	0	1	1	0	0
d	1	0	0	0	0	1	1
σ	1	0	0	1	1	1	1
π	1	1	1	1	2	2	2

TABLE XXII. *Reduction table for dodecahedral bonds.*

V_d	A_1	A_2	B_1	B_2	E
s	1	0	0	0	0
p	0	0	0	1	0
d	1	0	1	1	1
σ	2	0	0	2	2
π	2	2	2	2	4

TABLE XXIII. *Reduction table for face-centered prismatic bonds.*

C_{2v}	A_1	A_2	B_1	B_2
s	1	0	0	0
p	1	0	1	1
d	2	1	1	1
σ	3	0	2	1
π	4	4	4	4

TABLE XXIV. *Summary of stable bond arrangements and multiple bond possibilities.*

Coordination Number	Configuration	Arrangement	Strong π Orbitals	Weak π Orbitals	Table
2	sp	linear	p^2d^2	—	III
	dp	linear	p^2d^2	—	III
	p^2	angular	$d(pd)$	$d(sd)$	IV
	ds	angular	$d(pd)$	$p(pd)$	IV
	d^2	angular	$d(pd)$	$p(spd)$	IV
3	sp^2	trigonal plane	pd^2	d^2	II
	dp^2	trigonal plane	pd^2	d^2	II
	d^2s	trigonal plane	pd^2	p^2	II
	d^3	trigonal plane	pd^2	p^2	II
	dsp	unsymmetrical plane	pd^2	$(pd)d$	VI
	p^3	trigonal pyramid	—	$(sd)d^4$	V
	d^2p	trigonal pyramid	—	$(sd)p^2d^2$	V
4	sp^3	tetrahedral	d^2	d^3	VII
	d^3s	tetrahedral	d^2	p^3	VII
	dsp^2	tetragonal plane	d^3p	—	VIII
	d^2p^2	tetragonal plane	d^3p	—	VIII
	d^2sp	irregular tetrahedron	—	d	X
	dp^3	irregular tetrahedron	—	s	X
	d^3p	irregular tetrahedron	—	s	X
	d^4	tetragonal pyramid	d	$(sp)p$	IX
5	dsp^3	bipyramid	d^2	d^2	XI
	d^3sp	bipyramid	d^2	p^2	XI
	d^2sp^2	tetragonal pyramid	d	pd^2	XII
	d^4s	tetragonal pyramid	d	p^3	XII
	d^2p^3	tetragonal pyramid	d	sd^2	XII
	d^4p	tetragonal pyramid	d	sp^2	XII
	d^3p^2	pentagonal plane	pd^2	—	XIII
	d^5	pentagonal pyramid	—	$(sp)p^2$	XIV
6	d^2sp^3	octahedron	d^3	—	XV
	d^4sp	trigonal prism	—	p^2d	XVI
	d^5p	trigonal prism	—	p^2s	XVI
	d^3p^3	trigonal antiprism	—	sd	XVII
	d^3sp^2	mixed			
	d^5s	mixed			
	d^4p^2	mixed			
7	d^3sp^3	ZrF_7^{-3}	—	d^2	XVIII
	d^5sp	ZrF_7^{-3}	—	p^2	XVIII
	d^4sp^2	TaF_7^{-2}	—	dp	XIX
	d^4p^3	TaF_7^{-2}	—	ds	XIX
	d^5p^2	TaF_7^{-2}	—	ps	XIX
8	d^4sp^3	dodecahedron	d	—	XXII
	d^5p^2	antiprism	—	s	XXI
	d^5sp^2	face-centered prism	p	—	XXIII

directed nature of covalent bonds has little importance in determining the atomic arrangement.

Coordination number 8

Until very recently the spatial arrangement of no molecule involving a coordinate number of 8 had been determined experimentally. It had been supposed that the arrangements which were most probable were the cubic and the tetragonal antiprismatic. Hoard and Nordsieck[13] have now determined the arrangement of the ion $Mo(CN)_8^{-4}$ and have found that the structure is neither cubic nor antiprismatic, but instead that of a dodecahedron with triangular faces and symmetry $V_d(D_2{}^d)$. The reduction tables for these three cases are given in Tables XX, XXI, and XXII. Table XXIII is the reduction table for an arrangement which is derivable from a trigonal prism by placing two atoms at the centers of two of the rectangular faces. It is seen that the cubic requires the use of f orbitals, and even then arises only from the configurations d^3fsp^3 and d^3f^4s. The cubic arrangement should therefore not be ordinarily found. The antiprismatic arrangement is stable for the configurations d^4sp^3 and d^5p^3, and the dodecahedral for only d^4sp^3. The observed arrangement for $Mo(CN)_8^{-4}$, which has the configuration d^4sp^3, indicates that the dodecahedral arrangement has greater stability than the antiprismatic. The structure of such ions as TaF_8^{-3} and the molecule OsF_8 which should have the configuration d^5sp^2 should be the face-centered prismatic structure of Table XXIII.

Table XXIV summarizes these results. In it are given the most stable bond arrangements for each configuration of two to eight electrons in s, p or d orbitals. The orbitals available for strong π bonds and weak π bonds are also given. In those cases where there is a choice of two or more orbitals when only one can be chosen, the orbitals are enclosed in parentheses.

[13] Hoard and Nordsieck, J. Am. Chem. Soc. **61**, 2853 (1939).

The Absolute Rates of Heterogeneous Reactions

II. Electrode Reactions*

GEORGE E. KIMBALL
Department of Chemistry, Columbia University, New York, New York
(Received October 26, 1939)

The theory of the first paper of this series is extended to include reactions at electrode surfaces. The resulting expression for the rate of an electrode reaction includes both activation controlled and diffusion controlled reactions. The problem of the effect of stirring rate on reaction rate is discussed. The results are applied to the theory of reactions at "floating" electrodes, e.g. the solution of metals in acids. It is shown that the reaction rate expressions at such electrodes are of a very complex form, but can be approximated in special cases. It is found that the rate of such a reaction will in general depend not only on the concentration of the principal reactants, but also on the concentration of every ion in the solution.

ONE of the commonest types of chemical reaction takes place between a metal and a solution containing ions. As examples there are the processes of electrolytic deposition and solution, the solution of metals in acids, the displacement of one metal by another, and corrosion of metals. Each of these processes can be regarded as consisting of processes of formation of ions or discharge of ions at a metal surface. It is therefore appropriate to include them all in the category of electrode reactions.

As a metal atom leaves the electrode surface it passes through three regions: first, the surface of the metal, on which there may or may not be a layer of adsorbed atoms; second, a layer of adsorbed ions; and third, a diffusion layer in which the ionic concentration gradually changes from that near the layer of adsorbed ions to that of the main body of the solution. These layers are shown schematically in Fig. 1.

The rate at which metal atoms go into solution as ions, or vice versa, is therefore determined by two factors: the rate of formation of ions in the adsorbed layer and the rate of passage of these ions through the diffusion layer. Both of these processes have been discussed at great length in the literature.[1]

The principal difference between these reactions and other heterogeneous reactions is caused by the electrical effect of the layer of adsorbed ions and the electrical image of this layer in the electrode. This electrical double layer leads to a difference in potential between the solution and the electrode. It is, of course, impossible to measure absolutely the value of this potential difference[2] but nevertheless it is possible to measure changes in it. The effect of this potential on the reaction rate can be seen from Fig. 2. In this figure is given the potential energy of an atom as a function of its distance from the electrode surface. The curve *ABCD* is the curve for the potential energy of the neutral atom, while the curve *ECFG* is that for the ion. At the crossing point *C* quantum-mechanical resonance rounds off the crossing so that the two curves no longer intersect. The actual charging of the ion will therefore take place at this point. The energy difference between the point *C* and the point *B* is essentially the activation energy of the charging

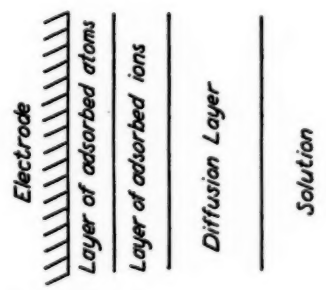

FIG. 1. Diagram of layers at an electrode surface.

* Publication assisted by the Ernest Kempton Adams Fund for Physical Research of Columbia University.

[1] For reviews see Glasstone, Annual Reports of the London Chemical Society **34**, 107 (1937); Bowden and Agar, *ibid.* **35**, 90 (1938).

[2] Guggenheim, *Modern Thermodynamics* (Methuen, 1933), Chapter X.

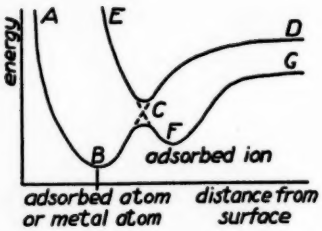

FIG. 2. Potential energy curves of adsorbed ions and atoms

process. The energy at C and at B, however, is a function of the potential difference between the solution and the electrode. The activation energy of the charging process is therefore also a variable quantity and will change with the potential difference.

According to the theory of absolute reaction rates[3] the rate of formation of ions in the adsorbed layer from the metal surface will be given by

$$\frac{kT}{h}e^{-[\Delta F_1^* + \epsilon(V_C - V_B)]/kT}[A],$$

where ΔF_1^* is the free energy difference between an atom at B and one at C when the potential drop is zero, V_C and V_B are the electrical potentials at C and B, $[A]$ is the activity of the atoms A in the surface or adsorbed on it, and ϵ is the charge of the ion. Letting

$$k_1 = \frac{kT}{h}e^{-\Delta F_1^*/kT},$$

this rate may be written in the form

$$k_1[A]e^{-\epsilon(V_C - V_B)/kT}.$$

The total current from the electrode due to this process is then given by

$$I_a' = \epsilon k_1[A]e^{-\epsilon(V_C - V_B)/kT}.$$

In a similar way the current (still measured as flowing *from* the electrode) caused by the discharge of ions is

$$I_a'' = -\epsilon k_2[A^+]_{ads}e^{-\epsilon(V_C - V_F)/kT},$$

where $[A^+]_{ads}$ is the activity of the ions in the adsorbed ion layer and k_2 is a constant. The net current I_a, flowing from the electrode, is therefore given by

$$I_a = \epsilon k_1 e^{-\epsilon(V_C - V_B)/kT}[A] - \epsilon k_2 e^{-\epsilon(V_C - V_F)/kT}[A^+]_{ads}. \quad (1)$$

The rate at which ions migrate through the diffusion layer will follow the Nernst[4] law.

$$\frac{D}{l}\{[A^+]_{ads} - [A^+]\},$$

where D is the diffusion constant, l is the thickness of the diffusion layer, and $[A^+]$ is the activity of the ions in the main body of the solution. The corresponding current, I_a''', is given by

$$I_a''' = \frac{\epsilon D}{l}\{[A^+]_{ads} - [A^+]\}. \quad (2)$$

Except for an extremely short period at the beginning of an experiment, during which the adsorbed ion layer is established, these two currents must be equal, for otherwise the adsorbed ion layer would not come to equilibrium. The activity $[A^+]_{ads}$ is therefore determined by the equation $I_a = I_a'''$. Setting these two equal and solving for $[A^+]_{ads}$ immediately gives

$$[A^+]_{ads} = \frac{k_1[A]e^{-\epsilon(V_C - V_B)/kT} + (D/l)[A^+]}{k_2 e^{-\epsilon(V_C - V_F)/kT} + D/l}.$$

Substitution of this equation in (2) gives for the current when the adsorbed ion layer is at equilibrium

$$I_a = \epsilon\lambda\left\{\frac{k_1}{k_2}e^{\epsilon(V_B - V_F)/kT}[A] - [A^+]\right\}, \quad (3)$$

where

$$\lambda = \frac{(k_2 D/l)e^{-\epsilon(V_C - V_F)/kT}}{k_2 e^{-\epsilon(V_C - V_F)/kT} + D/l}. \quad (4)$$

If we adopt the arbitrary convention that the potential of the solution is zero, and assume furthermore that $V_B = V$, the potential of the electrode, $V_F = 0$ (neglect of the diffusion potential), and put $V_C = \alpha V$, Eqs. (3) and (4) can be

[3] Eyring, J. Chem. Phys. 3, 107 (1935); Eyring and Wynne-Jones, *ibid.* 3, 492 (1935); Kimball, *ibid.* 6, 447 (1938); Eyring, Glasstone and Laidler, *ibid.* 7, 1053 (1939).

[4] Nernst, Zeits. f. physik. Chemie 47, 52 (1904).

put in the form

$$I_a=\epsilon\lambda\left\{\frac{k_1}{k_2}e^{\epsilon V/kT}[A]-[A^+]\right\}, \tag{5}$$

$$\lambda=\frac{(k_2D/l)e^{-\epsilon\alpha V/kT}}{k_2e^{-\epsilon\alpha V/kT}+D/l}. \tag{6}$$

We may simplify these equations still further if we note that at the equilibrium potential V_a, $I_a=0$ if $[A]=[A^+]$. This condition gives immediately

$$k_1/k_2=e^{-\epsilon V_a/kT}$$

and

$$I_a=\epsilon\lambda\{e^{\epsilon(V-V_a)/kT}[A]-[A^+]\}. \tag{7}$$

The equation for λ can be put in the form

$$\lambda=\frac{PQe^{-\epsilon\alpha(V-V_a)/kT}}{Pe^{-\epsilon\alpha(V-V_a)/kT}+Q}$$

where $P=k_2e^{-\epsilon\alpha V_a/kT}$ and $Q=D/l$, or

$$1/\lambda=(1/P)e^{\epsilon\alpha(V-V_a)/kT}+1/Q. \tag{8}$$

This equation may be simplified in the two limiting cases

$$Q\gg Pe^{-\epsilon\alpha(V-V_a)/kT} \quad \text{and} \quad Q\ll Pe^{-\epsilon\alpha(V-V_a)/kT}.$$

In the first case the reaction is activation controlled, and approximately

$$\lambda=Pe^{-\epsilon\alpha(V-V_a)/kT}, \tag{8a}$$

$$I_a=\epsilon P\{e^{(1-\alpha)\epsilon(V-V_a)/kT}[A]-e^{-\epsilon\alpha(V-V_a)/kT}[A^+]\}. \tag{7a}$$

In this case the kinetics are essentially those of Eyring, Glasstone and Laidler.[3] In the second case

$$\lambda=Q, \tag{8b}$$

$$I_a=\epsilon Q\{e^{\epsilon(V-V_a)/kT}[A]-[A^+]\}. \tag{7b}$$

It is interesting to note in this case that the rate is independent of the value of α.

The transition from activation control to diffusion control comes when

$$Q=Pe^{-\epsilon\alpha(V-V_a)}. \tag{9}$$

If the electrode process involves the charge or discharge of a positive ion the reaction will be diffusion controlled for $V\gg V_a$ and activation controlled for $V\ll V_a$, while for negative ions the reverse is true. It is quite possible that when several electrode processes are taking place at one electrode some may be diffusion controlled while others are simultaneously activation controlled.

The effect of the stirring rate on these reactions is essentially the effect of the change of the thickness of the diffusion layer. If we assume simply that the thickness of this layer is inversely proportional to the stirring rate, σ, then Q will be of the form

$$Q=\sigma Q_0, \tag{10}$$

where Q_0 is a constant. The form assumed by Eq. (7) is then

$$I_a=K_1K_2\sigma/(K_1+K_2\sigma), \tag{11}$$

where K_1 and K_2 are independent of σ. The form of this equation is shown in Fig. 3. This equation is of the same form as the Langmuir adsorption isotherm, and has the same relationship to the usual form of stirring curve

$$I=A\sigma^n$$

as the Langmuir isotherm does to the Freundlich isotherm. Thus the suggestion of Nernst and Merriam[5] and of Brunner[6] that the rate is proportional to the two-thirds power of the stirring rate must be regarded as open to doubt, for their data may be fitted about as well by Eq. (11).

With the exception of overvoltage measurements, which will not be discussed here, most of the experimental data on rates of electrode reactions have been obtained from experiments with what might be called a "floating" electrode, i.e., a piece of metal simply immersed in a

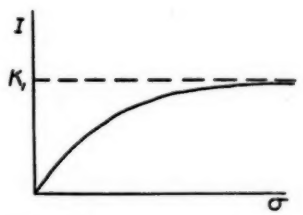

FIG. 3. The effect of stirring rate on solution rate.

[5] Nernst and Merriam, Zeits. f. physik. Chemie **53**, 235 (1905).
[6] Brunner, Zeits. f. physik. Chemie **47**, 56 (1904).

solution with no control over its electrical potential. In such a situation there are always at least three reactions which may take place: formation of metal ions in the solution from the metal, discharge of positive ions on the metal, and discharge of negative ions on the metal. It is a characteristic of electrode reactions that each of these processes tends to produce a potential in the metal of such a sign as to slow down the reaction producing it. The first and last of these reactions tend to produce a negative potential on the metal, while the second tends to produce a positive potential. After a very short time, therefore, the potential of the electrode will reach such a value that the positive current from the metal caused by reactions of the first and third types is exactly equal to the negative current caused by reactions of the second type. When this potential is once attained, the reactions proceed with no net current, so that this potential is maintained.

To illustrate this process, let us consider a case in which the discharge of negative ions is negligible, one in which a metal A is dissolving to form singly charged positive ions A^+ and simultaneously singly charged positive ions B^+ are discharging to form a second metal B. Since reactions of this type are usually diffusion controlled, we shall also assume that the currents due to these reactions are given by equation (7b). We shall also assume that the back reactions (discharge of A^+ and solution of B) can be neglected. With these simplifying assumptions the currents due to the two reactions are

$$I_a = \epsilon Q_a e^{\epsilon(V-V_a)/kT}[A], \tag{12}$$

$$I_b = -\epsilon Q_b[B^+]. \tag{13}$$

The steady-state potential is then determined by

$$Q_a e^{\epsilon(V-V_a)/kT}[A] = Q_b[B^+],$$

so that

$$e^{\epsilon(V-V_a)/kT} = \frac{Q_b}{Q_a}\frac{[B^+]}{[A]}. \tag{14}$$

If this is substituted into (12) we find

$$I_a = \epsilon Q_b[B^+]. \tag{15}$$

In other words the potential of the electrode adjusts itself to just such a value that the rate of solution of A is exactly equal to the rate at which B^+ ions can pass through the diffusion layer.

It is obvious that this result is oversimplified, for it gives a rate of solution which is independent of the metal dissolving, the same, for example, for sodium as for platinum. The difficulty is obviously in the neglect of the back reactions, in particular the solution of B, for the activity of the discharged B atoms rises very rapidly. If the volume of the solution is large, however, the discharge of A^+ can be safely neglected, so that only Eq. (13) needs to be modified. If we include the back reaction in this equation it becomes

$$I_b = \epsilon Q_b\{e^{\epsilon(V-V_b)/kT}[B] - [B^+]\}. \tag{16}$$

The equation determining V is now

$$Q_a e^{\epsilon(V-V_a)/kT}[A] + Q_b e^{\epsilon(V-V_b)/kT}[B] - Q_b[B^+] = 0$$

or

$$e^{\epsilon V/kT} = \frac{Q_b[B^+]}{[A]Q_a e^{-\epsilon V_a/kT} + [B]Q_b e^{-\epsilon V_b/kT}}. \tag{17}$$

Now if B is more noble than A, V_b will be larger than V_a and unless Q_a is much smaller than Q_b, the term

$$[B]Q_b e^{-\epsilon V_b/kT}$$

will be small compared to

$$[A]Q_a e^{-\epsilon V_a/kT}.$$

Then we will have approximately

$$e^{\epsilon V/kT} = \frac{Q_b}{Q_a}\frac{[B^+]}{[A]}e^{\epsilon V_a/kT}$$

and

$$I_a = \epsilon Q_b[B^+] \tag{18}$$

as before. On the other hand, if B is less noble than A, the term

$$[B]Q_b e^{-\epsilon V_b/kT}$$

will be large compared to

$$[A]Q_a e^{-\epsilon V_b/kT}$$

and

$$e^{\epsilon V/kT} = \frac{[B^+]}{[B]}e^{\epsilon V_b/kT},$$

that is, the potential becomes the equilibrium potential of the B electrode and the solution of

A proceeds at the rate determined by this potential:

$$I_a=\epsilon Q_a\frac{[B^+][A]}{[B]}e^{\epsilon(V_b-V_a)/kT}. \qquad (19)$$

Since in this case $V_b \ll V_a$, the solution proceeds very slowly. The net effect is therefore a slow corrosion of the electrode.

To illustrate the effect of negative ions let us consider an electrode consisting of a metal A in contact with a solution containing positive ions B^+ and negative ions C^-. The three currents from the electrode are then

$$I_a=\epsilon Q_a\{[A]e^{\epsilon(V-V_a)/kT}-[A^+]\},$$
$$I_b=\epsilon Q_b\{[B]e^{\epsilon(V-V_b)/kT}-[B^+]\},$$
$$I_c=-\epsilon Q_c\{[C]e^{-\epsilon(V-V_c)/kT}-[C^-]\}.$$

The steady-state potential is therefore given by

$$ax+b-c/x=0, \qquad (20)$$

where

$$a=Q_a[A]e^{-\epsilon V_a/kT}+Q_b[B]e^{-\epsilon V_b/kT},$$
$$b=Q_c[C^-]-Q_a[A^+]-Q_b[B^+],$$
$$c=Q_c[C]e^{\epsilon V_c/kT},$$
$$x=e^{\epsilon V/kT}.$$

The solution of (20) is

$$x=\frac{-b\pm(b^2+4ac)^{\frac{1}{2}}}{2a},$$

where, since x must necessarily be positive, only the positive sign before the radical is significant. Hence

$$x=\frac{-b+(b^2+4ac)^{\frac{1}{2}}}{2a}. \qquad (21)$$

We shall distinguish three cases. First suppose $b\gg(4ac)^{\frac{1}{2}}$. This corresponds to a reaction in which the fastest reaction is the discharge of the negative ions. In this case (Case I) we may approximate Eq. (21) by

$$x=\frac{-b+b(1+(2ac/b^2))}{2a}$$
$$=c/b.$$

To a first approximation

$$b=Q_c[C^-],$$

so that

$$x=\frac{[C]}{[C^-]}e^{\epsilon V_c/kT}$$

and

$$V=V_c+\frac{kT}{\epsilon}\ln\frac{[C]}{[C^-]}.$$

In other words the potential is the equilibrium potential for the discharge and charge of C^-. Then, if I_a' is the solution current of A,

$$I_a'=\epsilon Q_a\frac{[A][C]}{[C^-]}e^{\epsilon(V_c-V_a)/kT}, \qquad (22)$$

the condition for this case is

$$Q_c[C^-]^2\gg 4[C]e^{\epsilon V_c/kT}$$
$$\times\{Q_a[A]e^{-\epsilon V_a/kT}+Q_b[B]e^{-\epsilon V_b/kT}\},$$

which will usually hold if $V_a\gg V_c$, $V_b\gg V_c$, and $Q_c\gg Q_a+Q_b$. Because of the negative value of the exponent in Eq. (22) reactions of this type are necessarily slow.

Case II is that in which $|b|\ll(4ac)^{\frac{1}{2}}$, in which case Eq. (21) becomes approximately

$$x=(2c/a)^{\frac{1}{2}}.$$

This case in turn may be subdivided into two subcases, depending on whether A is more or less noble than B. If A is less noble than B (Case IIa), a is given approximately by

$$a=Q_a[A]e^{-\epsilon V_a/kT}$$

and x and I_a' become

$$x=\left[\frac{2Q_c[C]e^{\epsilon V_c/kT}}{Q_a[A]e^{-\epsilon V_a/kT}}\right]^{\frac{1}{2}},$$
$$I_a'=\epsilon(2Q_aQ_c[A][C])^{\frac{1}{2}}e^{\epsilon(V_c-V_a)/2kT}. \qquad (23)$$

On the other hand, if A is more noble than B (Case IIb),

$$a=Q_b[B]e^{-\epsilon V_b/kT},$$
$$x=\left[\frac{2Q_c[C]e^{\epsilon V_c/kT}}{Q_b[B]e^{-\epsilon V_b/kT}}\right]^{\frac{1}{2}},$$
$$I_a'=Q_a[A]\left[\frac{2Q_c[C]}{Q_b[B]}\right]^{\frac{1}{2}}e^{\epsilon[\frac{1}{2}(V_b+V_c)-V_a]/kT}. \qquad (24)$$

The condition for this case is

$$\{Q_c[C^-]-Q_a[A^+]-Q_b[B^+]\}^2 \ll 4Q_c[C]e^{\epsilon V_c/kT}\{Q_a[A]e^{-\epsilon V_a/kT} + Q_b[B]e^{-\epsilon V_b/kT}\},$$

which may be expected to hold if $V_c \gg V_a$ or $V_c \gg V_b$. Eq. (23) will therefore hold if $V_c \gg V_b \gg V_a$ or $V_b \gg V_c \gg V_a$ and Eq. (24) when $V_c \gg V_a \gg V_b$ or $V_a \gg V_c \gg V_b$.

Case III arises when $b \ll -(4ac)^{\frac{1}{2}}$, when approximately

$$x = -b/a$$

and

$$I_a' = \epsilon Q_a[A]e^{-\epsilon V_a/kT} \times \frac{Q_a[A^+]+Q_b[B^+]-Q_c[C^-]}{Q_a[A]e^{-\epsilon V_a/kT}+Q_b e^{-\epsilon V_b/kT}}. \quad (25)$$

If $V_a \ll V_b$ (Case IIIa) this is approximately

$$I_a' = \epsilon Q_a[A^+]+\epsilon Q_b[B^+]-\epsilon Q_c[C^+]. \quad (26)$$

If $V_b \ll V_a$ (Case IIIb) Eq. (25) approximates to

$$I_a' = \epsilon[A]\frac{Q_a}{Q_b}e^{\epsilon(V_b-V_a)/kT} \times \{Q_a[A^+]+Q_b[B^+]-Q_c[C^-]\}. \quad (27)$$

The conditions for this case are $V_a \gg V_c$, $V_b \gg V_c$, $Q_a+Q_b \gg Q_c$. If $V_a \gg V_b \gg V_c$ either Eq. (22) or Eq. (27) will hold, depending on whether $Q_c \gg Q_a+Q_b$ or whether $Q_c \ll Q_a+Q_b$. If $V_b \gg V_a \gg V_c$ Eq. (22) or Eq. (26) will hold.

It should be noted that the conditions given apply only when $[C]$ is appreciably large. If $[C]$ is extremely small, Case II becomes impossible, and the kinetics will belong to Case I or Case III according to the relative magnitudes of Q_a, Q_b and Q_c. Case I and Case IIIb will give very slow rates under these conditions, which include most corrosion problems. The reactions of metals with acids and similar reactions belong principally to Case IIIb.

The complexity of these rate expressions indicates very strongly that the experimental study of electrode reactions by means of experiments with "floating" electrodes is apt to be quite unreliable. The rates obtained for the solutions of metals in acids, for example, show very complicated behavior when the negative ion is changed and when salts are added to the solution. In part these effects are due to changes in activity coefficients, but the results derived above show that there is always a direct effect due to discharge of the negative ions.

It would seem best, therefore, to conduct experiments with controlled potential between the electrode and the solution. If the above theory is correct, the rate of solution of a metal, whatever the solution used, should depend only on the potential difference between the electrode and the solution. Experiments are now being carried out in this laboratory to investigate the truth of this assumption and to obtain measurements of the constants P, Q and α.

On Phase Changes in Crystals Arising from Hindered Molecular Rotation

JOHN G. KIRKWOOD
Baker Laboratory, Cornell University, Ithaca, New York

(Received October 30, 1939)

A theory of phase changes due to hindered molecular rotation in crystals is developed on the basis of classical statistical mechanics. It is demonstrated that local hindrance of relative rotation of neighboring molecules in the lattice can produce a non-uniform distribution in orientation below a certain critical temperature. The theory provides a semi-quantitative description of the behavior of the hydrogen halides in certain of their lambda-transitions, with a relative torque potential of the form $(\epsilon/2)\cos\gamma$ for a pair of neighboring molecules, the axes of which are inclined at an angle γ to each other. The barrier height ϵ is estimated to be between 200 and 300 cal./mole for hydrogen iodide and hydrogen bromide.

ANOMALIES are frequently observed in the heat capacity-temperature curves of crystals containing molecular or ionic groups capable of rotation in the lattice. The relationship of such anomalies to hindered molecular rotation has been established by Pauling.[1] Since they generally occur not as smooth maxima but in the form of lambda-points with a discontinuity on the high temperature side, it must be concluded that they are associated with phase changes of the second kind. In order to account for phase changes either of the first or second kinds on the hypothesis of hindered molecular rotation, it is necessary to suppose that the hindering torque acting on a molecule in the lattice depends upon the state of rotation of its neighbors. Processes of this type have been called cooperational phenomena by Fowler. Fowler[2] has developed a cooperational theory of the freezing of molecular rotation in crystals which provides a qualitative description of the observed phase changes. However, since Fowler's theory contains certain arbitrary features, it seems desirable to formulate a theory based more directly on the principles of statistical mechanics and in which the detailed role of molecular interaction is made more clear. It is the purpose of the present article to describe such a theory, carried to a stage of approximation equivalent to that of the Bragg-Williams[3] theory of super-lattices in alloys. In place of the Bragg and Williams long range order parameter, a set of functions of molecular orientation appear, each of which specifies the distribution in orientation of the molecules located on one of the interpenetrating lattices of the crystal. By straightforward methods, the conditions for a transition from a state of uniform to non-uniform distribution in molecular orientation are formulated, and expressions for the thermodynamic functions of the crystal in terms of the distribution functions are presented. From this point of view, the transition manifests itself as a segregation of the molecules from a random distribution in orientation to regions of preferred orientation, rather than as a change from rotating to librating states as in the Fowler theory. Local hindrance of the relative rotation of neighboring molecules in the lattice is assumed permanently present, and the existence of a transition temperature is demonstrated, below which local hindrance becomes effective in producing a non-uniform distribution in orientation of the crystal as a whole. The applicability of the general method of the present theory is not limited to phase changes associated with molecular rotation. Work is now in progress on a theory of fusion in which the method is applied to the lattice vibrational motion of a crystal.

We consider a crystal composed of n interpenetrating simple lattices, each site of which is occupied by one of a set of N identical molecules possessing rotational degrees of freedom. The rotational configuration of the entire crystal may be partially characterized by a set of distribution functions $g_1(\omega), \cdots g_n(\omega)$, so defined that $(N/n)g_k(\omega)$ specifies the density of molecules

[1] Pauling, Phys. Rev. **36**, 430 (1930).
[2] Fowler, *Statistical Mechanics* (Cambridge, 1936), Second edition, Chap. XXI.
[3] Bragg and Williams, Proc. Roy. Soc. **A145**, 699 (1934).

on lattice k in orientation ω. To an arbitrary specification of the functions $g_k(\omega)$, subject to normalization,

$$\int g_k(\omega)d\omega=1; \quad k=1, \cdots n, \tag{1}$$

there corresponds a subset of the entire set of rotational states accessible to the crystal. If the fluctuation in energy among the states of the subset is neglected, the entropy S corresponding to the specified distribution functions $g_k(\omega)$ may be calculated as $k \log \Omega$ where Ω is the total number of states in the subset. Assigning the quasi-classical statistical weights $dp_{\omega i}d\omega_i/h^r$ in the rotational momentum-configuration space of each molecule i of r rotational degrees of freedom, we calculate

$$S/Nk=-\frac{1}{n}\sum_{k=1}^{n}\int g_k \log g_k d\omega+S'/k, \tag{2}$$

where S' is the nonconfigurational rotational entropy of a free molecule. We shall henceforth suppress S' since it plays no role in the transitions with which we are concerned. The average potential energy E, calculated with a similar neglect of fluctuations in energy in the subset of configurations corresponding to the specified $g_k(\omega)$, is

$$E/N=\frac{1}{2n}\sum_{k=1}^{n}\sum_{l=1}^{n}\int\int V^{(kl)}(\omega, \omega')g_k(\omega)g_l(\omega')d\omega d\omega' \tag{3}$$

$$V^{(kl)}(\omega, \omega')=\sum_{b=1}^{N/n} V_{ab}{}^{(kl)}(\omega, \omega'),$$

where $V_{ab}{}^{(kl)}$ is the mutual potential energy of two molecules, respectively situated on site a of lattice k in orientation ω and site b of lattice l in orientation ω'. In the same approximation the configurational free energy F may be written

$$F/NkT=-\frac{1}{n}\sum_{k=1}^{n}\int g_k \log g_k d\omega \tag{4}$$

$$+\frac{1}{2nkT}\sum_{k=1}^{n}\sum_{l=1}^{n}\int\int V^{(kl)}(\omega, \omega')g_k(\omega)g_l(\omega')d\omega d\omega'.$$

Extremalization of the free energy, by means of the calculus of variations, with respect to the functions $g_k(\omega)$, subject to the normalization restraint, leads to the following set of integral equations

$$\log \lambda_k g_k(\omega)=\sum_{l=1}^{n}\int K_{kl}(\omega, \omega')g_l(\omega')d\omega', \tag{5}$$

$$\lambda_k=\int \exp\left[\sum_{l=1}^{n}\int K_{kl}g_l d\omega'\right]d\omega; \quad k=1, \cdots n.$$

$$K_{kl}(\omega, \omega')=-V^{(kl)}(\omega, \omega')/kT.$$

The form of the solutions of these equations is determined by the kernels K_{kl}, which in turn depend upon the form of the $V^{(kl)}(\omega,\omega')$ as functions of molecular orientation. As we shall demonstrate, interactions of certain types lead to phase changes of the second kind and lambda-points. Other types of interaction may lead to phase changes of the first kind, which are also observed in crystals with degrees of molecular rotational freedom.

We shall now undertake the solution of Eqs. (5), in the case of cubic crystals composed of diatomic molecules, under certain assumptions concerning the interaction hindering relative molecular rotation. We shall suppose the potential energy of a pair of nearest neighbors depends only on the angle γ between the molecular axes of figure and that the interaction of molecules which are not nearest neighbors can be neglected. The potential $V_{ab}{}^{(kl)}$ may be expanded in a Fourier series in γ with an arbitrary constant term, conveniently assigned the value zero, and an initial term depending on molecular symmetry,

$$V_{ab}{}^{(kl)}=\frac{\epsilon}{2}\cos(m\gamma) \tag{6}$$

if the molecule has an m-fold axis perpendicular to its axis of figure. For homonuclear diatomic molecules m has the value two and for heteronuclear diatomic molecules such as the hydrogen halides m is unity. ϵ is height of the potential barrier between adjacent minima. For cubic crystals, it is of course independent of the lattice indices k and l and on the neighbor indices a and b, since all nearest neighbor sites of an arbitrary lattice site are equivalent. We shall consider here only the heteronuclear case,

$m=1$, for which Eqs. (3), (5) and (6) yield

$$\begin{aligned} K_{kl} &= -\alpha \cos\gamma; \quad k \neq l \\ &= 0; \quad\quad\quad k = l \\ \alpha &= z\epsilon/2kT, \end{aligned} \tag{7}$$

where z is the number of nearest neighbors of an arbitrary site on one of the n interpenetrating lattices, belonging to each of the remaining $n-1$ lattices. For a body-centered lattice n is equal to 2 and z is 8; for a face-centered lattice n is 4 and z is 4. If orientations are referred to an arbitrary polar coordinate system, substitution of Eqs. (7) into Eqs. (5) yields

$$\log \lambda_k g_k(\vartheta, \varphi) = -\alpha \sum_{l=1\neq k}^{n} \int_0^{\pi}\int_0^{2\pi} \cos\gamma g_l(\vartheta', \varphi') \sin\vartheta' d\vartheta' d\varphi',$$

$$\lambda_k = \int_0^{\pi}\int_0^{2\pi} \exp\left[-\alpha \sum_{l=1\neq k}^{n} \int_0^{\pi}\int_0^{2\pi} \cos\gamma g_l \times \sin\vartheta' d\vartheta' d\varphi'\right] \sin\vartheta d\vartheta d\varphi, \tag{8}$$

$$\cos\gamma = \cos\vartheta\cos\vartheta' + \sin\vartheta\sin\vartheta'\cos(\varphi-\varphi').$$

Due to the degeneracy of the kernels, $\cos\gamma$, the solutions of Eq. (8) may be constructed without difficulty.

$$\begin{aligned} \lambda_k g_k &= e^{\alpha s_k \cos\vartheta}, \\ \lambda_k &= \frac{4\pi}{\alpha s_k}\sinh(\alpha s_k); \quad k = 1, \cdots n \\ -s_k &= \sum_{l=1\neq k}^{n} L(\alpha s_l), \end{aligned} \tag{9}$$

where $L(x)$ is the Langevin function, $\coth x - 1/x$. The transcendental Eqs. (9) determining the parameters S_k may be put in an alternative form

$$L(\alpha s_k) = s_k - \sigma_0/(n-1), \quad \sigma_0 = \sum_{l=1}^{n} s_l. \tag{10}$$

We shall consider here only those solutions of Eqs. (10) for which α is positive (minimum interaction in antiparallel orientation) and σ_0 vanishes. In the body-centered case ($n=2$), we have

$$s_k = \pm(-1)^k s; \quad k = 1, 2, \tag{11}$$

where S is the positive real solution, minimizing the free energy, of the equation,

$$s = L(\alpha s). \tag{12}$$

In the face-centered case ($n=4$), we have several alternatives, all of which are equivalent, two of the s_k being equal to the positive real root s of Eq. (12) and two equal to the negative real root, $-s$, for example,

$$s_k = \pm(-1)^k s; \quad k = 1, 2, 3, 4. \tag{13}$$

In both cases, there exists a critical value of α, equal to 3, below which Eq. (12) has no real solutions different from zero, and above which a single nonzero positive real root s, of minimum free energy, exists. This situation leads to a phase change of the second kind with a transition temperature, T_c, given by

$$\begin{aligned} T_c &= z\epsilon/6k \\ z &= \begin{cases} 8; \text{ b.c.} \\ 4; \text{ f.c.} \end{cases} \end{aligned} \tag{14}$$

The parameter s is tabulated as a function of T/T_c in Table I.* Above the transition temperature, the stable distribution functions g_k have the uniform value $1/4\pi$, corresponding to a random

TABLE I. *The order parameter s as a function of the temperature.*

T/T_c	s	T/T_c	s
1.0	0.00	0.5	0.79
.9	.39	.4	.84
.8	.54	.3	.89
.7	.65	.2	.93
.6	.72	.1	.96

* If Eq. (12) is to be solved graphically, the change of variable, $y=\alpha s$, is convenient.

$$y/\alpha = L(y).$$

The intersections of a straight line through the origin, with slope $1/\alpha$, and the graph of $L(y)$ provide the desired solutions of the above equation. When $1/\alpha$ is greater than $\frac{1}{3}$, the limiting slope of $L(y)$, the line and the curve intersect only at the origin, and s is constrained to the value zero. When $1/\alpha$ is less than $\frac{1}{3}$, there are three intersections at zero and $\pm\alpha s$, where s is the equilibrium value of the order parameter. For actual computation it is more convenient to assign a set of values to y and to calculate α and s by the parametric equations,

$$\begin{aligned} \alpha &= y/L(y) \\ s &= L(y), \end{aligned}$$

from which a tabulation of s as a function of α may be obtained by analytical methods.

distribution in orientation on each lattice. Below the critical temperature, the distribution becomes non-uniform, the molecules of half of the interpenetrating lattices partially oriented parallel to and the molecules of the remaining lattices antiparallel to the polar axis of the reference system. The orientation of this axis relative to the lattice vectors is of course arbitrary, as is to be expected from the fact that the interaction between neighbors depends only on their relative orientation. In Fowler's theory[3] of hindered rotation, distribution functions of the form exp $(\alpha s \cos \vartheta)$ were introduced in an *ad hoc* manner. Fowler's surmise that s was the fraction of molecules librating turns out to be unjustified. Eqs. (8), (9) and (10) show that s is the mean value of $\cos \vartheta$ for molecules of the lattice under consideration. The transcendental equation determining s is therefore quite different from that of Fowler.

The thermodynamic functions of the crystal, when expressed in terms of the order parameter s, have the form

$$\begin{aligned} S/R &= \log\left[\frac{4\pi}{\alpha s}\sinh \alpha s\right]-\alpha s^2, \\ E/RT &= -\alpha s^2/2, \\ F/RT &= -\log\left[\frac{4\pi}{\alpha s}\sinh \alpha s\right]+\alpha s^2/2. \end{aligned} \tag{15}$$

From Eqs. (12) and (15), the configurational contribution to the heat capacity C_v may be calculated as

$$C_v/R=\frac{\alpha^2 s^2 L'(\alpha s)}{1-\alpha L'(\alpha s)}, \quad L'(x)=\frac{dL}{dx}. \tag{16}$$

Eqs. (12) and (16) yield the following value for the heat capacity anomaly, ΔC_v, at the transition temperature,

$$\Delta C_v/R=5/2. \tag{17}$$

The heat capacity anomaly ΔC_v of 5 cal./mole is considerably smaller than anomalies in the constant pressure heat capacity ΔC_p observed at lambda-points which are attributed to hindered rotation. A theory based on two accessible relative molecular orientations rather than a continuous set only increases ΔC_v to 6 cal./mole. Moreover, the neglect of fluctuations in energy cannot be expected to introduce an error of more than about 20 percent in ΔC_v, if it is of the same magnitude as in the superlattice case. It seems necessary to attribute the large observed ratios of $\Delta C_p/\Delta C_v$ to a dependence of the barrier height ϵ on the expansion of the lattice.[4, 5] A general formula relating ΔC_p and ΔC_v in phase changes of the second kind has been given by Bethe and the writer.[5]

$$\frac{\Delta C_p}{\Delta C_v}=\frac{(1+\sigma\beta_+ T_c)^2}{1-\sigma^2\kappa_+ T_c \Delta C_v/v}, \quad \sigma=-\frac{v\,d\epsilon}{\epsilon\,dv}, \tag{18}$$

where β_+ and κ_+ are the coefficients of expansion and compressibility of the crystal just above the transition temperature and v is the molar volume. If σ is sufficiently large, the ratio, $\Delta C_p/\Delta C_v$, may become very large. If the denominator of Eq. (18) becomes zero or negative, the transition of the second kind must be replaced by one of the first kind occurring at a higher temperature than T_c. If ϵ is supposed to be proportional to a power $-m$ of the lattice parameter, σ is equal to $m/3$. Supposing m to be of the order of magnitude 10, we may estimate rather crudely that σ is of the order of magnitude unity. However, since theoretical calculation of ϵ and σ is not yet feasible, it is necessary to leave them as parameters to be determined from experiment.

If the molecules of the crystal are polar, the influence of rotational transitions on dielectric behavior is of considerable interest. It is first necessary to consider the influence of dipole-dipole interaction in the present theory and the possibility of electric Curie points. Thus far we have considered only short range interaction between the molecules, effectively limited to nearest neighbors in the crystal. Electric Curie points can be produced by short range interactions if ϵ and α, Eq. (7), are negative. It seems likely that the few observed examples of electric Curie points are in fact due to short range interaction, although for their discussion a more complicated potential than $(\epsilon/2)\cos\gamma$ is doubtless necessary. In cubic crystals, nearest neighbor dipole-dipole interaction makes no contribution to the kernels K_{kl} of Eq. (7). However, due to

[4] Eisenschitz, Proc. Roy. Soc. **A168**, 546 (1938).
[5] Bethe and Kirkwood, J. Chem. Phys. **7**, 578 (1939).

the long range character of dipole-dipole forces, they are found to make a contribution when summed over the entire crystal. If this is done, Eq. (7) is modified as follows,

$$\begin{aligned} K_{kl} &= (\beta-\alpha)\cos\gamma; \quad k \neq l \\ &= \beta\cos\gamma; \qquad\quad k = l \qquad (19) \\ \beta &= f\mu^2/\Delta kT, \end{aligned}$$

where Δ is the volume of the unit cell, μ the molecular dipole moment, and f is a factor depending on the shape of the crystal, ranging from zero for a spherical specimen to $8\pi/3$ for a slab bounded by two parallel planes of infinite extent. We shall not discuss in detail the solutions of Eqs. (5) with the kernels (18), but remark that electric Curie points ($\sigma_0 \neq 0$) are excluded if $\epsilon > 4f\mu^2/z\Delta$. Eqs. (14) and (15) remain valid, the transition temperature and thermodynamic functions being determined by the short range parameter α alone. Otherwise electric Curie points determined by both α and β are predicted. Unfortunately, Curie points are predicted by the above criterion for crystals in which they are not observed, for example the hydrogen halides. We must therefore conclude that the degree of approximation of the present theory is insufficient for the treatment of long range forces due to dipole-dipole interaction. However, the short range force theory based on Eq. (7) remains formally valid for a spherical specimen or for a specimen of arbitrary shape immersed in an infinite medium of its own dielectric constant. Since there is no evidence that rotational lambda-points are affected by the shape of the crystal, the difficulty appears to lie entirely in Eq. (19) and the manner in which dipole-dipole interaction is introduced there. Were fluctuations in energy among states of specified rotational distribution taken into account, we surmise that the long range effects of dipole-dipole interaction would be nullified leaving a residual short range effect which would appear in a higher approximation of the present theory.

Direct application of the present theory to the polarization of a crystal in an external electric field is prevented by similar difficulties with dipole-dipole interaction. In fact, if the short range interaction is zero, the present theory leads to results identical with the Lorentz theory of dielectric polarization. Fortunately, a general theory of dielectric polarization can be formulated in which the long-range effects of dipole-dipole interaction are taken properly into account at the beginning.[6, 7] This theory leads to the following formula for the mean dielectric constant ϵ of a polar crystal,* where v is the molar volume α_0 the optical polarizability of a molecule and $\bar{\boldsymbol{\mu}}$

$$\frac{(\epsilon-1)v}{4\pi} = \frac{3\epsilon N}{2\epsilon+1}\left[\alpha_0 + (\boldsymbol{\mu}\cdot\bar{\boldsymbol{\mu}})_{Av}/3kT\right] \qquad (20)$$

is the average dipole moment of a macroscopic spherical specimen of the dielectric, immersed in an infinite medium of its own dielectric constant, produced by fixing one of its molecules in a specified orientation, and $(\boldsymbol{\mu}\cdot\bar{\boldsymbol{\mu}})_{Av}$ is the mean value of the scalar product of $\bar{\boldsymbol{\mu}}$ and the dipole moment $\boldsymbol{\mu}$ of the fixed molecule averaged over all orientations of the latter. In the original formulation of the theory for liquids, the final average was unnecessary since in that case $\boldsymbol{\mu}\cdot\bar{\boldsymbol{\mu}}$ is independent of the orientation of the fixed molecule. Although in liquids $\bar{\boldsymbol{\mu}}$ reduces to the sum of the moment of a molecule and that which it induces in its immediate environment, this is not in general true of crystals. Long range dipole-dipole interaction having been implicitly taken into account in Eq. (20), it is possible to obtain a moderately good approximation to $(\boldsymbol{\mu}\cdot\bar{\boldsymbol{\mu}})_{Av}$ with the rotational distribution functions of Eq. (9). For $(\boldsymbol{\mu}\cdot\bar{\boldsymbol{\mu}})_{Av}$ we may write, where $(\cos\gamma_{ij})_{Av}$ is the

$$(\boldsymbol{\mu}_i\cdot\bar{\boldsymbol{\mu}}_i)_{Av} = \mu^2\left[1+\sum_{j=1\neq i}^{N}(\cos\gamma_{ij})_{Av}\right], \qquad (21)$$

mean value of the cosine of the angle γ_{ij} between a pair of molecules i and j, averaged over the orientations of both, the sum extending over all molecules of the spherical specimen except the specified molecule i. The condition that the specimen be immersed in an infinite medium of its own dielectric constant, involved in the definition of $\bar{\mu}$, seems at first irrelevant if the

[6] L. Onsager, J. Am. Chem. Soc. 58, 1486 (1936).
[7] J. G. Kirkwood, J. Chem. Phys. 7, 911 (1939).
* The mean dielectric constant is defined as one-third of the diagonal sum of the dielectric constant tensor. It is of course the observed dielectric constant of the crystal powder.

distribution functions of Eq. (9) are employed, until it is remembered that these functions are in fact only valid under these conditions and otherwise would require correction due to a reaction field produced by the fixed molecule i and the exterior boundary of the specimen. Making use of Eqs. (9) and (11) or (13), we calculate

$$(\cos \gamma_{ij})_{Av} = (-1)^{k+l} s^2, \tag{22}$$

where k and l are the indices of the lattices on which the molecular pair i and j are situated and the sum of Eq. (21) becomes

$$\sum_{j=1\neq i}^{N} (\cos \gamma_{ij})_{Av} = (-1)^k (Ns^2/n) \sum_{l=1\neq k}^{n} (-1)^l + [(N/n)-1](-1)^{2k} s^2 \tag{23}$$

which, with n equal to two or four, is exactly equal to $-s^2$, so that $(\mathfrak{y} \cdot \bar{\mathfrak{y}})_{Av}$ for both body-centered and face-centered cubic crystals is equal to $\mu^2(1-s^2)$ and Eq. (20) becomes

$$\frac{(\epsilon-1)}{4\pi} v = \frac{3\epsilon N}{2\epsilon+1}\left[\alpha_0 + \frac{\mu^2}{3kT}(1-s^2)\right]. \tag{24}$$

From Eq. (24), we observe that the dielectric constant is a continuous function of the temperature but has a discontinuous temperature derivative since the parameter s of Eq. (12) has a discontinuous temperature derivative. Above the transition temperature Eq. (23) reduces to the Onsager equation, which is a fairly good approximation for such substances as the hydrogen halides. Below the transition temperature, the dipole contribution to the dielectric constant diminishes to zero as s increases to its saturation value, unity.

Phase changes of the second kind possibly attributable to hindered molecular rotation were found for the solid hydrogen halides by Giauque and Wiebe.[8] Two lambda-points at 70°K and 125°K were found in the heat capacity curve of hydrogen iodide, and three at 89°K, 113°K, and 117°K in the heat capacity curve of hydrogen bromide. None were found for hydrogen chloride, but instead one transition of the first kind. Considering only the transitions of the second kind, we may ask which of them are directly attributable to hindered rotation. The dielectric constant measurements of Smyth and Hitchcock[9] provide a fairly conclusive answer to this question. The two upper transitions in hydrogen bromide and the upper transition in hydrogen iodide produce no marked effect on the dielectric constant. Below the 89°K transition in hydrogen bromide, the dielectric constant decreases rapidly with diminishing temperature. Although the measurements on solid hydrogen iodide were not carried through the transition at 70°K, their trend suggests a behavior similar to that of hydrogen bromide. The transitions of interest in the light of the present theory therefore appear to be the transition at 89°K in hydrogen bromide and the transition at 70° in hydrogen iodide. However, before discussing them, a few remarks concerning the other transitions should be made. The special solutions of Eq. (5) for cubic crystals predict only one rotational lambda-point. For rhombic crystals more than one lambda-point could result. But, since the hydrogen halide structures are face-centered cubic or face-centered tetragonal with an axial ratio differing only slightly from unity, and since the other transitions should have a marked effect on the dielectric constant if they were purely rotational, it seems necessary to attribute them to other causes, possibly to a coupling between molecular rotation and the lattice vibrations. The occurrence of a transition of the first kind in hydrogen chloride, evidently to be associated with hindered rotation from the dielectric constant evidence, is difficult to understand unless the dependence of ϵ on lattice expansion is admitted. On the basis of the present theory it could be attributed to a torque potential of different form than $(\epsilon/2)\cos\gamma$. It is interesting to remark the solutions of Eq. (5) with a two-minima potential, $(\epsilon/2)\cos 2\gamma$, lead to a phase change of the first kind. Such a potential should be appropriate to homonuclear diatomic molecules such as oxygen or nitrogen, but is difficult to see why hydrogen chloride should conform to it. It seems more likely that the parameter σ of Eq. (18) is sufficiently large to replace a transition of the second kind by one of the first kind in the case of hydrogen chloride.

[8] Giauque and Wiebe, J. Am. Chem. Soc. **50**, 2193 (1928); **51**, 1441 (1929).

[9] Smyth and Hitchcock, J. Am. Chem. Soc. **155**, 1830 (1933).

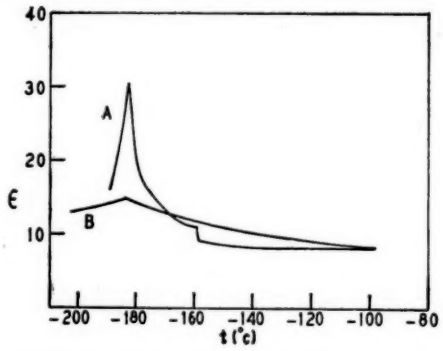

FIG. 1. The dielectric constant of solid hydrogen bromide as a function of temperature. Curve *A*, measurements of Smyth and Hitchcock at 20 kc. Curve *B*, theoretical, Eq. (24).

Identifying them as the rotational lambda-points, we may use the present theory to interpret the transition at 70°K in hydrogen iodide and the transition at 89°K in hydrogen bromide. We shall treat the lattices of both as face-centered cubic. The hydrogen iodide[10, 11] lattice is face-centered tetragonal with an axial ratio of 1.08, thus very nearly cubic. The lattice of hydrogen bromide has not been determined with certainty, but it appears to be face-centered cubic above the transition, changing to one of lower symmetry at lower temperatures. From Eq. (4) with z equal to 4, and the values of the transition temperatures, we calculate the barrier height ϵ as 210 cal./mole for hydrogen iodide and 267 cal./mole for hydrogen bromide. In both cases the ratio $\Delta C_p/\Delta C_v$ is large, about 4 for hydrogen iodide and 94 for hydrogen bromide, if the experimental values of ΔC_p and the theoretical value of ΔC_v, Eq. (17), are used. Unfortunately, no data on the coefficients of expansion and compressibility of the solid hydrogen halides seem to be available. In the case of hydrogen iodide, a value of approximately 1.6×10^{-3} for the mean expansion coefficient between 82°K and 100°K may be calculated from the dependence of the lattice parameters on temperature. The molar volumes of solid hydrogen iodide and hydrogen bromide at their melting points are 42 cc and 33 cc, respectively. In the absence of the necessary data, a very rough estimate of the magnitude of σ may be obtained from the ratios $\Delta C_p/\Delta C_v$ and Eq. (18), with a value 10^{-5} atmos.$^{-1}$ for κ_+ and a value 10^{-3} for $\beta+$ assigned to both of the hydrogen halides. For hydrogen iodide σ turns out to be about 6 and for hydrogen bromide 9. Only the order of magnitude of these values and the fact that σ is greater for hydrogen bromide than for hydrogen iodide are significant.

It is of interest to compare the temperature dependence of the dielectric constant predicted by Eq. (24) with the measurements of Smyth and Hitchcock on the dielectric constant of hydrogen bromide. In Fig. 1, the experimental values of ϵ at a frequency of 20 kc are compared with the theoretical values at zero frequency calculated by Eq. (24). The dipole moment of the HBr molecule is assigned a value 1.17 Debye units to bring the observed and calculated values of ϵ into agreement at 186°K. Although the moment of an HBr molecule in the crystal may differ somewhat from its value, 0.78 Debye, in the vapor, the rather large value 1.17 doubtless reflects a lack of accuracy in the theory, due to neglect of local ordering of the relative orientations of neighboring molecules in the crystal. The agreement between the theoretical and experimental curves is far from quantitative, but it will be observed that the kink at the transition temperature is reproduced by the theory. The theory fails to reproduce the very sharp peak in the experimental curve at the transition temperature, which is probably due to local ordering of orientations. It should of course be remarked that the experimental curve at 20 kc is not strictly comparable with the theoretical curve which is valid only at zero frequency. However, hysteresis effects prevent an unambiguous extrapolation of the experimental dielectric constants to zero frequency.

We seem justified in concluding that the present theory provides a semi-quantitative description of phase changes of the second kind produced by the ordering of molecular orientations in crystals. From its application to the solid hydrogen halides, we estimate a barrier height for the relative rotation of neighboring molecules in the lattice of the magnitude of several hundred calories per mole. From the ratio of $\Delta C_p/\Delta C_v$ the rough estimates of σ indicate a marked sensitivity of the barrier height to the lattice parameter of the crystal, greater for

[10] Ruhemann and Simon, Zeits. f. physik. Chemie (B) **15**, 389 (1932).
[11] Natta, Mem. Accad. Italia Chim. **2**, 15 (1931).

hydrogen bromide than for hydrogen iodide. We surmise that in hydrogen chloride, the sensitivity of the barrier height to the lattice parameter is the cause of a transition of the first kind instead of one of the second kind. In the case of hydrogen bromide, the behavior of the dielectric constant in the transition is qualitatively described. The theory is subject to corrections of two types. The first of these would involve taking into account energy fluctuations in states of the same orientational distribution. The second relates to deviations from classical statistical mechanics. The present theory must be regarded as inadequate when the separation between neighboring rotational energy levels in the crystal becomes large relative to kT. Evidence for the necessity of a quantum-mechanical theory of cooperative phenomena in the case of molecules of low moment of inertia at low temperatures is provided by the differences in the heat capacity curves of methane and the deutero-methanes, which cannot reasonably be attributed to differences in intermolecular forces between neighbors in the lattice.

FEBRUARY, 1940 JOURNAL OF CHEMICAL PHYSICS VOLUME 8

Kinetics of Phase Change. II

Transformation-Time Relations for Random Distribution of Nuclei*

MELVIN AVRAMI
School of Mines, Columbia University, New York, New York

(Received July 5, 1939)

Following upon the general theory in Part I, a considerable simplification is here introduced in the treatment of the case where the grain centers of the new phase are randomly distributed. Also, the kinetics of the main types of crystalline growth, such as result in *polyhedral*, *plate-like* and *lineal* grains, are studied. A relation between the actual transformed volume V and a related *extended volume* $V_{1\,ex}$ is derived upon statistical considerations. A rough approximation to this relation is shown to lead, under the proper conditions, to the empirical formula of Austin and Rickett. The exact relation is used to reduce the entire problem to the determination of $V_{1\,ex}$, in terms of which all other quantities are expressed. The approximate treatment of the beginning of transformation in the isokinetic range is shown to lead to the empirical formula of Krainer and to account quantitatively for certain relations observed in recrystallization phenomena. It is shown that the predicted shapes for isothermal transformation-time curves correspond well with the experimental data.

A. RESUMÉ

IN the previous paper[1] we have developed some of the general theory of phase change with the following assumptions strongly supported by experiment.

(I) The new phase is nucleated by tiny "germ nuclei" which already exist in the old phase and whose effective number $\bar{N}$ per unit nucleation region can be altered by temperature and duration of superheating. These germ nuclei, which may be heterogeneities of any sort, usually consist of small particles of the subcritical phase or tough films of the latter surrounding foreign inclusions.

(II) The number of germ nuclei per unit region at time t, $N \equiv N(t)$ decreases from $\bar{N}$ in two ways: (a) through becoming active growth nuclei, with number $N' \equiv N'(t)$, as a result of free energy fluctuations with probability of occurrence n (a function of temperature, concentration, etc.) per germ nucleus; (b) through being swallowed by grains of the new phase whose linear dimensions are growing at rate G (also a function of temperature, concentration, etc.). Letting $V \equiv V(t)$ represent the volume of the new phase per unit volume of space we are led to

* Publication assisted by the Ernest Kempton Adams Fund for Physical Research of Columbia University.

[1] J. Chem. Phys. **7**, 1103 (1939). Referred to hereafter as K.P.C. I.

the relation

$$N(t)=\bar{N}e^{-nt}[1-V(t)]$$

between the density of germ nuclei and transformed volume. For the density of growth nuclei we find

$$N'(t)=\bar{N}\int_0^t e^{-nz}[1-V(z)]dz.$$

It is very useful to express these relations as well as the others in terms of the *characteristic time scale* of the substance and process, defined by changing the unit of time so that $ndt=d\tau$. This gives

$$N(\tau)=\bar{N}e^{-\tau}[1-V(\tau)], \qquad (5')$$

$$N'(\tau)=\bar{N}\int_0^\tau e^{-z}[1-V(z)]dz. \qquad (5'')$$

Beyond $\tau=\bar{\tau}$, roughly corresponding to the time when the germ nuclei are exhausted, i.e., where

$$N=1=\bar{N}e^{-\bar{\tau}}[1-V(\bar{\tau})]$$

these expressions are to be replaced by*

$$N=0,$$

$$N'=\bar{N}'=\bar{N}\int_0^{\bar{\tau}} e^{-z}[1-V(z)]dz.$$

(III) Besides (5'), we found another relation in that V is a functional $V|[N(\tau)]|$ of N, i.e., at any time τ, it depends upon the values of $N(\tau)$ throughout the interval 0 to τ. Assuming, as is usually true in crystalline growth, that where one grain impinges upon another, growth ceases, we found the form and significance of the terms $V_{m\,ex}$ in the expansion of the functional

$$V=V_{1\,ex}-V_{2\,ex}+V_{3\,ex}+\cdots(-1)^{m+1}V_{m\,ex}\cdots. \qquad (9)$$

(IV) If now it is assumed, as is plausible from the underlying mechanisms and as the experiments verify, that

$$G/n\equiv\alpha$$

is approximately independent of temperature and concentration in a given "isokinetic range," for a given substance and crystal habit, we have

$$V_{m\,ex}=\int_0^\tau N(z_1)dz_1\int_0^{z_1}N(z_2)dz_2\cdots$$

$$\times\int_0^{z_{m-1}}N(z_m)\bar{v}_m[\alpha(\tau-z_1),\cdots\alpha(\tau-z_m)]dz_m. \qquad (6'')$$

In particular

$$V_{1\,ex}=\sigma\alpha^3\int_0^\tau(\tau-z)^3N(z)dz, \qquad (16)$$

for pseudospherical or polyhedral grains, where σ is a shape factor, equal to $4\pi/3$ for spherical grains. $\bar{v}_m$, $V_{m\,ex}$, and therefore the transformed volume V, in the characteristic time scale depend upon n and G only through the ratio α, which has been supposed constant. Therefore, the relative internal history of the transformation is independent of temperature, concentration, or other variables (in the range in which n and G are proportional); or, to restate our conclusion: *For a given substance and crystal habit, there is an "isokinetic range" of temperatures and concentrations throughout which the kinetics of phase change in the characteristic time scale remains unchanged.* This observation enables us to translate results of isothermal reaction curve analysis to the description of phenomena under conditions of varying temperature and concentration.

The calculation of $V_{m\,ex}$, and the determination thereby (with Eqs. (9) and (5')) of the complete kinetics of the process, was shown to depend upon complex statistical considerations. Fortunately, in the important case of *random* distribution of the grain centers, we may use a general method which, expressing all quantities in terms of a suitably defined $V_{1\,ex}$ alone, enables us to avoid these detailed statistical calculations. We note that the assumption of random distribution of grain centers throughout the volume should be applicable with good approximation to cases where the germ nuclei tend to segregate at the boundaries of a fine grained structure in the old phase, as with many solid-solid phase changes, especially in metals. The results of this

* If we wished to be meticulous we should add to the above the contribution of the last germ nucleus. This is most likely to nucleate at ordinary time $t+1/n$ or characteristic time $\bar{\tau}+1$.

TABLE II.

τ	$E_3(-\tau)$	τ	$E_3(-\tau)$	τ	$E_3(-\tau)$
0.1	0.0000041	2.4	0.914	11	171.33
0.2	0.0000641	2.5	1.057	12	227
0.3	0.000318	2.6	1.223	13	293.67
0.4	0.000987	2.7	1.4025	14	372.33
0.5	0.00236	2.8	1.5995	15	464
0.6	0.00481	2.9	1.815	16	569.67
0.7	0.00874	3.0	2.050	17	690.33
0.8	0.01462	3.1	2.305	18	827
0.9	0.02307	3.2	2.582	19	980.67
1.0	0.0346	3.3	2.881	20	1152
1.1	0.050	3.4	3.204	25	2315.67
1.2	0.069	3.5	3.553	30	4079
1.3	0.095	3.6	3.923	35	6567.33
1.4	0.124	3.7	4.322	40	9905.67
1.5	0.161	3.8	4.748	45	14,219
1.6	0.205	3.9	5.202	50	19,632
1.7	0.258	4.0	5.685	60	34,259
1.8	0.317	5.0	12.34	70	54,786
1.9	0.387	6.0	23.00	80	82,212
2.0	0.468	7.0	38.67	90	117,539
2.1	0.560	8.0	60.33	100	161,766
2.2	0.666	9.0	89.00	↓	↓
2.3	0.783	10.0	125.67	∞	$\tau^3/3!$

theory should then check approximately with those of a theory which explicitly takes into account the distribution along grain boundaries.

Before proceeding, we should point out that the special formulae (12), (15), and (16) given in the preceding paper apply only to the case of pseudospherical or polyhedral grains, i.e., those growing at approximately the same rate in all directions. In the general case, where the growth is considerably unsymmetrical, we have to deal with an interesting and complex problem. We shall not study it here but merely note that besides the case, given above, of what we can call *polyhedral* growth, we may have two important situations: First, where growth is primarily along two dimensions so that the grain is *plate-like* in shape; and second, where growth is primarily along one direction when we shall call it *lineal*. In these two cases, the expressions corresponding to (16) are

$$V_{1\,ex}=\sigma'\alpha^2\int_0^\tau(\tau-z)^2N(z)dz, \qquad (16')$$

$$V_{1\,ex}=\sigma''\alpha\int_0^\tau(\tau-z)N(z)dz, \qquad (16'')$$

respectively. Here α represents the ratio, in each case, of a suitably chosen G to n. Like (16), these formulae are applicable only if we are in a range approximately isokinetic, i.e., for G/n constant. In general for most substances, as crystallization velocities are made higher the type of growth changes from polyhedral to lineal.

B. Relation Between V and $V_{1\,ex}$ [2]

1. Approximation. The Austin-Rickett formula as a special case

In any region, selected arbitrarily, let us designate as "nonoverlapped" that part of the volume in which there is no transformed matter, i.e., no grains or parts of grains of the new phase. Then we have that, *on the average, the ratio of nonoverlapped volume v' to extended volume $v_{1\,ex}$ of a randomly selected region is equal to the density of untransformed matter* $1-V$ at that time, i.e.,

$$\frac{v'}{v_{1\,ex}}=1-V. \qquad (17)$$

If now we suppose that the grains of the new phase themselves have formed at random during the reaction, we might hope to apply (17) to these on the average. We cannot, however, do this directly because any actual grain is not randomly located in the *entire* unit volume. Its position is subject to the restriction that its nucleus lay somewhere outside of the transformed volume $V(z)$ at the time z of its origin. We can circumvent this complication in one of two ways. In either case we get the same result. First we can restore complete randomness by including in our consideration all the "phantom" grains associated with germ nuclei which would have been activated into growth if they had not been absorbed by the growing new phase. At time z, the total rate of grain formation, including phantoms, is $\bar{N}e^{-z}$ (per unit volume), and it is this value of $N(z)$ which should be used in the calculation of the various extended volumes $V_{m\,ex}$. In particular

$$V_{1\,ex}=\bar{N}\int_0^\tau e^{-z}v(\tau,z)dz \qquad (18)$$

where, as in (6) of the previous paper,

$$v(\tau,z)\equiv v_{1\,ex}(\tau,z)$$

[2] R. F. Mehl and W. Johnson in Metals Technology, T.P. No. 1089 (1939), have used arguments similar to those in this section in the special case of spherical grains appearing at a constant rate per unit untransformed volume.

is the extended volume, at time τ, of a grain which started at z. The contributions of the phantom grains to the nonoverlapped and actual volumes, V_1' and V, respectively, are zero, so that there is no physical difference introduced by their consideration. Strictly, we should distinguish between $V_{m\,ex}$ as defined in this way and as used before, but for brevity's sake we employ the same notation. From now on, unless otherwise specified, we shall work with the phantom-included population in calculating $V_{m\,ex}$. This way of thinking is particularly useful in proving the theorem of the Appendix. Now we may apply (17) to the nonoverlapped volume of an average grain (over the phantom included population) in relation to its extended volume. Summing both numerator and denominator over all the grains (including phantoms) in unit volume we get

$$\frac{V_1'}{V_{1\,\mathrm{ex}}}=1-V$$

or

$$\frac{V_1'}{1-V}=\bar{N}\int_0^\tau e^{-z}v(\tau,z)dz \qquad (17')$$

An alternative approach, without the use of "phantom" grains, which leads to the same result is as follows: The nucleus or center of an actual grain originating at time z was, with equal likelihood, anywhere in the volume $1-V(z)$ (and only in this region). Then, at a later time τ, when the untransformed volume has diminished to $1-V(\tau)$, the ratio of nonoverlapped to extended volume of the grain is, on the average, given by

$$\frac{v_1'}{v_{1\,\mathrm{ex}}}=\frac{1-V(\tau)}{1-V(z)} \quad \text{or} \quad \frac{v_1'}{1-V(\tau)}=\frac{v_{1\,\mathrm{ex}}}{1-V(z)}.$$

If we multiply both sides of the equation by the number of (actual) grains forming in time interval dz, and integrate from 0 to τ, we get

$$\frac{V_1'}{1-V}=\bar{N}\int_0^\tau e^{-z}v(\tau,z)dz$$

which agrees entirely with (17').

We shall now consider an interesting special case: For transformations in which the new phase is very fine grained, and therefore the overlapping is small, we may write as a rough approximation

$$V_1'=V$$

and, combining with (17'), this gives

$$V/(1-V)=V_{1\,\mathrm{ex}}. \qquad (17'')$$

Under isothermal conditions, and for phases which remain uniform in concentration, growth of linear dimensions is frequently at a constant rate G. n too is constant and as before, with $\alpha\equiv G/n$ and polyhedral growth, we get

$$V_{1\,\mathrm{ex}}=\sigma\alpha^3\bar{N}\int_0^\tau(\tau-z)^3e^{-z}dz.*$$

In assuming the constancy of G under isothermal conditions, we have supposed that, once activated, the germ nucleus soon passes the region of slow growth beyond which its rate becomes constant. This amounts to neglecting any "incubation period" in the growth nucleus. Integrating, we get

$$V_{1\,\mathrm{ex}}=\frac{6\sigma G^3\bar{N}}{n^3}\left[e^{-\tau}-1+\tau-\frac{\tau^2}{2!}+\frac{\tau^3}{3!}\right]\equiv\beta E_3(-\tau) \qquad (18')$$

where we have introduced the convenient abbreviations

$$\beta\equiv 6\sigma G^3\bar{N}/n^3, \qquad (18'')$$

$$E_m(-x)=\frac{1}{m!}\int_0^x(x-z)^me^{-z}dz=(-1)^{m+1}\times\left[e^{-x}-1+x\cdots(-1)^{m+1}\frac{x^m}{m!}\right].$$

TABLE III.

τ	$E_1(-\tau)$	$E_2(-\tau)$
0.1	0.0048375	0.0001625
0.5	0.10653	0.01847
1.0	0.36788	0.13212
2	1.13534	0.86466
3	2.04979	2.45021
4	3.01832	5.98168
5	4.00674	8.49326
6	5.00248	12.99752
7	6.00091	18.49909
8	7.00034	24.99966
9	8.00012	32.49988
10	9.00005	40.99995
20	19	181
100	99	4901
↓	↓	↓
∞	τ	$\tau^2/2!$

* The generalization to the nonisothermal case as in quenching, and to that of varying concentrations (as in precipitation from noneutectic solutions), has the same form in the isokinetic range, but the unit of τ in ordinary time is variable.

(18′) is valid only up to $\tau=\bar{\tau}$, the time corresponding to the exhaustion of the germ nuclei. Beyond this, the upper limit of the integral should be replaced by $\bar{\tau}$, and we may express the result of integration by

$$V_{1\,ex}=\beta\{E_3(-\tau)-e^{-\bar{\tau}}E_3[-(\tau-\bar{\tau})]\}. \quad (18''')$$

Formulae similar to (18′) and (18‴), with E_3 replaced by E_2 and E_1, respectively, are obtained when we suppose the grain growth to be plate-like or lineal as in (16′) and (16″). For brevity's sake we shall use the designation $E(\tau)$ with the understanding that

$$E(\tau)=\begin{cases}E_3(-\tau) & \text{for polyhedral growth}\\ E_2(-\tau) & \text{for plate-like growth}\\ E_1(-\tau) & \text{for lineal growth.}\end{cases}$$

$E_3(-\tau)$, $E_2(-\tau)$, and $E_1(-\tau)$ are tabulated as functions of τ in Tables II and III.

For n very large, (18′) goes over to

$$\beta\tau^3/3!=\sigma G^3\bar{N}t^3.$$

For τ small, i.e., t small compared with $1/n$, it goes into

$$\beta\tau^4/4!=\sigma G^3\bar{N}nt^4/4.$$

In either case, and for different types of crystal growth, it approximates the form Bt^k, where B is a function of temperature only and k is a constant. (17″) gives then

$$V(t)/(1-V(t))=Bt^k \quad (17''')$$

and this is exactly the formula for isothermal transformation of super-cooled austenite into bainite found empirically by J. B. Austin and R. L. Rickett.[3] The reasons for the approximate independence of temperature of k are now clear. Any observed deviations from (17‴) can be understood as due to the approximations involved in deriving it from (17′).

2. Exact relation

To obtain the exact relation between V and $V_{1\,ex}$ we may employ the following argument: Applying the same reasoning as in the previous section, not to the volumes of the single grains, but to the nonoverlapped and extended portions of the *increments* of these grains in an element of time, we get for the average grain (including phantoms)

$$dv_1/dv_{1\,ex}=1-V$$

since the nonoverlapped increment of a grain is nothing other than the increment in transformed volume of that grain. For the unit volume

$$\frac{dV}{dV_{1\,ex}}=1-V. \quad (19)$$

Integrating, and rearranging, this gives

$$V=1-e^{-V_{1\,ex}} \quad (20)$$

as the desired fundamental relation, which is applicable in the case of random distribution of the grains.

The derivation of (20) is entirely independent of any assumption about isothermal or isokinetic conditions. Thus even in the case where the distribution of grain centers is not uniformly random, as for instance in solidification in an ingot mold where there is a temperature gradient, as long as the distribution is fine grained and *locally random*, we may expect to be able to apply (20). $V_{1\,ex}$ and V are then functions not only of the ordinary time t, but also of the space coordinates which, together with t, determine the thermal history and the local characteristic time at any point.

Substituting (20) into (5) and (5′), we get

$$N=\bar{N}e^{-(\tau+V_{1\,ex})}, \quad (21)$$

$$N'=\bar{N}\int_0^{\tau}e^{-[z+V_{1\,ex}(z)]}dz. \quad (22)$$

Thus the entire problem of determining the kinetics of reaction has been reduced to finding $V_{1\,ex}$ from (18) in any particular case. The isokinetic case will be examined in detail in this and the next paper.

Considerable doubt might have been raised as to the validity of (19), on the following grounds chiefly. The fraction $1-V$ measures the ratio of nonoverlapped to extended volume of any *volume region* selected at random. We cannot too easily assume that it also measures the corresponding ratio in what is effectively a *selected surface region*, i.e., the layers of grain increments in an element of time. The assumption requires

[3] J. B. Austin and R. L. Rickett, Metals Technology, September 1938, T.P., No. 964.

therefore more rigorous justification. It does turn out to be correct, primarily because of the complete randomness which we assume. The rigorous justification given in Appendix I brings out a number of very interesting relations. Expressions, which are valid in our case of random nucleation, for all $V_{k\,ex}$, V_k, and V_k' in terms of $V_{1\,ex}$ alone, are also derived there.

C. Transformation-Time Phenomena in the Isokinetic Range

1. The beginning of transformation, isothermal and nonisothermal. Derivation of Krainer's formula. Recrystallization phenomena

The kinetics of phase change, as concerning transformation-time and nucleation-time relations are completely determined by (20) to (22), when $V_{1\,ex}$ is known. In the isokinetic case, $V_{1\,ex}$ is given by (18′) up to $\tau=\bar{\tau}$, and we have

$$V(\tau)=1-e^{-\beta E(\tau)}, \tag{23}$$

$$N(\tau)=\bar{N}e^{-[\tau+\beta E(\tau)]}, \tag{24}$$

$$N'(\tau)=\bar{N}\int_0^{\tau} e^{-[z+\beta E(z)]}dz \tag{25}$$

$\tau=\bar{\tau}$ is determined by

$$\bar{\tau}+\beta E(\bar{\tau})=\lg \bar{N} \tag{26}$$

and for $\tau>\bar{\tau}$ we have, from (18′′′)

$$V(\tau)=1-e^{-\beta[E(\tau)-e^{-\bar{\tau}}E(\tau-\bar{\tau})]}, \tag{23′}$$

$$N=0 \text{ (or, more exactly, 1 up to } \bar{\tau}+1), \tag{24′}$$

$$N'=\bar{N}'=\bar{N}\int_0^{\bar{\tau}} e^{-[z+\beta E(z)]}dz. \tag{25′}$$

In all cases when τ is very small, i.e., at the beginning of transformation, and for polyhedral grain growth, (23) goes over into

$$V=1-e^{(-\beta\tau^4/4!)}=1-e^{(-\sigma G^3 N n t^4)/4} \tag{27}$$

or, even more approximately,

$$V\backsimeq\frac{\beta\tau^4}{4!}=\frac{\sigma\alpha^3\bar{N}}{4}\tau^4=\frac{\sigma G^3\bar{N}n}{4}t^4, \tag{27′}$$

indicating that the $V-t$ curve begins like a fourth degree parabola. The physical significance of this is that in the early stages of transformation the number of growth nuclei present is proportional to the first power of the time and their respective volumes to the third power giving for the total volume transformed a dependence on the fourth power of the time.

(27′) shows that V begins to depart appreciably from zero, i.e., the transformation "begins" when $\beta\tau^4/4!$ becomes appreciably different from zero. Now, for ordinary magnitudes of β, this happens rather abruptly around $\tau=1$. Thus we would expect that, generally, the time of "beginning" t_b of isothermal transformation would be approximately equal to $1/n$ at that temperature, i.e.,

$$t_b(T)\backsimeq 1/n(T)$$

or, if the circumstances under which transformation is taking place are nonisothermal, the condition for the "beginning" is

$$\tau=\int n(T)dt\backsimeq\int\frac{dt}{t_b(T)}\backsimeq 1$$

and this is precisely the result obtained empirically by H. Krainer[4] in his experiments on the decomposition of austenite in steels. The root of the formula is seen to be the dependence of V upon the exponential of a high power of τ, a quantity which changes its value very considerably in the neighborhood of $\tau=1$.

For constant β (isokinetic case), not only does the "beginning" time vary inversely with n at different temperatures, but also the temperature —lg time curves for different degrees of transformation are all parallel. We have indicated the form of these curves in the previous paper.

It is especially interesting to consider recrystallization phenomena in metals in the light of (27′). Here, even if α remains approximately constant (isokinetic range), we may vary $\bar{N}$ considerably through the degree of deformation which the old phase is made to undergo. Now there is strong experimental evidence[5] for believing that the "degree of deformation" in a polycrystalline material is measured by Nadai's "octahedral shear."[6] This measure has the advantage of giving results which are independent of the mode of

[4] H. Krainer, Archiv f. Eisenhüttenwesen **9**, 619 (1936).
[5] H. F. Kaiser and H. F. Taylor, Trans. A. S. M. **27**, 227 (1939).
[6] M. Nadai, J. App. Phys. **8**, 205 (1937).

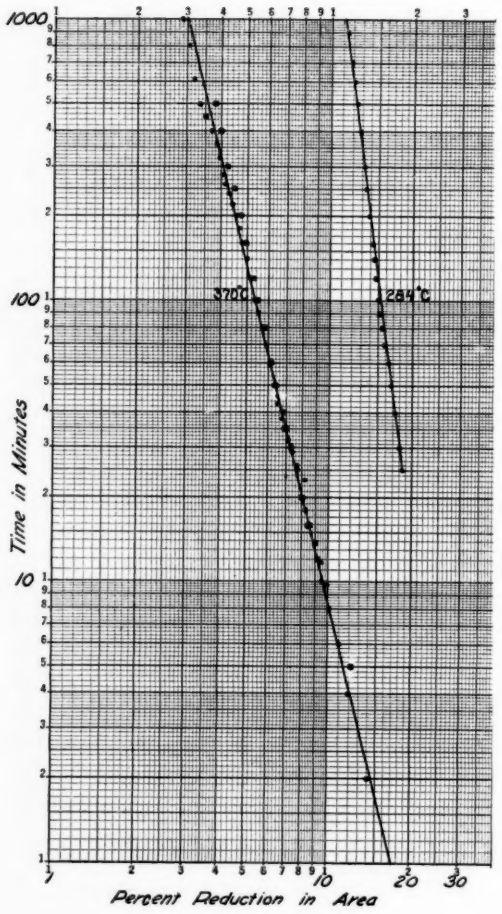

FIG. 4.

deformation, whether, for instance, tension, torsion or rolling. Nadai has given formulae whereby the octahedral shear may be computed, in any case, from the principal specific extensions or contractions. Thus, for instance, in deformation by elongation in tension, the octahedral shear γ_n is related to the specific reduction q through the formula

$$\gamma_n = \sqrt{2} \lg (1+q).$$

For small plastic deformations γ_n will evidently be proportional to q. For larger deformations, we must distinguish between the two.

Now, an inspection of the data on the number of nuclei which appear as a function of the deformation, e.g., that of Kornfeld and Pawlow,[7] suggests a parabolic dependence of $\bar{N}$ upon q, or γ_n, i.e.

$$\bar{N} \propto \gamma_n^4.$$

Since, by (27′), if we keep temperature and other things constant, t_b varies inversely as the 4th root of $\bar{N}$, we would expect to find

$$t_b^4 \propto \frac{1}{\gamma_n^4} \quad \text{or} \quad -8 \lg t_b \propto \lg \gamma_n \propto \lg \lg (1+q)$$

which for small deformations can be written

$$-8 \lg t_b \propto \lg q.$$

If the recrystallizing grains are growing lineally, instead of polyhedrally, t_b varies inversely as the 2nd root of $\bar{N}$ and we would expect to find

$$-4 \lg t_b \propto \lg \lg(1+q) \sim \lg q$$

In the absence of data on the "time of beginning" we use, as a rough indication, the data on the so called "time of recrystallization." This is generally taken to mean the time $t_{0.5}$ required for approximately 50 percent transformation. As will be seen, this is not, by any means, always simply related to t_b. In many cases, however, it is found that the transformation, once started, proceeds rapidly, i.e., the rise of the S-shaped transformation-time curve is quite steep and $t_{0.5}$ does not differ very much from t_b. Here we may expect the data to fit an inverse fourth or eighth power relation depending on whether the growth is lineal or polyhedral.

In the experiments of Karnop-Sachs[8] on the recrystallization of stretched copper wires, the deformations were small enough to permit us to replace the octahedral shear by the specific reduction. In Fig. 4 we have plotted the logarithm of "time of recrystallization" against the logarithm of percentage reduction in area as obtained by Karnop and Sachs. We note that the data, over the entire range, all plot on straight lines with remarkable accuracy. The slope of the line passing through the points taken (from several wires) at 370°C is exactly equal to -4, and the slope of the line through the points taken at 284° is equal to -8. This tends to verify our assumption that the number of germ nuclei is proportional to the square root of the de-

[7] Kornfeld and Pawlow, Physik. Zeits. der Sowjetunion **6**, 537 (1934).

[8] R. Karnop and G. Sachs, Zeits. f. Physik **60**, 464 (1930).

gree of deformation, and suggests that the growth is lineal at the upper temperature and polyhedral at the lower temperature.

If we suppose α to be approximately constant and fix a definite time of annealing, (27) indicates that the $\bar{N}$ required to produce appreciable recrystallization varies inversely as n^4 or, taking logarithms,

$$\lg \bar{N} \propto -4 \lg n = 4(Q+A)/RT$$

where, as shown in the first paper of this series, $Q+A$ is the total energy (per mole) required for a germ nucleus to become a growth nucleus. We shall suppose that we are in the temperature range where this has become constant. Now if we assume, as above, that

$$\bar{N} \propto \gamma_n^{\frac{1}{4}} \propto [\lg (1+q)]^2$$

we may write, for a given time of anneal t_b,

$$\lg \lg (1+q) \propto 1/T.$$

This proportionality is well satisfied over a wide range of deformation as may be seen from the straightness of the lines in Fig. 5, where we have plotted $1/T$ against $\lg \lg (1+q)$ for the data of Oberhoffer-Oertel[9] on electrolytic iron and of Hanemann[10] on hot forged mild steel. This result also constitutes evidence in favor of the assumption of proportionality of $\bar{N}$ to some power of the degree of deformation

2. Transformation-time curves in the isothermal range

Let us consider the entire $V-t$ curve, for polyhedral grain growth as given by (23) and (23′). We first examine the case where $\bar{N}$ is very large, i.e., exhaustion of the germ nuclei does not occur until the end of transformation. Under such conditions we may consider two limiting cases. When n is very small (τ small), (27) will be an adequate representation over the entire transformation, and this corresponds to the special case considered by Mehl-Johnson.[2] On the other hand, for n very large, τ will be large during most of the reaction, and (23) is represented by

$$V = 1 - e^{-\sigma G^3 \bar{N} t^3}. \tag{28}$$

For intermediate values of n the dependence of V upon t will lie between (27) and (28).

If $\bar{N}$ is small so that exhaustion occurs near the beginning of transformation, i.e., for

$$\bar{\tau} \backsimeq \lg \bar{N}$$

which (26) becomes in this case, most of the region of transformation is represented by

$$V = 1 - e^{-\sigma G^3 (\bar{N}-1) t^3} \tag{28′}$$

which is practically the same as (28). The occurrence of the factor $\bar{N}-1$ instead of $\bar{N}$ is due to the neglect of the last germ nucleus in the derivation of (23′). Had we included this we should have obtained a result identical with (28).

The physical interpretation of the two limiting cases is readily given. (27) was seen to be interpretable in terms of a linear increase in number and a third power increase in extended volume of the growth nuclei with time. (28) evidently corresponds to the case where the great majority of the growth nuclei start near the beginning of transformation, and the growth in total extended volume is due merely to their continued growth. A little analysis will show that all other cases, of nucleus exhaustion at intermediate stages of the reaction, give a dependence of $V_{1\ ex}$ upon t somewhere in between t^3 and t^4.

For plate-like and lineal growth an analysis similar to the above gives for limiting cases

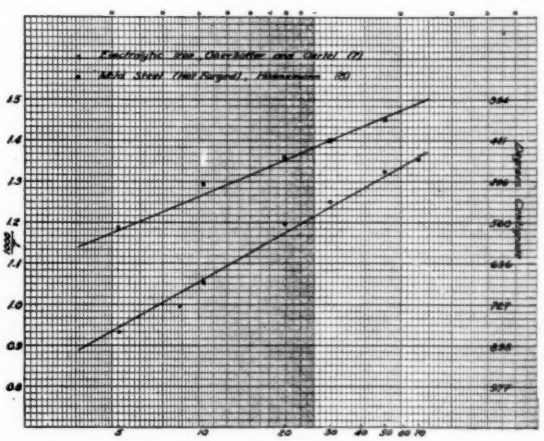

FIG. 5.

[9] Oberhoffer and Oertel, Stahl und Eisen **44**, 560–561 (1924); *ibid.* **39**, 1061 (1919).

[10] H. Hanemann and F. Lucke, Stahl und Eisen **47**, 1117 (1925). H. Hanemann, Zeitschrift für Metallkunde **17**, 316 (1925).

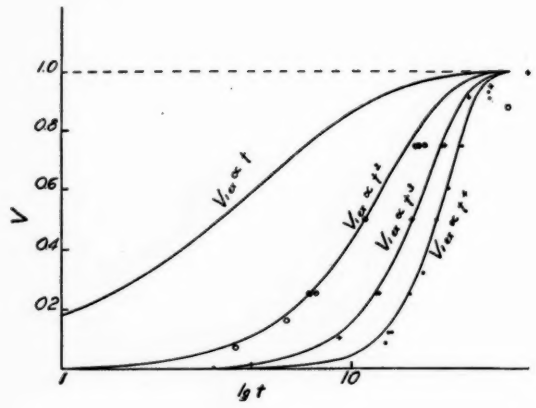

FIG. 6.

Plate-like, n small:

$$V=1-e^{(\sigma' G^2 \bar{N} n t^3)/3}. \tag{29}$$

Plate-like, n large:

$$V=1-e^{-\sigma' G^2 \bar{N} t^2}. \tag{30}$$

Lineal, n small

$$V=1-e^{(-\sigma'' G \bar{N} n t^2)/2}. \tag{31}$$

Lineal, n large:

$$V=1-e^{-\sigma'' G \bar{N} t} \tag{32}$$

all of which may be written, by analogy with the Austin Rickett formula,

$$V=1-e^{-Bt^k}. \tag{20'}$$

It is interesting to note that all of the cases (29) to (32) (except the last which has the shape of a first-order reaction curve) give the typical S-shape for V against t, starting slowly, rising rapidly, and then leveling off again. Since, in each, β and τ appear only in the combination $\beta\tau^k$ or Bt^k ($k=1, 2, 3, 4$), on a $V-\lg t$ plot all isothermal reaction curves for a particular value of k will have the same shape, differing only in position. Thus it will be convenient to designate as *the shape* of a $V-t$ curve the form which it takes in such a plot. We have plotted the four type curves in this fashion in Fig. 6. We note the increasing flatness of the reaction curves as the growth changes from polyhedral to lineal. This is in conformity with the available experimental data, which shows that when the habit changes from a polyhedral to an "acicular" needle-like, lineal type (e.g., for lowered temperature), *the transformation-time curves become flatter*. The effect is quite apparent in the data of Bain and Davenport on various alloys.[11]

For purposes of rough comparison with experiment, the difference in shape between the various limiting cases may be indicated by taking the ratio of times for two fixed degrees of transformation. A convenient representative index is the ratio of times for 75 percent and 25 percent transformation, respectively. This is equal in the various limiting cases to the fourth, third, second, and first roots, respectively, of

$$\frac{\lg (1-0.75)}{\lg (1-0.25)}=4.82.$$

Thus we should expect to find observed values of the ratio lying between the corresponding limits for the various types of growth, i.e.,

$$1.48 \leqslant \frac{t_{0.75}}{t_{0.25}}=\frac{\tau_{0.75}}{\tau_{0.25}} \leqslant 1.69 \quad \text{for polyhedral growth.}$$

$$1.69 \leqslant \frac{t_{0.75}}{t_{0.25}} \leqslant 2.2 \quad \text{for plate-like growth.}$$

$$2.2 \leqslant \frac{t_{0.75}}{t_{0.25}} \leqslant 4.82 \quad \text{for lineal growth.}$$

TABLE IV.

Steel	Temperature °C	$t_{0.75}$ in seconds	$t_{0.25}$ in seconds	$\frac{t_{0.75}}{t_{0.25}}$	Type of Growth
A	340	500	365	1.37	
	275	2000	1350	1.48	Polyhedral, n small
	250	4900	3200	1.53	" " "
	200	25500	17500	1.46	" " "
B	340	110	60	1.83	Plate-like
	320	130	70	1.86	"
	300	170	96	1.89	"
	275	290	155	1.86	"
	260	420	180	2.33	Lineal, n small
	250	540	220	2.45	" " "
C	340	33	16	2.08	
D	340	69	41	1.68	Polyhedral, n large
E	340	245	145	1.69	" " "
	275	680	410	1.66	" " "
	250	880	390	2.26	Lineal, n small
F	340	650	480	1.35	
	275	4500	3300	1.36	
	250	10100	7400	1.37	

[11] Bain and Davenport, Trans. A.I.M.E. **90**, 117 (1930); **100**, 13 (1932).

To test these conditions, we have examined the ratios as observed in a set of different steels studied very completely by Bain and Davenport.[12] The results are tabulated in Table IV. We notice two things. First, the ratios for a given steel, at different temperatures within an appreciable range, are approximately the same. This is evidence that the phenomena in this range are isokinetic.† Second, except for A at 340°C and for F, all of the ratios lie within the theoretically predicted limits. What is more, the values for A lie approximately at the polyhedral—n small limit, i.e., where

$$V_{1\,ex} \propto t^4$$

those for D and E above 250°C at the polyhedral —n large limit where

$$V_{1\,ex} \propto t^3$$

and for C, B and E below 260° at the lineal—n small limit where

$$V_{1\,ex} \propto t^2.$$

When we consider that the time dependences of $V_{1\,ex}$ leading to the indicated limits were derived completely theoretically, these agreements are strong confirmation of the suggested mechanisms.

The values for B above 260°C are, of course, within the allowed range. They correspond to the 5/2th root of 4.82, and we have suggested that the growth is plate-like in this region. It may be, however, that plate-like growth is not common, and that this intermediate value is due to some other cause. The whole question will bear further experimental and theoretical investigation. It is interesting that the outstanding discrepancy, that of A at 340°C and F, corresponds almost exactly to the 5th root of 4.82. Whether this is connected with some time variation of n which leads to a 5th power dependence of $V_{1\,ex}$ upon t we cannot at present say.

We have plotted the experimental data, associated by Table IV, with each of the limits, upon the corresponding limit curve in Fig. 6. We note the falling off of the experimental values from the curve at the end of reaction in each case. A still more clearcut comparison of the data with the limit curves may be made on the basis of (20′), which implies that a plot of lg lg $1/1-V$ against lg t should give a straight line with slope k. In fact, it is found that the experimental data plot even more accurately on these straight lines than on those given by Austin-Rickett. This is especially true at the beginning and end points. There is, however, the same falling off of the experimental points at the end of reaction as we observe in Fig. 6. We can trace this deviation to two factors both operating in the same direction: First, in writing

$$V_{1\,ex} = Bt^k$$

with k constant, we have ignored the fact that the dependence of $V_{1\,ex}$ upon t, as given by (18), occurs with a diminishing power of t as τ increases in $E(\tau)$. Second, as apparent in (18‴), there is an additional dropping off of $V_{1\,ex}$ from the limit curve after the exhaustion of the germ nuclei. To obtain an exact fit for the experimental data we should use (23) and (23′) with properly chosen values of β and $\bar{\tau}$. This, we have not attempted here. The deviation of experimental data from (17‴) or (20′), always in the same direction (falling off), is important in affording strong additional confirmation of the whole germ nucleation mechanism, for if we assumed only a constant rate of spontaneous nucleation per unit untransformed volume we should obtain only the limit curves (27) to (31).

Appendix I

Expression of V_k, $V_{k\,ex}$ and V_k' in Terms of $V_{1\,ex}$

First we shall show how (20), and therefore (19), may be derived by taking into account all of the higher order terms in V. To do this we proceed as follows. Let $v_{m\,ex}$ represent the extended volume of an average region in which m grains overlap, and let v_m' represent the volume of that part of the region in which *only* m grains overlap. Then, assuming complete randomness, we have by the same reasoning as that which leads to (17)

$$v_m'/v_{m\,ex} = 1 - V.$$

Multiplying both numerator and denominator by the total number of regions of this sort in

[12] The compositions and descriptions of the steels are given in the Trans. A.I.M.E. 90, 117 (1930). I wish here to acknowledge my indebtedness, not only to Messrs. Bain and Davenport for making available their original data, but also to Dr. J. B. Austin of the U. S. Steel Research Laboratory for his help in reading the values off the charts.

† K.P.C. I.

unit volume, we get

$$V_m'/V_{m\,\mathrm{ex}}=1-V, \qquad \text{(I, 1)}$$

where V_m' and $V_{m\,\mathrm{ex}}$ have the significance discussed in the previous paper. If we put this expression for V_k' into Eq. (10′) of that paper

$$V_m'=\sum_{p=m}^{\infty}(-1)^{p-m}C_m{}^pV_{p\,\mathrm{ex}}, \qquad (10')$$

we get

$$(1-V)\ V_{m\,\mathrm{ex}}=\sum_{p=m}^{\infty}(-1)^{p-m}C_m{}^pV_{p\,\mathrm{ex}}$$

which, upon rewriting and putting down together with (9), gives us an infinite system of linear equations for the determination of the infinite set of $V_{p\,\mathrm{ex}}$ in terms of V.

$$-V=-V_{1\,\mathrm{ex}}+V_{2\,\mathrm{ex}}-\cdots(-1)^pV_{p\,\mathrm{ex}}\cdots \qquad \text{(I, 2)}$$

$$0=VV_{m\,\mathrm{ex}}+\sum_{p=m+1}^{\infty}(-1)^{p-m}C_m{}^pV_{p\,\mathrm{ex}}.$$

The determinants involved in the solution of this system do not seem to have been studied in the literature. They are connected with the rather remarkable type of continued fraction to be discussed below. Since the matter is largely of pure mathematical interest we shall confine ourselves here to the consideration only of the determinants which appear in the solution for $V_{1\,\mathrm{ex}}$.

$$\begin{vmatrix} -V & 1 & -1 & \cdots & (-1)^p & \cdots \\ 0 & -2 & 3 & \cdots & (-1)^{p-1}C_1{}^p & \cdots \\ & V & -3 & \cdots & (-1)^{p-2}C_2{}^p & \cdots \\ & & \cdots & & \cdots & \\ \cdots & V & -k & \cdots & (-1)^{p-k}C_k{}^p & \cdots \\ & & \cdots & & \cdots & \end{vmatrix} \Bigg| \begin{vmatrix} -1 & -1 & -1 & \cdots & (-1)^p & \cdots \\ V & -2 & 3 & \cdots & (-1)^{p-1}C_1{}^p & \cdots \\ & V & -3 & \cdots & (-1)^{p-2}C_2{}^p & \cdots \\ & & \cdots & & \cdots & \\ \cdots & V & -k & \cdots & (-1)^{p-k}C_k{}^p & \cdots \\ & & \cdots & & \cdots & \end{vmatrix}.$$

Upon multiplying alternate rows and columns by -1 all the minus signs become plus. Expanding both numerator and denominator according to the elements of the first column, and dividing through, we get

$$V_{1\,\mathrm{ex}}=V/(1-fV), \qquad \text{(I, 3)}$$

where f is the fraction

$$\begin{vmatrix} 1 & 1 & 1 & \cdots & 1 & \cdots \\ V & 3 & 6 & \cdots & C_2{}^p & \cdots \\ & V & 4 & \cdots & C_3{}^p & \cdots \\ & & \cdots & & \cdots & \\ \cdots & V & k & \cdots & C_k{}^p & \cdots \\ & & \cdots & & \cdots & \end{vmatrix} \Bigg| \begin{vmatrix} 2 & 3 & 4 & \cdots & C_1{}^p & \cdots \\ V & 3 & 6 & \cdots & C_2{}^p & \cdots \\ & V & 4 & \cdots & C_3{}^p & \cdots \\ & & \cdots & & \cdots & \\ \cdots & V & k & \cdots & C_k{}^p & \cdots \\ & & \cdots & & \cdots & \end{vmatrix}.$$

The numerator and denominator of this fraction separately approach infinity, but the ratio is finite for values of V in the range of physical interest between 0 and 1. For $V=0$ f is evidently equal to $\frac{1}{2}$; for $V=1$ it goes over into a ratio of determinants of a type studied by Zeipel.[12] Terminating the rows and columns after any fixed number, e.g., $p-1$, the numerator and denominator have the values $p-1$ and $p+2$, respectively. For $p\to\infty$ the ratio approaches 1. f then varies between $\frac{1}{2}$ and 1 as V goes from 0 to 1, and we see how the Austin Rickett formula with $f=1$ can give an approximate representation of (I, 3). We shall now proceed to show how $V_{1\,\mathrm{ex}}$, and therefore f, may be obtained as a function of V.

If, by convention, we set $V_{0\,\mathrm{ex}}$, "the extended volume of no transformation," equal to 1, (I, 2) may be written in the compact form

$$0=VV_{k\,\mathrm{ex}}+\sum_{m=k+1}^{\infty}(-1)^{m-k}C_k{}^mV_{m\,\mathrm{ex}}, \qquad k=0, 1\cdots. \qquad \text{(I, 2′)}$$

Now let us arbitrarily cut off each of the equations after the term containing $V_{p\,\mathrm{ex}}$. We may later allow p to become infinite. Our system becomes

$$0=VV_{k\,\mathrm{ex}}+\sum_{m=k+1}^{p}(-1)^{m-k}C_k{}^mV_{m\,\mathrm{ex}}, \qquad k=0, 1\cdots p-1. \qquad \text{(I, 4)}$$

Let us add to each equation the last equation multiplied by

$$(-1)^{p-k}\frac{C_k{}^p}{C_{p-1}{}^p}.$$

Our system becomes

$$0=VV_{k\,\mathrm{ex}}+\sum_{m=k+1}^{p-2}(-1)^{m-k}C_k{}^mV_{m\,\mathrm{ex}}+(-1)^{p-k-1}C_k{}^{p-1}\left[1-\frac{V}{p-k}\right]V_{p-1\,\mathrm{ex}}, \qquad k=0, 1\cdots p-2, \qquad \text{(I, 4′)}$$

[12] V. v Zeipel, *Lunds Universitets Arsskrift*, II (1865); VIII (1871).

of which the last $(p-2)$ equation has the form

$$0 = VV_{p-2\text{ ex}} - (p-1)\left[1-\frac{V}{2}\right]V_{p-1\text{ ex}}.$$

If now we add to each of the equations in (I, 4′) the last equation multiplied by

$$(-1)^{p-k-1}\frac{C_k{}^{p-1}\left[1-\dfrac{V}{p-k}\right]}{(p-1)\left[1-\dfrac{V}{2}\right]},$$

our system becomes

$$0 = VV_{k\text{ ex}} + \sum_{k+1}^{p-3}(-1)^{m-k}C_k{}^{m}V_{m\text{ ex}} + (-1)^{p-2-k}C_k{}^{p-2}\left[1-\frac{V}{p-k-1}\,\frac{1-\dfrac{V}{p-k}}{1-\dfrac{V}{2}}\right]V_{p-2\text{ ex}},$$

$$k=0,\ 1,\ \cdots p-3. \quad \text{(I, 4″)}$$

Continuing in similar fashion, we find that the last remaining term in the kth equation after the jth operation of this type is

$$(-1)^{p-k-j}C_k{}^{p-1}\left[1-\frac{V}{p-k-j+1}\,\frac{1-\dfrac{V}{p-k-j+2}\,\dfrac{1-\dfrac{V}{p-k-j+3}\cdots}{1-\dfrac{V}{2}\,\dfrac{1-V/3}{1-V/2}\cdots}}{1-\dfrac{V}{2}\,\dfrac{1-\dfrac{V}{3}\,\dfrac{1-V/4}{1-V/2}\cdots}{1-\dfrac{V}{2}\,\dfrac{1-V/3}{1-V/2}\cdots}}\right], \quad \text{(I. 5)}$$

in which there appears a remarkable novel type of generalized ascending-descending continued fraction. It is characterized by the property that from each and every branch except the terminating ones there are two branches of higher order. We may perhaps describe it as a "tree fraction," and define its order as the order number of branchings, e.g., j in (I, 5). Upon letting the number of operations j equal $p-1$, the sole remaining equation for $k=0$ is

$$V=\left[1-\frac{V}{2}\,\frac{1-\dfrac{V}{3}\,\dfrac{1-\dfrac{V}{4}\,\dfrac{1-V/5}{1-V/2}\cdots}{1-\dfrac{V}{2}\,\dfrac{1-V/3}{1-V/2}}}{1-\dfrac{V}{3}\,\dfrac{1-\dfrac{V}{2}\,\dfrac{1-V/4}{1-V/2}\cdots}{1-\dfrac{V}{2}\,\dfrac{1-V/3}{1-V/2}\cdots}}\right]V_{1\text{ ex}} \quad \text{(I, 6)}$$

and this determines $V_{1\text{ ex}}$ in terms of V.

In general a tree fraction, like that in the brackets, defines a function which could be evaluated approximately for any value of the parameter by cutting off the "tree" after a certain number of branchings. In our case the function defined is a familiar elementary one as we shall now show. Let us designate the expression in the brackets by y. Then

$$V = yV_{1\text{ ex}}. \quad \text{(I, 6′)}$$

Since, for our infinite tree fraction, each successive *lower* branch is always exactly the same in structure as the entire tree, and is therefore equal to y, we have the relation

$$y=1-\frac{V}{2y}\left\{1-\frac{V}{3y}\left[1-\frac{V}{4y}(\cdots)\right]\right\}$$

which may be rewritten

$$y=1-\frac{V}{2!y}+\frac{V^2}{3!y^2}-\frac{V^3}{4!y^3}+\cdots=\frac{y}{V}(1-e^{-V/y}),$$

from which

$$V=1-e^{-V/y}$$

and

$$y = -V/\lg(1-V).$$

Upon substituting into (I, 6′) this gives

$$-\lg(1-V) = V_{1\,ex} \qquad \text{(I, 7)}$$

which, upon rearrangement, gives

$$V = 1 - e^{-V_{1\,ex}}, \qquad (20)$$

thus establishing the desired result.

Comparing (I, 7) with (I, 3), we find f in terms of V,

$$f = \frac{1}{V}\left[1 + \frac{V}{\lg(1-V)}\right],$$

an interesting result for the ratio of the two infinite determinants given above.

Upon expanding (20) we get

$$V = V_{1\,ex} - \frac{V_{1\,ex}^{\,2}}{2!} + \frac{V_{1\,ex}^{\,3}}{3!} - \cdots + (-1)^{m-1}\frac{V_{1\,ex}^{\,m}}{m!} - \cdots. \qquad (20')$$

If we compare this with (9) the suggestion crops up that, in our case of complete randomness, the relations

$$V_{k\,ex} = V_{1\,ex}^{\,k}/k!$$

hold. That this is true can be seen as follows. From the previous paper

$$V_k = \sum_{m=k}^{\infty} V_m', \qquad (8')$$

from which

$$V_k' = V_k - V_{k+1}$$

and, combining with (I, 1) and (20), this gives

$$V_k - V_{k+1} = V_{k\,ex}\, e^{-V_{1\,ex}}. \qquad \text{(I, 8)}$$

Now we must compare this with another relation, the generalization of (19), which we shall now obtain. Applying the same reasoning as above to increments in extended volume $dv_{k\,ex}$ and volume dv_k of the average kth-order region, we find

$$\frac{dv_k}{dv_{k\,ex}} = 1 - V = e^{-V_{1\,ex}}.$$

For unit volume

$$\frac{dV_k}{dV_{k\,ex}} = e^{-V_{1\,ex}}. \qquad \text{(I, 9)}$$

Differentiating (I, 8) and comparing with equations of the form (I, 9) we get

$$dV_{k+1\,ex} = V_{k\,ex}\, dV_{1\,ex}$$

which is evidently equivalent to the desired result

$$V_{k\,ex} = \frac{V_{1\,ex}^{\,k}}{k!}. \qquad \text{(I, 10)}$$

To express the V_k also in terms of $V_{1\,ex}$ we use the recursion formula (I, 8) successively to get

$$V_{k+1} = 1 - e^{-V_{1\,ex}}(1 + V_{1\,ex} + \cdots + V_{k\,ex})$$

and, substituting (I, 10) and rearranging, this becomes

$$V_{k+1} = (-1)^{k+1} e^{-V_{1\,ex}} E_k(V_{1\,ex}), \qquad \text{(I, 11)}$$

where E_k has the significance defined in (18″). Also

$$V_m' = \frac{V_{1\,ex}^{\,m}}{m!} e^{-V_{1\,ex}}, \qquad \text{(I, 12)}$$

which is evidently identical with (10′) in our case, since

$$V_m' = \sum_{p=m}^{\infty} (-1)^{p-m} C_m^{\,p} \frac{V_{1\,ex}^{\,p}}{p!} = \frac{V_{1\,ex}^{\,m}}{m!} \sum_{p=m}^{\infty} (-1)^{p-m} \frac{V_{1\,ex}^{\,p-m}}{(p-m)!}. \qquad (10'')$$

This completes the process of expressing all the other geometrical quantities in terms of $V_{1\,ex}$ alone.

The Magnetic Susceptibility of Silver Sub-Fluoride

SIMON FREED, NATHAN SUGARMAN, AND RICHARD P. METCALF
G. H. Jones Laboratory, University of Chicago, Chicago, Illinois

(Received December 4, 1939)

The metallic character of the crystals of silver sub-fluoride was studied in terms of the magnetic susceptibility. It was found that the conduction electrons contribute a considerable diamagnetism which was related especially to the anisotropy of the crystals.

CRYSTALS of silver sub-fluoride (Ag_2F) were prepared electrolytically from a solution of silver fluoride according to the procedure of A. Hettich[1] as modified by Scholder and Traulsen.[2] At the beginning of the electrolysis, the plates depositing on the cathode resembled highly burnished brass in their luster, but later the reflections became predominantly dark green. The different colors were re lected from different faces of the same crystal.[3]

There is no longer any question concerning the stoichiometrical relation between silver and fluorine. According to x-ray measurements, the silver atoms are in equivalent positions in a cadmium iodide lattice and at the same distance from each other as prevails between the silver atoms in metallic silver. The distance between the silver and fluorine is the same as the interionic distance in silver fluoride (AgF).

The magnetic measurements were undertaken to obtain information concerning the conduction electrons. The crystals conduct the electric current about as well as graphite.[4] In addition they rectify an alternating current.[3] Such properties corresponding to partially bound electrons might be expected to lead to a net paramagnetism somewhat higher than furnished by free electrons, not only because of a higher paramagnetic contribution by partially bound electrons but also because of the diminished diamagnetic susceptibility.[5]

The magnetic susceptibility was measured by the standard Gouy method at room temperature and at 77°K by an adaptation for low temperatures resembling one already described.[6] The curve shown in Fig. 1 represents the apparent change in weight as the current was varied in the electromagnet. The calibration was derived from the change in weight observed when water filled the tube in place of the crystals. Corrections for the empty tube were determined at 77°K since the method of substitution by water was no longer applicable. The molal susceptibility of silver sub-fluoride (Ag_2F) was found to be -64.3 ± 1.2 e.m.u.$\times10^{-6}$ both at room temperature and at 77°K.

The molal susceptibility of silver fluoride (AgF) as computed from the measurements of Kido[7] are -26.2 $(Ag^+)+(-12.2)(F^-)=-38.4$ (AgF). On the other hand, Brindley and Hoare[8] obtained -23.6 ± 0.06 for the molal susceptibility potassium fluoride (KF) whereas Kido's value was -25.7 by direct measurement. We shall accept -37.0 as the average value for the molal susceptibility of silver fluoride. The susceptibility of metallic silver has been measured by de Haas and van Alphen[9] and found to be -20.5 ± 0.2 per gram atom, independent of the temperature from 289°K to 20.4°K. According to Wiedemann's law, the molal susceptibility of the sub-fluoride would be $-37.0+(-20.5)=-57.5$. However, the ideal independence of the constituent magnetic susceptibilities would also allow for an increase in the paramagnetism of the conduction electrons because of the increase in molal volume—the difference between the molal volume of silver sub-fluoride and of silver.

[1] A. Hettich, Zeits. f. anorg. Chemie **167**, 67 (1927).
[2] R. Scholder and K. Traulsen, Zeits. f. anorg. Chemie **197**, 57 (1931).
[3] H. Steinmetz and A. Hettich, Zeits. f. anorg. Chemie **167**, 75 (1927).
[4] H. Terry and H. Diamond, J. Chem. Soc. 2820 (1928).
[5] N. F. Mott and H. Jones, *Properties of Metals and Alloys* (Oxford, 1936), p. 209.
[6] S. Freed, J. Am. Chem. Soc. **52**, 2702 (1930).
[7] K. Kido, Sc. Repts. Tohoku Imp. Univ. (1) **21**, 149 (1932); Sc. Repts. Tohoku Imp. Univ. (1) **21**, 288 (1932).
[8] G. W. Brindley and F. E. Hoare, Proc. Roy. Soc., London **49**, 342 (1937).
[9] W. J. de Haas and P. M. van Alphen, Proc. Acad. Sci., Amsterdam **36**, 263 (1933).

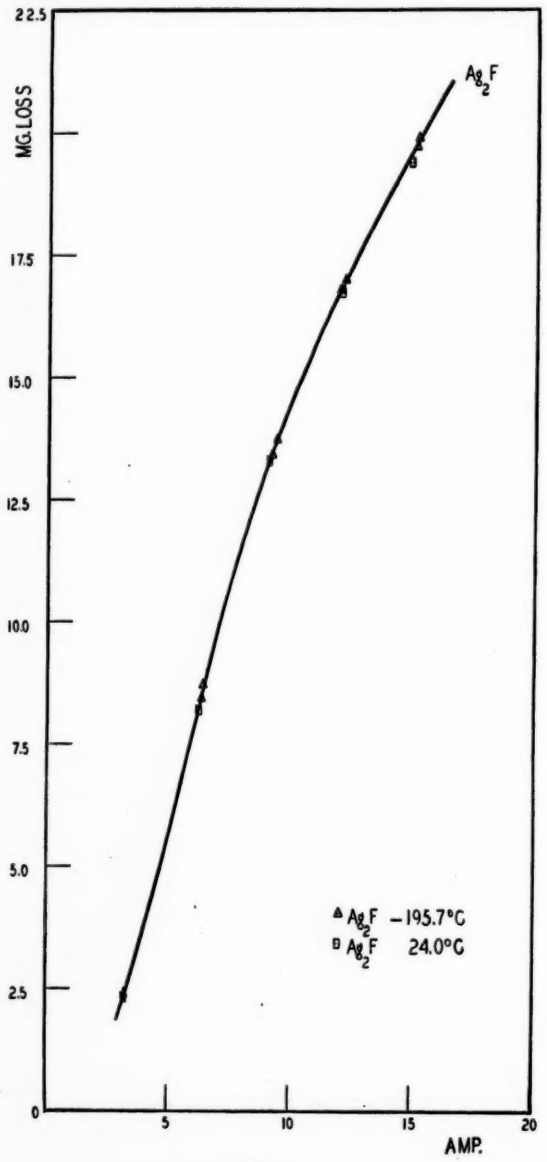

FIG. 1.

If the electrons be regarded as free, the additional net paramagnetic susceptibility is

$$\chi=\tfrac{2}{3}\left[\frac{4\pi m\mu^2}{h^2}\left(\frac{3n}{\pi}\right)^{\frac{1}{3}}\Delta V^{\frac{1}{3}}\right]=\tfrac{2}{3}(1.88\Delta V^{\frac{1}{3}})$$

$$=\tfrac{2}{3}[1.88(27.7^{\frac{1}{3}}-10.3^{\frac{1}{3}})]=5.6,$$

where m is the mass of the electron, h is Planck's constant, n is the number of free electrons per molecule $=1$, μ is the Bohr unit of magnetic moment and $\Delta V^{\frac{1}{3}}$ is the increase in the $\frac{2}{3}$ power of the molal volume. The factor $\frac{2}{3}$ before the bracket includes the subtraction effected by the diamagnetism of free electrons the magnitude of which is one-third of the spin paramagnetism.[10] The additivity on an "ideal" basis leads to the susceptibility $-57.5+5.6=-51.9$, a value which differs from -64.3 the observed susceptibility by considerably more than any experimental uncertainties.

The plate-like form of the crystals suggests that the enhanced diamagnetism is to be related to their anisotropic character, that is, to the "bindings" of the electrons which differ in magnitude with the directions in the crystal. If the surface of constant energy can be represented by a spherical surface, the "binding" or the increase in the "effective mass" of the electrons would, as we have mentioned in the introduction, have increased the paramagnetism and decreased the diamagnetism. However, anisotropic binding may lead to large diamagnetic contributions.[11] Instead of the Landau formula for the diamagnetism of free electrons

$$\chi=-\frac{4\pi m\mu^2}{3h^2}\left(\frac{3n}{\pi}\right)^{\frac{1}{3}}V^{\frac{1}{3}},$$

the diamagnetic susceptibility becomes

$$\chi=-\frac{4\pi m\mu^2}{3h^2}\left(\frac{3n}{\pi}\right)^{\frac{1}{3}}V^{\frac{1}{3}}\left\{\frac{(\alpha_1\alpha_2)^2}{\alpha_3}\right\}^{\frac{1}{3}},$$

where α_1, α_2, α_3 represent the bindings in different directions, α_3 corresponding to the direction of the magnetic field. This formula was derived on the supposition that the surfaces of constant energy could be approximated by ellipsoidal surfaces, instead of spherical surfaces. It is clear that the diamagnetism becomes very large when the ratio in the brackets is large. In the case of silver sub-fluoride, a rather weak anisotropy can account for the diamagnetic susceptibility which was obtained experimentally.

[10] L. Landau, Zeits. f. Physik **64**, 629 (1930); N. F. Mott and H. Jones, reference 5, p. 203.
[11] H. Jones, Proc. Roy. Soc. **A147**, 296 (1934); N. F. Mott and H. Jones, reference 5.

Lattice Vibrations of Crystals and the Corresponding Vibrations of Their Solutions

S. I. WEISSMAN AND SIMON FREED
G. H. Jones Laboratory, University of Chicago, Chicago, Illinois

(Received December 4, 1939)

Crystals of hydrated europium chloride possess structures in their absorption spectrum which are faint but accurate repetitions of the intense patterns arising from electronic transitions in in the europium ions. These repetitions occur on both sides of the intense patterns at intervals which are ascribed to oscillations of the lattice, thermally as well as optically excited oscillations. The spectra of aqueous solutions of europium chloride and also of europium nitrate closely parallel the structures in the spectrum of the crystals. In the region where the crystals absorb, the solutions absorb also. The structures in the spectra of the solutions are somewhat more diffuse than the corresponding structures in the spectra of the crystals. Especially is this true for the structures at the intervals corresponding to lattice vibrations.

THE spectra of crystals of the rare earths consist of rather widely spaced groups of lines. The separate groups owe their origin, it is generally accepted, to the decomposition of the electronic levels of the rare earth ions by the electric fields of their environment, somewhat as a line in the spectrum of a gas separates into a group of lines in the presence of an external electric field. Recently H. Ewald[1] has taken the absorption spectra through thick layers of crystals at the temperature of liquid hydrogen. He examined neodymium chloride $NdCl_3 \cdot 6H_2O$, the nitrate $Nd(NO_3)_3 \cdot 6H_2O$ the mixed magnesium neodymium nitrate $3Mg(NO_3)_2 \cdot 2Nd(NO_3)_3 \cdot 24H_2O$, the corresponding zinc salt $3Zn(NO_3)_2 \cdot 2Nd(NO_3)_3 \cdot 24H_2O$ and the sulfate $Nd_2(CO_4)_3 \cdot 8H_2O$. He found most of the intense groups accurately repeated at intervals toward shorter wave-lengths. The intervals between the intense pattern and the repetitions which were less intense conformed in most instances to well-known vibrational frequencies. For example the patterns from the crystal of the hydrated nitrate were repeated at intervals which accurately matched the frequencies of the internal vibrations of the nitrate ion as derived from Raman spectra. The intervals associated with the vibrations of nitrate ion were the same in the mixed as in the simple salt. In addition, repetitions of the patterns existed at intervals equivalent to the vibrations of water molecules. And when heavy water was substituted for light water the faint patterns were moved toward the main pattern, that is, the intervals now accurately represented the lower frequencies characteristic of heavy water. The intervals we have been discussing range from about 800 cm^{-1} to 1600 cm^{-1}. There were, however, smaller separations from the main patterns, from 100 cm^{-1} to about 500 cm^{-1}. At these intervals the faint structures were usually rather diffuse. When heavy water replaced the light water, these lines also moved toward the main pattern and the lines were nearer the main group from the mixed zinc nitrate than they were from the isomorphous mixed magnesium nitrate. That is, an increase in the mass of the constituents of the lattice brought about a lower frequency and for this reason, especially, Ewald identified these intervals with lattice vibrations. To summarize, it may be stated that the electronic transitions in these crystals couple with the internal vibrational frequencies of the molecules as well as with various modes of oscillation of the lattice. In neodymium chloride, only the intervals of the water and lattice vibrations were observed in the spectrum. Hellwege[2] confirmed this interpretation. Reststrahlen revealed frequencies in these crystals which agreed with the intervals in the visible spectrum.

The crystals of europium homologous to those of neodymium possess such sharp absorption spectra at room temperature that we examined them for the phenomena Ewald described. The

[1] H. Ewald, Ann. d. Physik **34**, 209 (1939).

[2] K. H. Hellwege, Zeits. f. Physik **113**, 192 (1939).

spectra of hydrated europium chloride at room temperature showed faint repetitions of the main pattern (especially at 4650A) not only on the side at shorter wave-lengths but also on the side toward longer wave-lengths. The intervals in both directions were the same. The lattice frequencies 115 cm^{-1} and 127 cm^{-1} were especially prominent. When the crystals of the hydrated chloride were placed in liquid nitrogen the spectrum no longer contained the lines on the long wave-length side. These represent then thermally activated lattice vibrations.

Rather concentrated aqueous solutions of europium chloride (0.15M, 0.75M, 1.7M and the corresponding light paths 90 cm, 24 cm, 12 cm) possessed definite regions of absorption in the spectrum on both sides of the main electronic pattern at 4650A and at intervals which paralleled closely the lattice vibrations in the crystals. The lines were diffuse and the resulting patches extended with especial intensity over a range about the width of the main pattern and were removed from the latter on both sides by the same interval, about 125 cm^{-1}. The solutions of europium nitrate possessed practically the same features in absorption. From more dilute solutions the structures were more diffuse and appeared to extend over a greater range of frequencies.

In as much as reststrahlen confirmed the presence of the lattice oscillations in the crystals, there is reason to expect that infra-red or Raman frequencies would register these quasi-lattice vibrations in the liquid.

This investigation was made possible with the aid of the Penrose Fund of the American Philosophical Society.